Speech-brain synchronization: a possible cause for developmental dyslexia

The research presented in this thesis was partially supported by: grants CONSOLIDER-INGENIO2010 CSD2008-00048 and PSI2012-31448 from the Spanish Ministry of Science and Innovation, the AThEME project funded by the European Commission 7th Framework Programme and ERC-2011-ADG-295362 from the European Research Council to Dr. Manuel Carreiras; grant PSI2012-32350 from the Spanish Ministry of Economy and Competitiveness to Dr. Nicola Molinaro; grant PSI2012-32128 from the Spanish Ministry of Economy and Competitiveness to Dr. Marie Lallier.

Mikel Lizarazu Ugalde

BCBL

Basque Center on Cognition Brain and Language

Paseo Mikeletegi, 69, Donostia-San Sebastián

November, 2016

BASQUE CENTER ON COGNITION, BRAIN AND LANGUAGE

eman ta zabal zazu

Universidad del País Vasco

Euskal Herriko Unibertsitatea

Speech-brain synchronization: a possible cause for developmental dyslexia

By Mikel Lizarazu Ugalde

A dissertation submitted to the Department of Linguistic and Basque Studies of the University of the Basque Country in candidacy for the Degree of Doctor in Linguistics

Thesis Supervised by Dr. Nicola Molinaro and Dr. Marie Lallier

San Sebastian, 2017

ACKNOWLEDGMENT

The work presented in the thesis was carried out at the “Basque Center on Cognition Brain and Language” (BCBL), under the supervision of Dr. Nicola Molinaro and Dr. Marie Lallier.

Firstly, I would like to express my sincere gratitude to Dr. Molinaro and Dr. Lallier for the continuous support of my Ph.D study and related research, for their patience, motivation, and immense knowledge. Their guidance helped me in all the time of research and writing of this thesis. It was a real pleasure to be under their supervision and learn from them.

Besides my advisor, I would like to thank the rest of my thesis committee: Prof. Franck Ramus, Prof. Martin Cooke, and Dr. Iria SanMiguel, for their insightful comments and encouragement, but also for the hard question which incented me to widen my research from various perspectives.

I thank my fellow lab mates in for the stimulating discussions and for all the fun we have had in the last five years. My sincere thanks also go to all the participants and families that took part in the experiments.

Last but not the least, I would like to thank my family: my parents and my brother, girlfriend and friends for supporting me spiritually throughout writing this thesis.

ABSTRACT

Dyslexia is a neurological learning disability characterized by the difficulty in an individual´s ability to read despite adequate intelligence and normal opportunities. The majority of dyslexic readers present phonological difficulties. The phonological difficulty most often associated with dyslexia is a deficit in phonological awareness, that is, the ability to hear and manipulate the sound structure of language. Some appealing theories of dyslexia attribute a causal role to auditory atypical oscillatory neural activity, suggesting it generates some of the phonological problems in dyslexia. These theories propose that auditory cortical oscillations of dyslexic individuals entrain less accurately to the spectral properties of auditory stimuli at distinct frequency bands (delta, theta and gamma) that are important for speech processing. Nevertheless, there are diverging hypotheses concerning the specific bands that would be disrupted in dyslexia, and which are the consequences of such difficulties on speech processing.

The goal of the present PhD thesis was to portray the neural oscillatory basis underlying phonological difficulties in developmental dyslexia.

We evaluated whether phonological deficits in developmental dyslexia are associated with impaired auditory entrainment to a specific frequency band. In that aim, we measured auditory neural synchronization to linguistic and non-linguistic auditory signals at different frequencies corresponding to key phonological units of speech (prosodic, syllabic and phonemic information). We found that dyslexic readers presented atypical neural entrainment to delta, theta and gamma frequency bands. We focused on atypical auditory entrainment to delta oscillations that might be underlying (i) the reduced sensitivity to prosodic contours in speech, ii) the *encoding* difficulties during speech processing and (ii) the speech-related attentional and phonological deficits observed in dyslexia.

In addition, we characterized the links between the anatomy of the auditory cortex and its oscillatory responses, taking into account previous studies which have observed structural alterations in dyslexia. We observed that the cortical pruning in auditory regions was linked to a stronger sensitivity to gamma oscillation in skilled readers, but to stronger theta band sensitivity in

dyslexic readers. Thus, we concluded that the left auditory regions might be specialized for processing phonological information at different time scales in skilled and dyslexic readers (phoneme vs. syllable, respectively).

Lastly, by assessing both children and adults on similar tasks, we provided the first evaluation of developmental modulations of typical and atypical auditory sampling (and their structural underpinnings). We found that atypical neural entrainment to delta, theta and gamma are present in dyslexia throughout the lifespan and is not modulated by reading experience.

TABLE OF CONTENTS

ABBREVIATIONS

AC	auditory cortex
ADHD	attention deficit hyperactivity disorder
AM	amplitude modulation
AMFR	amplitude modulation following response
ANOVA	analysis of variance
AST	asymmetric sampling in time
BCBL	Basque Center on Cognition, Brain and Language
BEM	boundary element method
CSD	cross spectral density
CT	cortical thickness
dB	decibel
DICS	dynamic imaging of coherence sources
DMGB	dorsal medial geniculate body
EEG	electroencephalography
ECD	equivalent current dipole
ECoG	electrocorticography
ENV	envelope
EOG	electrooculography
FDR	false discovery rate
FDM	finite difference method
FDMa	frequency-domain multivariate analysis
FEM	finite element method

fMRI	functional magnetic resonance imaging
HPI	head position indicator
IFG	inferior frontal gyrus
IC	inferior colliculus
ICA	independent component analysis
IQ	intelligence quotient
LI	lateralization index
MEG	magnetoencephalography
MGB	medial geniculate body
MI	mutual information
MRI	magnetic resonance imaging
MMGB	medial medial geniculate body
MN	minimum norm
MNI	Montreal Neurological Institute
NIRS	near-infrared spectroscopy
PAC	phase amplitude coupling
PET	positron emission tomography
PDC	partial direct coherence
PLV	phase locking value
RAN	rapid automatized naming
ROI	region of interest
SLI	speech language impairment
SOI	source of interest

SPECT	single photon emission computed tomography
SPL	sound pressure level
SPM	statistical parametric mapping
SSS	signal space separation
SQUID	superconducting quantum interference device
TE	transfer entropy
VMGB	ventral medial geniculate body
WAIS	Wechsler adult intelligence scale
WISC	Wechsler intelligence scale for children

1 OVERVIEW OF THE WORK: SUMMARY, OBJECTIVES AND STUDIES

As the title of the present thesis suggests, the present work will focus on the neural basis of the phonological deficit in dyslexia. This section will serve as a brief introduction to the main concepts and research aims that will be further developed throughout the whole manuscript.

Firstly, we will shortly introduce the basic assumptions of the phonological deficits in dyslexia (Ramus et al., 2003). We will present different hypotheses suggesting that phonological deficits observed in dyslexia could be associated to atypical oscillatory mechanisms at one or more temporal rates in auditory integration (Tallal, 1980; Goswami, 2011). We will mention data coming from different studies that describe the role of cortical oscillations when processing linguistic (speech) and non-linguistic (white noise amplitude modulated (AM)) auditory stimuli in normal and dyslexic readers (Lehongre, Ramus, Villiermet, Schwartz and Giraud, 2011; Hämäläinen, Rupp, Soltész, Szücs and Goswami, 2012; Gross et al., 2013; Hyafil, Giraud, Fontolan and Gutkin, 2015). We will also introduce neural mechanisms that are important during auditory processing and that will be addressed throughout the thesis, e.g. neural entrainment, neural *de-multiplexing* and neural *encoding*. Beside functional evidence, we will present various studies suggesting that structural abnormalities in auditory regions could underlie phonological deficits in dyslexia (Galaburda, Sherman, Rosen, Aboitiz and Geschwind, 1985).

After the Introduction, we will formulate the unresolved questions that our literature review has revealed and that the present thesis will try to answer by means of three studies that will be further described.

The phonological theory of dyslexia

Dyslexia is a neurological disorder with a genetic basis that affects the acquisition and processing of written language. Varying in degrees of severity, it is mainly manifested by difficulties in learning to read despite adequate intelligence, no obvious sensory deficits and appropriate educational opportunities. It affects an

estimated 10% of the population and seems to be more prevalent amongst males than females. The phonological theory is the prevalent cognitive-level explanation for the cause of dyslexia (Ramus et al., 2003). The phonological theory postulates that dyslexic readers have a specific impairment in the representation, access and/or retrieval of speech sounds. Multiple case studies have demonstrated that the phonological deficit might be a sufficient cause of dyslexia, independently of any sensory (magnocellular deficit) or motor (cerebellar deficit) impairment (Ramus et al., 2003). Phonological deficits in dyslexia are classically reflected by poor phonological awareness, poor verbal short-term memory, and slow phonological lexical retrieval (Vellutino, Fletcher, Snowling and Scanlon, 2004). Phonological awareness is the ability to identify and manipulate the sounds of language; for example, the ability to segment words into their parts, and understanding, for example, that 'car' is constituted of the onset and rime /c/-/ar/ and or of individual sounds (phonemes) /c/-/a/-/r/. Phonological awareness is also engaged in grapheme to phoneme conversion, which plays a critical role in reading and its disorders such as dyslexia (Goswami, 1998; Wheat, Cornelissen, Frost and Hansen, 2010). The phonological hypothesis of dyslexia is supported by numerous studies showing that individuals with dyslexia do poorly on behavioral tests which measure phonological awareness, phonological short term memory or lexical phonological access. In spite of these findings, the precise nature of the phonological impairment in dyslexia remains elusive (Bryant, 1998; Stanovich, 2000). It has been suggested that phonological deficits in dyslexia would result from auditory perceptual impairments (Lehongre et al., 2011, 2013; Hämäläinen et al., 2012; Goswami and Leong, 2013) (but see Boets et al., 2013 for an alternative proposal). Deficits were indeed demonstrated across a wide range of auditory tasks, from Tallal's (Tallal, 1980) classic temporal order judgment and repetition tests (De Martino, Espesser, Rey and Habib, 2001; Rey, De Martino, Espesser and Habib, 2002), to frequency and intensity discrimination (Amitay, Ahissar and Nelken, 2002; France et al., 2002), gap detection (Chiappe, Stringer, Siegel and Stanovich, 2002), frequency and AM detection (Amitay et al., 2002; Goswami et al., 2002; Witton, Stein, Stoodley, Rosner and Talcott, 2002) and categorical perception of phonemes and non-speech analogues (Breier et al., 2001; Serniclaes, Sprenger, Carré and Demonet, 2001).

The 'temporal sampling framework' (TSF) (Goswami, 2011) and the 'rapid temporal processing' hypothesis (Tallal, 1980) suggest that the auditory perceptual deficits observed in dyslexia are linked to atypical sampling of auditory temporal inputs. In other words, a temporal processing impairment would reduce the ability of dyslexic readers to accurately perceive critical phonological information in the speech stream. The TSF hypothesis suggests that dyslexic readers present difficulties in processing syllabic and prosodic information occurring at frequencies between 4-7 Hz (Theta band) and 0.5-2 Hz respectively (Delta band). The rapid temporal processing hypothesis, on the other hand, suggests that dyslexic readers could not accurately identify rapid changes in auditory signal, in the time scale of phonemic information (Gamma band: 25-80 Hz). Recent studies propose that atypical auditory entrainment to delta (prosodic), theta (syllabic) and gamma (phonemic) AMs underlies auditory deficits in dyslexia (Lehongre et al., 2011; Hämäläinen et al., 2012; Goswami, Power, Lallier and Facoetti, 2014). We note that there are diverging hypotheses concerning the specific frequency bands at which auditory processing would be disturbed in dyslexia, and the evidence so far seems contradictory.

The goal of the present PhD thesis is to better understand the neural oscillatory basis underlying the phonological difficulties observed in developmental dyslexia.

First, we wanted to clarify which cortical oscillations matter for speech processing in normal readers (Study 1), and which are disrupted in dyslexia (Study 2 and Study 3). For that, we recorded MEG signals from children and adults with and without dyslexia while they listened to continuous speech (Study 1 and Study 2) and to non-linguistic stimuli (Study 3). We evaluated the synchronization between the auditory signals and the MEG data at frequencies that correspond to the occurrence of phonological units of speech (prosodic, syllabic and phonemic information). Results from Study 1 highlighted the role of delta neural entrainment during normal continuous speech processing. We showed that cortical oscillations synchronized to prosodic contours in speech and modulated theta and gamma cortical oscillations during phonological *encoding* operations (for details see below). Furthermore, we suggested that delta entrainment is also important for

attentional operations during speech processing. Interestingly, in Study 2 and Study 3, our result suggest that reduced auditory entrainment to delta oscillations may underlie i) impaired sensitivity to prosodic information, ii) altered *encoding* of syllabic and phonemic units and, ii) speech-related attentional deficits during speech processing in dyslexia.

In addition, we investigated structural anomalies in the auditory cortex that could underlie atypical oscillatory activity in dyslexic readers (Study 3). We found that the development of the left auditory cortex (cortical pruning) in normal readers facilitates that sampling of rapid changes in auditory signals (gamma oscillations). Interestingly, the cortical pruning in dyslexic readers was linked to a stronger sensitivity to 4 Hz auditory modulations that could explain the atypical entrainment observed in the theta band.

Neural entrainment to speech rhythms in skilled and dyslexic readers

Phonological units in speech are distributed across different time scales. Across languages, syllables occur in the speech stream at relatively constant rates, every 200 ms (within the Theta band of 4-7 Hz), and the more prominent syllables (stress syllables) occur approximately every 500 ms (within the Delta band of 0.5-2 Hz) (Arvaniti, 2009). Phonetic information occurs approximately every 80 ms and shorter segmental speech features such as formant transitions are presented at even faster rates (within the Gamma band of 28-80 Hz) (Ghitza and Greenberg, 2009). The regularity in the timing of the successive phonological units modulates in a quasi-rhythmic manner the amplitude of the speech envelope.

The coding of these temporal speech modulations is thought to be performed in part through neural entrainment to the rhythmic components embedded in continuous speech (Poeppel, 2003; Lakatos, Karmos, Mehta, Ulbert and Schroeder, 2008; Giraud and Poeppel, 2012a). Neural entrainment refers to the adaptive function of the brain by which the endogenous neural oscillations can adjust to synchronize with a regularly repeating pattern of an external stimulus, e.g. the speech signal (Poeppel, 2003; Schroeder and Lakatos, 2009). Neural entrainment during speech processing entails at least two distinct neural mechanisms: the *de-multiplexing* step and the *encoding* step.

The de-multiplexing neural mechanism

Most of the speech processing models (Hickok and Poeppel, 2004; Rauschecker and Scott, 2009; Peelle, Johnsrude and Davis, 2010) involve frontal, temporal and parietal regions in the processing of speech. Importantly, different brain regions process different features of the speech stream in parallel before extracting meaning from speech. For that, neural oscillations within the fronto-temporo-parietal network synchronize their endogenous oscillations at the frequencies that match the temporal occurrence of phonological information in the acoustic speech signal. This speech processing step is termed as neural *de-multiplexing* (Gross et al., 2013). Frequency *de-multiplexing* during speech processing allows parallel analysis of phonological information at different time scales.

Importantly, the left and right hemispheres play different roles in frequency *de-multiplexing* mechanisms. According to the "asymmetric sampling in time (AST)" theory (Poeppel, 2003), the right hemisphere is specialized for processing slow modulations at the delta and theta frequency bands whereas bilateral auditory regions (also viewed as a left-biased hemispheric specialization) are associated with the processing of fast acoustic gamma fluctuations (> 30 Hz) (Poeppel, 2003; Boemio, Fromm, Braun and Poeppel, 2005; Vanvooren, Poelmans, Hofmann, Ghesquière and Wouters, 2014). This parallel processing allows sensory representations to be stable despite of the presence of distortions of the audio signal and increases the *encoding* capacity of neural responses (Panzeri, Brunel, Logothetis and Kayser, 2010). Furthermore, the asymmetric routing between cerebral hemispheres represents an important mechanism for temporal *encoding* (described below) in auditory regions (Poeppel, 2003).

The speech encoding step

After *de-multiplexing* the speech stream, speech entrained brain oscillations are hierarchically coupled for mediating speech *encoding* (Schroeder and Lakatos, 2009; Canolty and Knight, 2010; Hyafil et al., 2015). Recent studies on cross-frequency interactions have demonstrated modulations of the amplitude of fast oscillations in relation to the phase of slow oscillations (Canolty and Knight, 2012). For example, Hyafil and colleagues (2015) showed that gamma power is phase

locked to theta oscillations in auditory regions during speech processing. Thanks to cross-frequency coupling mechanisms, it is assumed that theta oscillations track the syllabic rhythms of speech to temporally organize the phoneme level responses of gamma-spiking neurons into segments that permit syllabic identification (Hyafil et al., 2015). Likewise, Gross and colleagues (2013) showed that delta-theta phase amplitude coupling extends to fronto-parietal regions, i.e. brain areas involved in higher order processes during speech comprehension. Consequently, syllabic segments are grouped into words or larger meaningful linguistic units, i.e. phrase and sentences, for further processing.

Although recent studies (Gross et a., 2013; Hyafil et al., 2015) suggest that neural entrainment may be the key for processing speech, previous models of speech processing (Hickok and Poeppel, 2004; Rauschecker and Scott, 2009; Peelle et al., 2010) did not characterize the *de-multiplexing* and/or *encoding* neural mechanisms (Jensen and Lisman, 1996; Tort, Komorowski, Eichenbaum and Kopell, 2010) or did not involve neural oscillations at all (Gütig and Sompolinsky, 2009; Yildiz, von Kriegstein and Kiebel, 2013). Furthermore, understanding the oscillatory mechanisms underlying speech processing could help us to better understand the cause of language developmental disorders such as dyslexia, since abnormal speech analysis has been proposed to result in the acoustic deficits observed in dyslexia (Goswami, 2011; Lehongre et al., 2011).

Unresolved question addressed in the present work: There is indeed a substantial body of literature suggesting that atypical neural entrainment to prosodic, syllabic and phonemic rhythms of speech might be underlying the auditory deficits and, in turn, the phonological difficulties observed in dyslexia (Goswami 2011; Lehongre et al., 2013; Leong and Goswami 2014). Nevertheless, none of the previous studies specify how these abnormalities might be reflected in the *de-multiplexing* and the *encoding* mechanisms involved in speech processing.

As stated before, the neural *de-multiplexing* mechanism relies on asymmetries in hemispheric specialization of the processing of speech sounds. Abnormal *de-multiplexing* of the speech stream in dyslexia could affect the asymmetric sampling in the auditory cortex (Poeppel, 2003). In contrast to normal

readers who present a right hemispheric asymmetry during prosody rate modulations, dyslexic readers rely on more bilateral networks (Hämäläinen et al., 2012). Moreover, the sensitivity to phoneme rate modulations is less left lateralized in dyslexia (Lehongre et al., 2011). There are several studies showing that atypical synchronization patterns affect reading performance. For example, Abrams and colleagues (2009) showed that good readers present consistent right-hemisphere dominance in auditory regions in response to slow temporal cues in speech, while poor readers showed a bilateral response. The aforementioned studies suggest that an adequate division of labor between the two hemispheres for processing acoustic information is critical for later temporal *encoding* steps.

We already mentioned that the *encoding* mechanism relies on the hierarchical coupling of the speech-entrained neural oscillations, where fast oscillations are nested within slow oscillations. Entrainment difficulties in the *de-multiplexing* mechanism could initiate a chain of errors in further *encoding* steps. Atypical neural synchronization to slow speech envelope variations (delta and/or theta) in dyslexia (Goswami, 2011; Hämäläinen et al., 2012) could disturb the control of faster oscillations (Lehongre et al., 2011). This being said, it is reasonable to suppose that the coupling between delta-theta and theta-gamma frequency bands might be disrupted in dyslexia. Nonetheless, there is no research that studies specifically the *de-multiplexing* and *encoding* neural mechanisms in dyslexia.

Neural entrainment to non-linguistic auditory signals in dyslexia

Like most complex natural sounds, the spectrum of the speech signal shows power increase at multiple frequency bands. The information within each frequency band contains different and sometimes non-independent linguistic information. Inter-frequential dependencies within the speech stream make it difficult to clearly identify the neural activity elicited by different frequency bands. To solve these issues, some studies analyzed the brain response to white noise (non-linguistic) AM at frequencies that independently represent prosodic, syllabic and phonemic fluctuations in speech. These auditory signals are perfectly periodic and entrain neural oscillations at the modulation frequency of the stimuli. Therefore, different neural groups responsible for the *de-multiplexing* process are

entrained separately. Furthermore, the processing of these stimuli does not involve *encoding* or predictive processes observed during speech processing.

Reduced sensitivity to slow AM white noise has been reported in dyslexic adults (Hämäläinen et al., 2012) and children (Lorenzi, Dumont and Fullgrabe, 2000; Rocheron, Lorenzi, Füllgrabe and Dumont, 2002). Hämäläinen and et al. (2012) used magnetoencephalography (MEG) to measure how consistently the phase of the neural activity tracks the AM at 2, 4, 10 and 20 Hz in adults with and without dyslexia. Typical readers exhibited stronger phase synchronization to AM at delta rate of 2 Hz in right auditory cortex, whereas adults with dyslexia showed bilateral synchronization. Two psychophysical studies conducted with children with dyslexia examined thresholds for perception of 4 Hz AMs (Lorenzi et al., 2000; Rocheron et al., 2002). In both studies, dyslexic children showed higher thresholds than control children indicating perceptual insensitivity to slower AM rates. In the same vein, atypical synchronization to fast AMs has been found in dyslexic adults (Menell, McAnally and Stein, 1999; Lehongre et al., 2011). Menell et al., used electroencephalography (EEG) to measure the scalp-recorded amplitude modulation following responses (AMFR) at rates of 10, 20, 40, 80 and 160 Hz. This test showed reduced AMFR amplitude across all modulation frequencies in adults with dyslexia compared to normal readers. Using MEG, Lehongre and colleagues (2011) showed that dyslexic adults present reduced entrainment to 30 Hz acoustic modulations in left auditory cortex, which furthermore correlated with measures of phonological processing and rapid naming.

Unresolved question addressed in the present work: Overall, these results indicate that dyslexic readers present atypical sensitivity to slow and fast AMs that could affect prosodic/syllabic and phonemic processing respectively. Nevertheless, the stimuli in the different experiments are heterogeneous which does not allow us to draw clear conclusions on the nature of the neural oscillatory deficit in dyslexia.

Reading-related developmental changes in the structure and function of the auditory cortex

In all the studies mentioned above, dyslexic and normal readers were age matched, without taking into account whether the auditory processing deficits highlighted in dyslexia were a consequence of the lack of print exposure in dyslexic

individuals. However, a comprehensive understanding of the "oscillatory" bases of developmental dyslexia should take into account how the deficit changes across development and with the amount of reading experience and exposure (Goswami et al., 2014).

We know that the size of the phonological units to which pre-readers are sensitive decreases as soon as their reading skills develop. Before reading, children are highly sensitive to the syllabic (large grain) structure of words and become progressively more sensitive to phonemic (small-grain) units as they learn how to read (Morais, Alegría and Content, 1987; Goswami and Bryant, 1990; Anthony and Francis, 2005; Ziegler and Goswami, 2005). Following the link between neural oscillations and phonological units at multiple time scales, it seems understandable that low frequency sampling linked to syllabic stress may be trained from birth until the exposure of alphabetic principles (e.g., Curtin, 2010; Molnar, Lallier and Carreiras, 2014). Sensitivity to higher AM frequencies could improve with reading acquisition and expertise.

Unresolved question addressed in the present work: Previous studies have shown that both prosodic/syllabic and phonemic dimensions of phonological processing are affected in dyslexic children (Serniclaes, Van Heghe, Mousty, Carré and Sprenger, 2004; Goswami and Leong, 2013) and adults (Pennington, Orden, Smith, Green and Haith, 1990; Soroli, Szenkovits and Ramus, 2010). However, such findings have been reported separately and could not provide evidence about the evolution of the trajectory of the phonological deficits in dyslexia (e.g., Lallier et al., 2009).

The neuroanatomy of the auditory cortex in dyslexic readers

Structural neuroimaging studies suggest that auditory regions are typically larger in the left hemisphere than in the right hemisphere (Geschwind and Levitsky, 1968; Galaburda, LeMay, Kemper and Geschwind, 1978; Rademacher et al., 1993; Penhune, Zatorre, MacDonald and Evans, 1996; Shapleske, Rossell, Woodruff and Davis, 1999; Altarelli et al., 2014). Structural hemispheric asymmetries in auditory regions (Galaburda et al. 1985) may underlie the auditory perceptual asymmetries for processing slow and fast AMs (Poeppel, 2013) and, in

turn, support the neural *de-multiplexing* mechanism. Neurons in left auditory regions are better equipped for processing fast AMs while neurons in right auditory regions are more sensitive to slow AMs (Giraud and Poeppel, 2012b).

Structural anomalies could compromise efficient sampling of the auditory stream at different frequencies (Giraud and Poeppel, 2012b) in dyslexia. Numerous studies reported macrostructural brain differences between dyslexic and controls in a variety of regions involved in reading (Pennington et al., 1999; Eliez et al., 2000; Robichon, Levrier, Farnarier and Habib, 2000; Robinchon, Bouchars, Démonet and Habib, 2000; Brown et al., 2001; Leonard et al., 2001; Rae et al., 2002). In post-mortem studies, Galaburda et al. (1985) reported an enlargement of the planum temporale (area Tpt in Galaburda and Sanides, 1980) of the right hemisphere in dyslexia. Although some of the subsequent work analyzing the size of temporal regions with magnetic resonance imaging (MRI) confirmed Galaburda's findings (Larsen, Høien, Lundberg and Odegaard, 1990), recent studies have failed to do so (Schultz et al., 1994; Leonard et al., 2001). Genetically driven microstructural (neural level) anomalies on cortex that includes ectopias, dysplesia and microgyria have been also reported in dyslexia (Galaburda, 1989; Galaburda, 1999). Nevertheless, microstructural results should be interpreted with caution due to the low sample size of these studies (low statistical power). Overall, the lack of replicability and consistency hampers the identification of a structural marker that could differentiate dyslexics from normal readers.

Unresolved question addressed in the present work: As mentioned before, it is possible that anatomical abnormalities in the auditory regions are linked to auditory sampling and reading deficits in dyslexia. However, there are no previous studies trying to link structural anomalies with atypical sampling properties of auditory cortex in dyslexic readers.

Objectives and studies of the present thesis

The previous brief review of literature led us to set the different objectives of our work in order to answer unresolved questions in the field of developmental dyslexia and oscillatory speech processing. In particular, this research was dedicated to explore further the neural substrates of the phonological deficit in

developmental dyslexia in the framework of multi-time resolution models of speech perception (Poeppel, 2003).

The specific aims of the present work are formulated below:

I. To better describe the neural mechanisms involved in speech processing in normal readers, i.e. *de-multiplexing* and *encoding* processing steps.

II. To clarify the specific frequency band that is disrupted in dyslexia during continuous speech or non-linguistic auditory sequential processing and how these abnormalities affect speech processing and phonological skills.

III. To provide a developmental evaluation of typical and atypical auditory sampling of both linguistic and non-linguistic auditory stimuli in skilled and dyslexia readers.

IV. To identify potential structural anomalies in the auditory cortex of dyslexic individuals in relation to their atypical neural oscillations and their phonological deficits.

In order to reach these objectives, we conducted three studies that examined behavioral, functional, and structural brain data from children and adults with and without dyslexia. Brain functional data was recorded using MEG, while brain structural data was acquired using MRI. We present briefly below each study and summarize the results obtained.

In Study 1, we examined the neural mechanism underlying speech processing in normal reader adults. Twenty healthy adults listened to continuous speech while their brain signals were recorded with whole-scalp MEG. We confirmed that neural oscillations within fronto-temporo-parietal regions deal with the *de-multiplexing* (Coherence analysis, see section 3.4.2) and the *encoding* (Mutual Information (MI) analysis, see section 3.4.5) steps at different frequency bands. During the *de-multiplexing* analysis delta and theta neural oscillations track prosodic and syllabic rhythms of speech respectively. After the *de-multiplexing* step, speech entrained brain oscillations were hierarchically coupled during the *encoding* step. Delta-theta and theta-gamma phase amplitude coupling emerged in

fronto-parietal and temporal regions respectively. Results from the first study shed light on the role of cortical oscillations during speech processing (Objective I).

In Study 2, we studied the neural mechanism underlying speech processing in children and adults with and without dyslexia. Brain activity during listening to natural speech was recorded using MEG in all participants. Here again, coherence and MI analysis were computed to identified *de-multiplexing* and *encoding* speech processing steps respectively. In line with the temporal sampling theory, we observed that dyslexic readers (both adults and children) present difficulties tracking slow (delta frequency band) fluctuation in the speech envelope. Differences emerged in the *de-multiplexing* step, but not in the *encoding* step.

Furthermore, using causal connectivity analysis (Partial Direct coherence (PDC)) we demonstrated that the source of the phonological processing difficulties in developmental dyslexia is a low-frequency processing deficit in right auditory regions. This deficit triggers a chain reaction that hinders the neural entrainment in left frontal regions. We suggested that the entrainment deficits in dyslexia emerged in auditory perceptual regions and could affect higher order regions involved in speech processing. Results from the first study shed light on the specific frequency band that is disrupted in dyslexia during continuous speech and how these abnormalities affect speech processing (Objective II). This study has been published in Human Brain Mapping (Molinaro, Lizarazu, Lallier, Bourguignon and Carreiras, 2016).

In Study 3, we better identified the frequency bands where dyslexic readers (children and adults) present auditory deficits. During the MEG recordings, participants listened to white noise AM at different rates (2, 4, 7, 30 and 60 Hz). The modulation frequencies correspond to relevant phonological spectral components of speech and strongly entrain auditory neural oscillations. These stimuli are non-linguistic and evaluate neural entrainment during the *de-multiplexing* step. Dyslexics showed atypical brain synchronization also at syllabic (theta band) and phonemic (gamma band) rates. From Study 2 and Study 3, we concluded that dyslexic readers present atypical neural entrainment to multiple frequency bands (delta, theta and gamma frequency bands). Furthermore, we suggested that abnormal entrainment to theta and gamma frequency bands could

compromise perceptual computations during speech processing, while reduced neural entrainment to delta could disrupt higher order operation during speech processing, e.g. speech-related attentional computations (Objective II). Results of this study have been published in Human Brain Mapping (Lizarazu et al., 2015; Molinaro et al., 2016).

Moreover, in Study 3, structural magnetic resonance imaging (MRI) was employed to estimate structural anomalies (cortical thickness (CT)) in auditory cortex in dyslexia. No CT difference in the auditory cortex was found between normal and dyslexic readers. Links between the anatomy of the auditory cortex and its oscillatory responses in normal and dyslexic readers were also studied in this experiment (Objective IV). We found that while a left biased hemispheric asymmetry in CT was functionally related to a stronger left hemispheric lateralization of neural synchronization to stimuli presented at the phonemic rate in skilled readers, the same anatomical index in dyslexics was related to a stronger right hemispheric dominance for neural synchronization to syllabic rate auditory stimuli. Results from this analysis are also published in Human Brain Mapping (Lizarazu et al., 2015).

Importantly, in Study 2 and Study 3, we assessed both children and adults on similar tasks. This allowed us to provide an evaluation of the developmental modulation of typical and atypical auditory sampling (Objective III). We concluded that abnormal entrainment to delta, theta and gamma is present already in early stages of reading development in dyslexia and is still present in adulthood. Regarding the structural analysis, we confirmed that the CT decrease with age due to cortical pruning in normal and dyslexic readers.

In the following section, we will review in more detail the literature that allowed us to formulate our hypotheses for each of our Study.

2 INTRODUCTION

In this section, we present some of the main concepts that we will discuss throughout different studies. We describe the central auditory neural pathway and we focus on the neural mechanisms involved in the processing of audio stimuli, in particular in the processing of speech. Finally, we focus on the phonological deficit theory in dyslexia and we present functional and structural evidences suggesting that abnormal cortical oscillations during auditory processing might be causing phonological deficits.

2.1 NEUROANATOMY OF AUDITORY SIGNAL PROCESSING

As mentioned previously, in this section we introduce basic information on the structure and function (based on neural oscillations) of the human auditory system. Although we explain that neural activity caused by an auditory input undergoes intermediate steps before reaching the auditory cortex (e.g. thalamus), we will focus on investigating neural oscillations in the neocortex. Then, we describe how cortical oscillations track amplitude fluctuations at different time-scales in simple audio signals. Finally, we extend this neural property to the processing of more complex sounds (e.g. speech).

2.1.1 CENTRAL AUDITORY NEURAL PATHWAY

The human ear is separated in three main parts: the outer ear, the middle ear and the inner ear. The outer ear is the external portion of the ear, which consists of the pinna and the ear canal, gathers sound waves and directs them to the middle ear. The middle ear contains three tiny bones (malleus, incus and stapes), called the ossicles. These three bones form a connection from the eardrum to the inner ear. As sound waves hit the eardrum, the eardrum moves back and forth causing the ossicles to move. As a result, the sound wave is changed to a mechanical vibration that is transferred to the cochlea. The cochlea is part of the inner ear and is filled with a watery liquid, the perilymph, which moves in response to the vibration. As the fluid moves, thousands of hair cells located on the basilar membrane in the cochlea sense the vibration and convert that motion to electrical signals that are communicated via neurotransmitters to thousands of nerve cells. Interestingly, the hair cells are tuned to a certain frequency based on

their location in the cochlea. In this way, lower frequencies cause movement in the base of the cochlea, and higher frequencies work at the apex. This characteristic is known as cochlear tonotopy (Figure 1). The human cochlea is capable of exceptional sound analysis, in terms of both frequency (between 20 Hz and 20.000 Hz) and intensity (between 0 decibel (dB) sound pressure level (SPL) and 120 dB SPL). Nerve impulses generated in the inner ear travel along the cochlear nerve (acoustic nerve) and enter the brainstem at the lateral aspect of the lower pons.

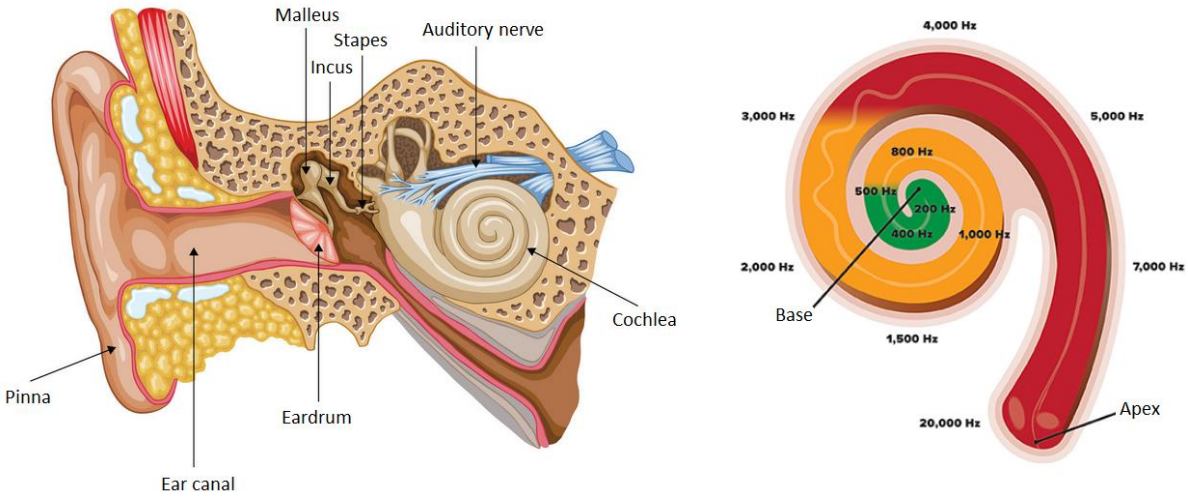

Figure 1. Peripheral auditory system. On the left part, a representation of the peripheral auditory system. On the right side, an illustration of the cochlea and its tonotopic across the frequency spectrum. Adapted from Lahav and Skoe (2014).

Upon entering the central nervous system, the auditory nerve fibers synapse with cell in the cochlear nuclei (Figure 2). Auditory fibers from more basal (high frequency) areas of the cochlea reach dorsomedial parts of the cochlear nuclei, and neurons from more apical (lower frequency) parts of the cochlea project to the ventrolateral parts of these nuclei. After ipsilateral processing in either the dorsal or the ventral cochlear nucleus impulses are projected bilaterally, but with a contralateral dominance, to the superior olivary complex. This is the first (lowest) level of the central auditory pathway that receives information originating from both sides of the head (bilateral representation). The pathway travels up through the lateral lemniscus to the inferior colliculus (IC) where there is a further partial decussation. The IC is located on the left and right sides of the midbrain and plays a role in multisensory integration. Ascending fibers from the IC project to the ipsilateral medial geniculate body (MGB). Neurons from both MGBs also receive input from the contralateral IC due to the commissure between the

two colliculi. This organization means that most MGB neurons are responsive to binaural signals.

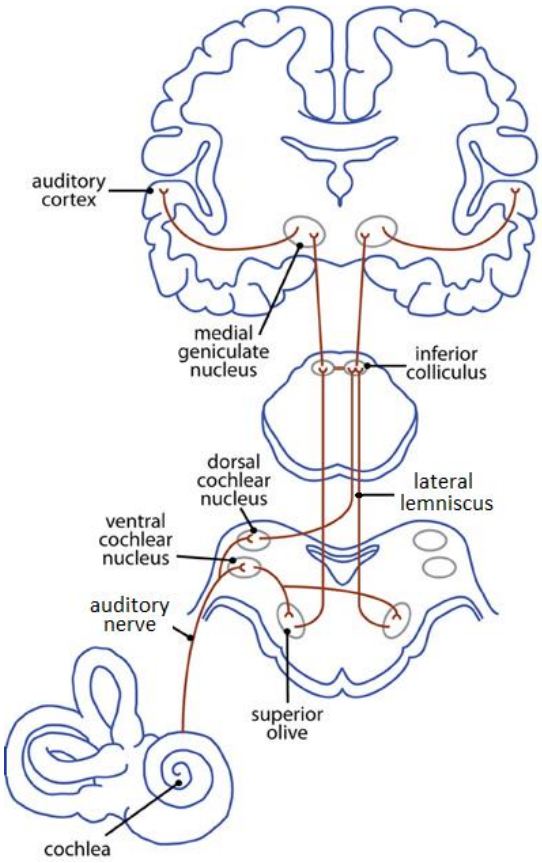

Figure 2. The ascending auditory pathway, from cochlea to cortex. Adapted from Butler and Lomber (2013).

The MGB can be subdivided in three regions: ventral (VMGB), dorsal (DMGB) and medial (MMGB) (Morest, 1965). The ventral division receives auditory signal from the central nucleus of the IC (Bartlett, 2013). This region is tonotopically organized (Wenstrup, 1999). Neurons in the VMGB are involved in the frequency, intensity and latency analysis of the auditory signal (Aitkin and Webster, 1972). The DMGB receives auditory signal from the IC and non-auditory information from brainstem and other thalamic inputs. The DMGB is not tonotopically organized (Wenstrup, 1999). Neurons in the dorsal region have a multimodal role: they respond to stimuli from different sensory modalities, and have a role in sensory integration. The MMGB receives both auditory (from the IC) and multisensory non-auditory (from the spinal cord, superior colliculus and spinal cord) inputs (Bartlett, 2013). Neurons within the MMGB seem to be preferentially tuned to certain frequencies, but they often respond to multiple

frequencies (Wenstrup, 1999). It is not clear whether there truly is one, none, or many tonotopic organizations maps present in the MMGB (Rouiller et al., 1989). The fact that sensory stimulation from other modalities modulates the response within the MMGB hinders the research. This region seems to be responsible for detection of the intensity and duration of the sounds. The MGB projects ipsilaterally to auditory cortex via the auditory radiations: white matter fibers that traverse the posterior limb of the internal capsule. Auditory radiations from the VMGB project to primary auditory cortex, while those from DMGB and MMGB project to primary and non-primary auditory cortices (belt and parabelt regions) (Winer and Larue, 1987).

It is important to remember that, in contrast to the visual system, there is significant signal processing at each nucleus in the pathway (e.g. brainstem and thalamus). Nevertheless, in the present work, the focus is set to the neural computations at the cortex.

2.1.2 THE HUMAN AUDITORY CORTEX

The human auditory cortex represents 8% of the surface of the cortex. The auditory cortex is located along the superior temporal gyrus (STG) (Figure 3). There are discrepancies among the various anatomical studies with respect to the number of defined auditory areas, the location and the nomenclature. Overall, these studies indicate that the human auditory cortex is hierarchically organized with a core or primary auditory cortex, surrounded by non-primary belt and parable regions (Hackett, Stepniewska and Kaas, 1998; Morosan et al., 2001).

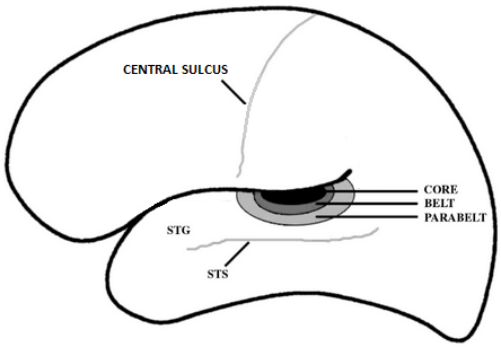

Figure 3. Schematic of the left hemisphere showing different regions within the auditory cortex. Concentric rings represent auditory core, belt and parabelt regions in the STG. Light grey lines represent the central sulcus and the superior temporal sulcus (STS).

The core or the primary auditory cortex is located deep in Sylvian fissure, on the temporal transverse gyrus (Heschl gyrus). The core region is characterized by a well-developed layer IV, reflecting the dense thalamic input from the MGB. It corresponds to the cytoarchitectonical area 41 of Brodmann (1909) and region TC of Von Economo and Horn (1930). The core region is tonotopically organized (Merzenich and Brugge, 1973); neurons responding to lower frequencies are located in the rostral portions of Heschl´s gyrus, and those responding to higher frequencies are located in the more caudal portions of the gyrus.

The core is surrounded postero-laterally by the belt region. This region corresponds to area 42 of Brodmann (1909) and area TB of Von Economo and Horn (1930). The auditory belt receives projections from the adjacent core regions and from the VMGB and MMGB (Kaas, Hackett and Tramo, 1999). Although the belt region shows evidence of tonotopic organization, neurons in this region also respond to spectrally complex sounds, such as bandpass noise (Rauschecker, Tian and Hauser, 1995; Rauschecker and Tian, 2004). Although further study is necessary to determine the functionality of the auditory belt, this region appears to serve as an intermediate processing stage between the core and parabelt regions (Morel and Kaas, 1992).

The auditory parabelt or auditory association cortex is located on the lateral aspect of the posterior STG, adjacent to the auditory belt. The parabelt region corresponds to area 22 of Brodmann (1909) and area TB/TA of Von Economo and Horn (1930). The auditory parabelt receives direct input from the adjacent belt region and from the DMGB and MMGB, but not from the core region. This is consistent with the traditional hierarchical model of cortical auditory processing (Boatman, Lesser and Gordon, 1995; Rauschecker et al., 1995; Kaas et al., 1999; Wessinger et al., 2001; Okada et al., 2010). Auditory association cortex is part of what has traditionally been referred to as Wernicke´s area. Lesions in this area are associated with impaired auditory comprehension (Wernicke, 1969; Luria, 1976) and phonological and lexical-semantic processing (Blumstein, Cooper, Zurif and Caramazza, 1977; Miceli, Caltagirone, Gainotti and Payer-Rigo, 1978; Binder et al., 1994; Woods, Herron, Kang, Cate and Yund, 2011). A network of pathways

connects auditory association cortex to other cortical areas, suggesting that this region is a gateway to higher-level language processing regions.

2.1.3 CORTICAL OSCILLATIONS DURING AUDIO SIGNAL PROCESSING

Before explaining how the brain processes auditory stimuli, we briefly introduce some properties of the auditory signals.

Within the waveform of a natural sound (e.g. speech) it is possible to distinguish between "fine structure" and "envelope" components (Figure 4). The fine structure constitutes the fast pressure variations that determine the spectral content. This fine structure waxes and wanes in amplitude, and the temporal contour of this amplitude modulations (AMs) defines the envelope. The envelope is the intensity-varying waveform that the ear receives, mainly reflecting energy variations over time.

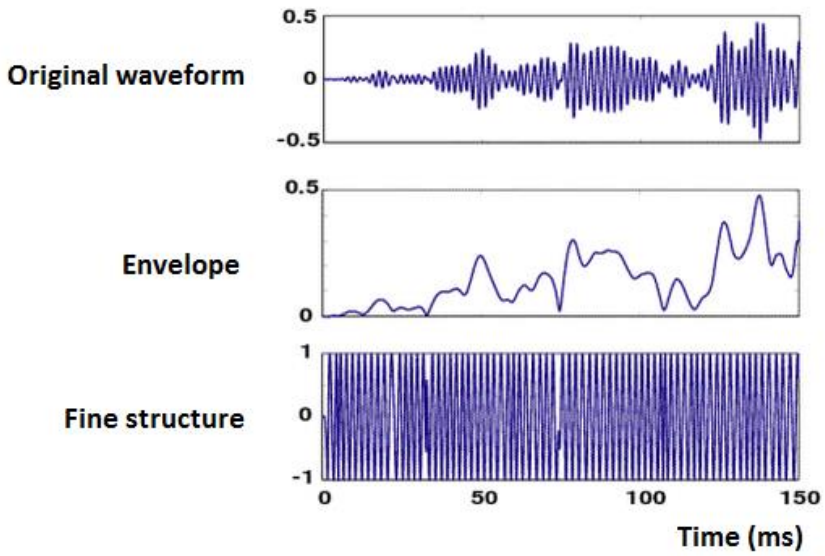

Figure 4. Decomposition of a complex sound in fine structure and envelope

The perception of complex audio signals at multiple temporal scales is essential for the efficient extraction of meaningful phonological elements that facilitate the comprehension of speech sounds.

Neural response to simple amplitude-modulated noise in normal readers

As a first step in understanding the way in which the brain processes complex sounds (e.g. speech), responses have been studied to simpler auditory stimuli which allow selective manipulation of specific features of the acoustic

waveform. One possibility is to sinusoidally modulate the amplitude of a non-linguistic sound (white noise) to generate a stimulus in which temporal features are determined by the frequency of the modulating waveform. Using this kind of non-linguistic audio stimuli, neuroimaging studies have shown that at all levels of the auditory system neurons precisely mimic the time-varying physical properties of the acoustic signal (Figure 5).

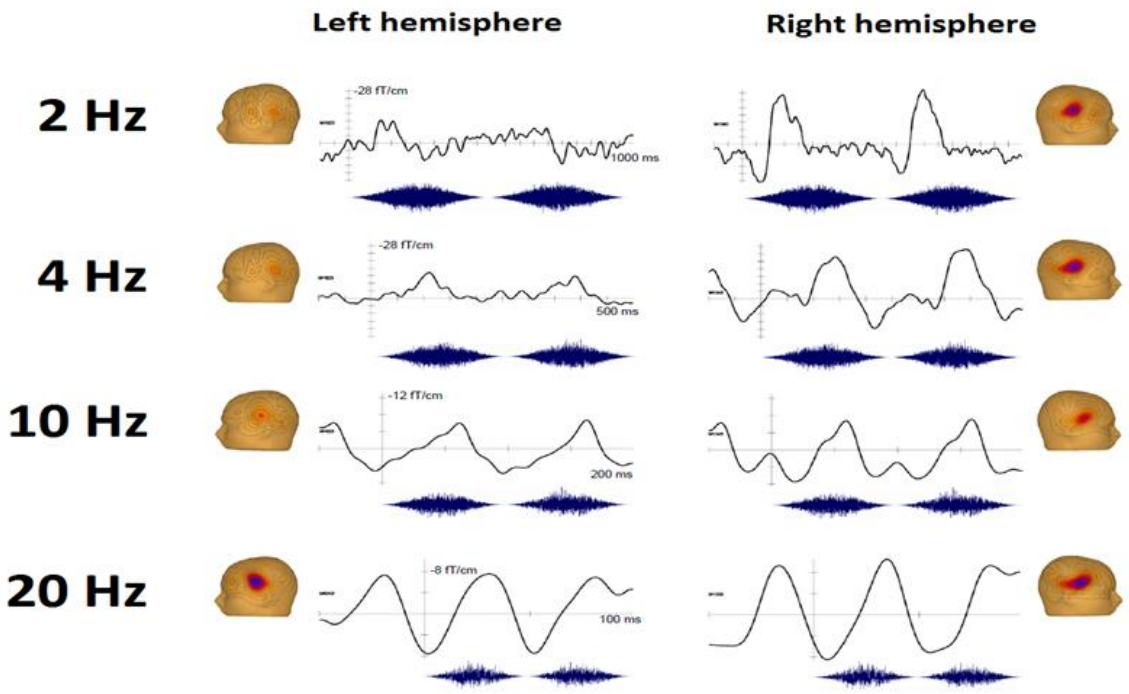

Figure 5. Averaged MEG responses to the 2, 4, 10 and 20 Hz AMs from the left (left hand panel) and right (right hand panel) gradiometers over the temporal area. Below each evoked response is the AM stimulus for reference. Close to each evoked response, the gradient map for the responses to each AM rate (modified from Hämäläinen et al., 2012).

From lower to higher layers of the auditory system there is a noticeable temporal downsampling of the acoustic signal. Neural activity in lower layers (inferior colliculus, superior olive, and cochlear nucleus) track acoustic AM up to 200 Hz. Thalamocortical neural discharges synchronize to acoustic fluctuations up to 100 Hz and in the cortex, neural oscillations time-lock to acoustic AM up to about 40-60 Hz (Bendor and Wang, 2007; Middlebrooks, 2008; Brugge et al., 2009).

Intracranial data on AM coding in humans suggest that there are differences in AM sensitivity across cortical auditory areas and hemispheres. Primary auditory

cortex seems to be more sensitive to high or moderately high frequencies (e.g. beta and gamma bands: 14-32 Hz), whereas neurons in non-primary auditory regions are mainly synchronized to lower frequencies (delta and theta band: 4-8 Hz) (Liégeois-Chauvel, Lorenzi, Trébuchon, Régis and Chauvel, 2004; Lizarazu et al., 2015).

Moreover, the left and right auditory cortices are functionally specialized in analyzing audio modulations at different rates: the right hemisphere preferably processes slow modulations - delta (0-2 Hz) and theta (4-7 Hz) frequency bands - whereas a bilateral processing (also viewed as a left-bias hemispheric specialization) is associated with the processing of fast acoustic fluctuations - gamma (>30 Hz) and beta (15-30 Hz) frequency bands (Poeppel, 2003; Boemio et al., 2005; Vanvooren et al., 2014).

The division of labor between the left and right auditory cortex to sample information in the frequency domain may well be linked to macrostructural pro-left hemispheric asymmetries (Geschwind and Galaburda, 1985; Foundas, Leonard, Gilmore, Fennell and Heilman, 1994). Several studies have shown structural pro-left asymmetries in the size of the planum temporale in approximately 70% of adult and infant post-mortem brains (Geschwind and Levitsky, 1968; Witelson and Pappiel, 1973). Differences in the cytoarchitectonic (microstructural) organization between the right and left auditory cortices could also explain the mentioned functional asymmetries. Specifically, right auditory cortex has relatively larger proportion of long term (delta-theta) integrating neurons, whereas left auditory cortex has higher proportion of short term (beta-gamma) integrating cell groups. Consequently, right hemisphere auditory cortex is better equipped for parsing low frequency AM, and left auditory cortex for parsing high frequency AM.

In summary, these studies suggest that neurons within successive layers of the auditory system can be differentiated by responding to different limited ranges of modulation rates. This neural mechanism allows *de-multiplexing* auditory inputs composed of multiple frequency components, e.g. the speech stream. Frequency division *de-multiplexing* mechanism enables parallel processing of different frequency streams in complex sounds.

Neural response to complex speech signals in normal readers

Across languages, continuous speech is organized into a hierarchy of quasi-rhythmic component with different time scales: prosodic information is present on average every 500 ms (Arvaniti, 2009), stream of syllables occur 4-7 times per second (mean duration 200 ms, core range 100-300 ms) and phonetic information can be found approximately in every 80 ms chunks (core range 60-150 ms) (Ghitza and Greenberg, 2009). Linguistic information at mentioned rates modulates the amplitude of the speech envelope in delta (0.5-4 Hz, indicating prosody), theta (4-7 Hz, syllables) and gamma (30-80 Hz, phonemes) frequency bands (Figure 6A and 6B). Interestingly, these quasi-rhythmic modulations entrain cortical oscillations at different frequency bands (Figure 6C and 6D) (Poeppel, 2003; Ghitza, 2011; Giraud and Poeppel 2012a).

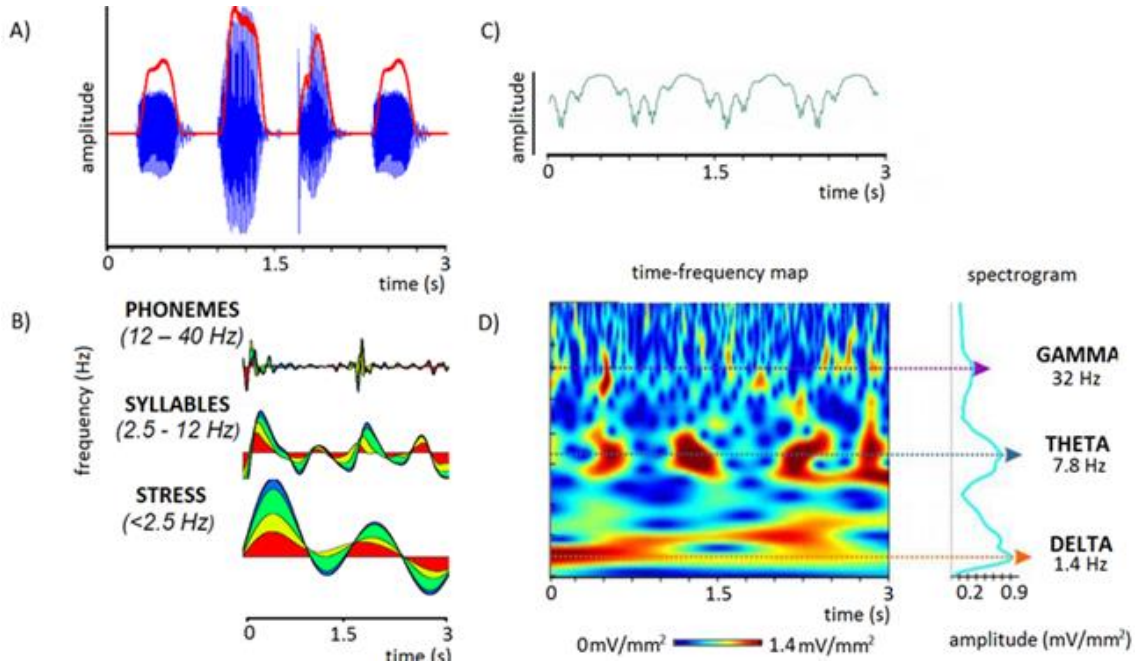

Figure 6. Speech-Brain signals. A) Speech waveform (blue) and speech envelope signal (red). B) The waveforms after bandpass filtering the speech signal in the delta (<2.5 Hz), theta/alpha (2.5 -12 Hz) and beta/gamma (12-40 Hz) frequency bands contain prosodic, syllabic and phonemic information respectively. C) Recorded oscillations (green) from auditory cortex reflect complex combinations of components at different frequencies. D) Time-frequency representation of the neural activity in auditory cortex in response to the same speech signal. The power of the neural activity within the auditory cortex is distributed through the frequency bands that contain essential linguistic information within the speech (delta (1.4 Hz), theta (7.8 Hz) and gamma (32 Hz) frequency band). Adapted from Lakatos et al., 2005.

Neural entrainment during speech processing involves two different neural mechanisms: the *de-multiplexing* step and the *encoding* step.

Neural *de-multiplexing* allows sampling the speech stream at different time scales in parallel. For that, neural groups within different brain regions simultaneously track quasi-rhythmic modulations of speech at different frequency bands. Delta and theta neural oscillations track prosodic and syllabic rhythms respectively (Bourguignon et al., 2013; Doelling, Arnal, Ghitza and Poeppel, 2014) whilst phonemic rhythms regulate gamma-spiking activity (Chan et al., 2014). Theta and gamma synchronization is restricted to auditory regions (Ahissar et al., 2001; Luo and Poeppel, 2007; Cogan and Poeppel, 2011; Morillon, Liégeois-Chauvel, Arnal, Bénar and Giraud, 2012) while delta entrainment extends to frontal and parietal areas (Gross et al., 2013). As in non-linguistic AM audio processing, the left and right auditory cortex play different roles in the temporal analysis of the speech envelope: the right hemisphere is specialized for processing slow AMs (delta and theta frequency bands), whereas a bilateral processing is associated with the processing of fast acoustic fluctuations (beta and gamma frequency bands) (Poeppel, 2003; Boemio et al., 2005; Vanvooren et al., 2014).

Before extracting the meaning of an utterance, speech entrained brain oscillations at different frequency bands (delta, theta and gamma) are hierarchically coupled for mediating the *encoding* of continuous speech in phonemic units. Cross-frequency phase amplitude coupling (PAC) has been proposed as the *encoding* mechanism in which the phase dynamics of lower frequency oscillations temporally organize the amplitude of higher frequency oscillations (Figure 7). Numerous studies have shown theta-gamma PAC during intelligible speech processing (Lakatos et al., 2005). Theta-gamma PAC provides a plausible mechanism through which the phase dynamics of theta oscillations regulate the spiking of gamma neurons involved in phonemic processing (Hyafil et al., 2015). Therefore, phonemic related gamma activity in left temporal regions is segmented into discrete chunks, each of which contains phonemes that make up each syllable. Delta-Theta PAC emerged in fronto parietal region during speech processing (Gross et al., 2013) (Figure 8). Delta-Theta PAC could be the mechanism through which syllabic information is grouped to form word and phrase

structures. Actually, the fronto-parietal network has been largely associated to the maintenance of language units during serial information processing (Berthier and Ralph, 2014), e.g. syllabic units in continuous speech.

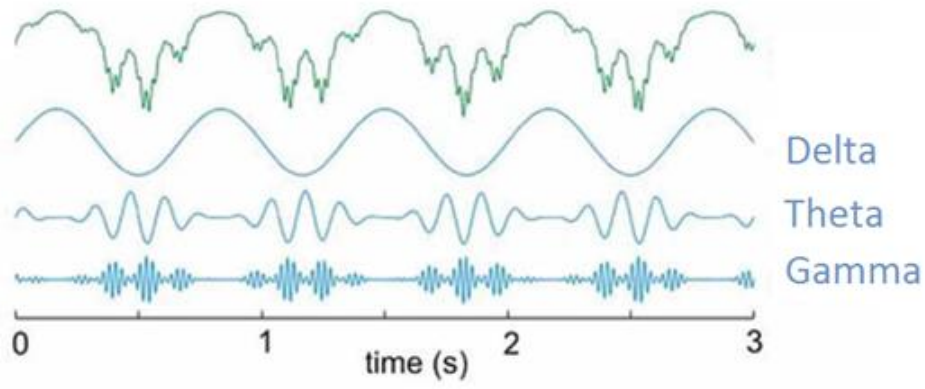

Figure 7. Cross-frequency coupling between delta, theta, and gamma frequency bands. The green oscillation reflects the combination of the different frequency components. . Blue traces independently illustrate delta, theta, and gamma frequency components that summed together make up the combined signal (green signal).

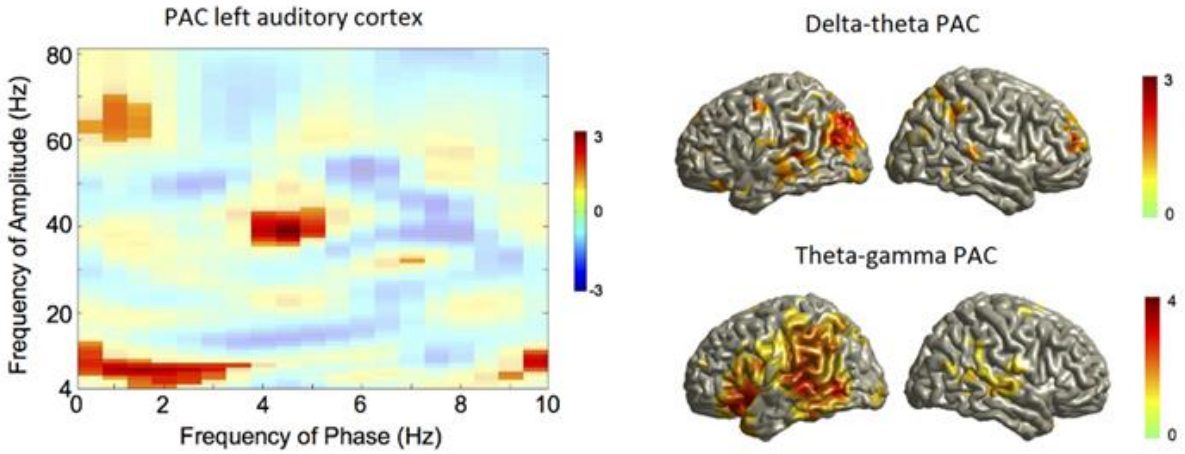

Figure 8. Cross frequency phase-amplitude coupling. Left panel: Spectral distribution of phase-amplitude coupling in the left auditory cortex. Pixels showing significant PAC when processing speech are displayed as opaque. Right panel: Spatial distribution of delta phase to theta amplitude coupling (top-right) and theta phase to gamma amplitude coupling (bottom-right) when processing speech. In both panels, color code represents t-values. Adapted from Gross et al., 2013.

In Study 1, we better characterized the neural mechanisms involved in speech processing. We computed coherence analysis (see section 3.4.2) between the speech envelope and neural oscillations at different frequencies (from 0.5 to 40 Hz with ~0.5 Hz frequency resolution) to evaluate the *de-multiplexing* step. We measured mutual information (see section 3.4.5) between the phase of low

frequency neural oscillations and the amplitude of high frequency oscillations to evaluate the *encoding* step.

Deeper understanding of the neural mechanisms underlying speech perception could shed light on the neurological basis of language learning disabilities, including dyslexia. Among other theories, it has been proposed that the phonological difficulties of dyslexia would reside in the poor sensitivity (or atypical sampling) of speech units dissociable by their temporal distributional properties in speech (Goswami and Leong, 2013).

2.2 DEVELOPMENTAL DYSLEXIA

Dyslexia is the most common reading disability. Around 10 % of the population suffers from dyslexia and it is more common in males than in females. Dyslexia is a neurological learning disability characterized by difficulties in accurate and/or fluent word recognition and by poor spelling and decoding abilities. Despite decades of intensive research, the underlying cognitive and biological causes of dyslexia are still under debated. At present, the more accepted causal viewpoint about dyslexia is the phonological deficit (Ramus et al., 2003). The phonological theory suggests that abnormalities in brain regions associated with language processing underlie dyslexic´s difficulties to properly identify, access and/or retrieve constituent sound of speech. In turn, anomaly of phonological processing results in problems with phoneme-to-grapheme conversion mechanisms required for reading (Ramus, 2003; Ramus et al., 2003; Vellutino et al., 2004). A study of 16 adult dyslexics by Ramus and colleagues (2003) showed that phonological deficits are the primary source of reading difficulties in dyslexia. In this detailed study, all dyslexic readers presented phonological deficits and some of them suffered from additional auditory, visual or motor disorders. Dyslexic readers have difficulties with a wide range of cognitive tasks that engage phonological processes (Vellutino et al., 2004).

Behavioral evidence of the phonological deficit in dyslexia

Phonological difficulties in dyslexia include limitations of short-term verbal memory (Brady, Shankweiler and Mann, 1983), problems with phonological

awareness (Fawcett, Nicolson and Dean, 1996; Swan and Goswami, 1997) and slow phonological lexical retrieval (Bowers and Wolf, 1993).

Short-term verbal memory usually refers to the ability to retain and immediately repeat verbal material of increasing length, e.g. non-words repetition of two to five syllables. Deficits in the storage of phonological information impede, for example, the learning of new phonological combinations and the development of automated reading. Poor short-term verbal memory is a very common cognitive difficulty for dyslexic readers (Brady et al., 1983; Jorm, 1983). Dyslexic readers have no trouble, however, with non-linguistic short-term memory tasks like picture, non-sense figure, or character recall (Katz et al., 1981; Gould and Glencross, 1990). Moreover, problems with *short-term verbal memory* naturally lead to difficulties with *long-term verbal memory*. Therefore, dyslexic readers may present difficulties learning letter names, memorizing the days of the week or the month of the year, mastering multiplication tables, and learning a foreign language (Miles, 2006).

Phonological awareness refers to an understanding of the sound structure of language. That is, that words are made of a combination of smaller units (syllables and phonemes), and to the ability to pay attention to these units and explicitly manipulate them. For example, it has been shown that dyslexic readers present difficulties counting the number of syllables or phonemes in a word, deleting the initial (or final) phoneme, detecting whether words rhyme, or performing simple spoonerisms (swapping the initial phonemes of two words) (Bradley and Bryant, 1978; Joanisse, Manis, Keating and Seidenberg, 2000; Catts, Adlof, Hogan and Weismer, 2005).

Lexical retrieval during rapid naming requires that the participant rapidly converts presented visual symbols to sounds retrieved from memory. *Lexical retrieval* speed can be predicted by performance on a rapid automatized naming task (RAN) (Denckla and Rudel, 1976), which involves the serial naming of letters, digits, objects or colors arranged in a 50 items array. There is a substantial body of evidence demonstrating a significant relation between rapid serial naming tasks and reading performance (Bowers, 1989; Uhry, 2002; Compton, 2003). This apparently simple task is problematic for dyslexic readers that present slower

naming times than normal readers (e.g., Denckla and Rudel, 1976; see Wolf and Bowers, 1999, for a review).

The impairment in various phonological aspects affects the acquisition of the skills necessary to decode new words and impacts on the ability to acquire reading skills (Vellutino et al., 2004 for a review). Difficulties in phonological awareness and the alphabetic principle would compromise the learning of grapheme-phoneme correspondences, i.e. the correspondences between letters and constituent sounds of speech, required for reading acquisition (Bradley and Bryant, 1978; Vellutino, 1979; Snowling, 1981). In support to the phonological deficit hypothesis, studies in preschool and kindergarten children documented a robust relationship between phonological skills development and subsequent reading achievement (Adams, 1994; Lonigan, Burgess and Anthony, 2000; but see Catts, Fey, Zhang and Tomblin, 2001). Moreover, there is evidence that training phonological awareness facilitates learning to read (see Ehri et al., 2001 for a review). Mounting evidence suggests that phonological disorders in dyslexia result from more basic auditory perceptual processing difficulties. This hypothesis is supported by experiments showing, for example, that dyslexic individuals present difficulties in temporal sequencing of auditory information (Tallal, 1980; Tallal and Gaab, 2006) and comprehension of speech in the presence of background noise (Dole, Hoen and Meunier, 2012). Disruptions at some point within the ascending auditory system (Fan et al., 2013) or at the cortical level (Galaburda, 1989), through intrahemispheric (Klingberg et al., 2000; Deutsch et al., 2005; Niogi and McCandliss, 2006), interhemispheric (Robichon et al, 2000b; von Plessen et al., 2002; Fine, Semrud, Keith, Stapleton, and Hynd, 2007; Hasan et al., 2012;) or association connections (see Vandermosten, Boets, Wouters and Ghesquière, 2012 for a review), may explain the inability of dyslexic readers to normally process linguistic input. Overall, it is reasonable to assume that poor auditory perception may affect temporal coding during speech processing and lead to less precise phonological representations in dyslexia.

Neural response to speech in dyslexic readers

As mentioned before, the speech signal contains modulations at multiple temporal rates, which convey information about different linguistic aspect of

speech such as prosodic (delta: 0.5-4 Hz), syllables (theta: 4-7 Hz) and phonemic segments (gamma: 30-80 Hz, phonemes) (Figure 6A and 6B). Speech processing is thought to be achieved by the synchronous neural activity in auditory regions that align their endogenous oscillations at different frequencies with matching temporal information in the acoustic speech signal (Giraud and Poeppel, 2012a). Specifically, for the "asymmetric sampling in time (AST)" theory (Poeppel, 2003), right auditory regions respond better to slow AMs in speech while left auditory regions are more sensitive to many aspects of fast modulated speech content. According to the "temporal sampling" hypothesis proposed by Goswami (2011), atypical synchronization of oscillatory brain signals to the slow amplitude modulations of speech could lead to degraded phonological representations in dyslexia. Brain functional studies showed that brain responses of dyslexic individuals fail to align with the delta and theta AMs in speech associated to prosodic and syllabic information (Goswami, 2011; Leong and Goswami, 2014) (but see Ramus and Szenkovits, 2008 for an alternative view). Reduced sensitivity to slow oscillations during the *de-multiplexing* step could affect further processing steps such as the *encoding*. We already stated that, after the *de-multiplexing* step, speech entrained neural oscillations are hierarchically coupled for mediating *encoding*. During *encoding*, slow oscillations modulate the power of faster oscillations. Atypical neural entrainment to slow rhythms could disrupt the hierarchical coupling between frequency bands and affect phonological *encoding* (Gross et al., 2013). Lehongre et al. (2013) reported an atypical neural entrainment to fast AMs representing phonemic cues in speech signal. Atypical brain synchronization at different rates affects the division of labor between the two hemispheres (Poeppel, 2003) for delta, theta, and gamma oscillations. Indeed, dyslexic individuals do not show the typical right and left hemispheric specialization for slow (delta/theta) (Hämäläinen et al., 2012; Cutini, Szücs, Mead, Huss and Goswami, 2016) and fast AMs (Lehongre et al., 2011).

Overall, these studies suggest that dyslexic readers present neural entrainment difficulties to speech rhythms that could compromise the *de-multiplexing* and the *encoding* speech processing mechanisms. In order to test this hypothesis, in Study 2, we recorded neural oscillations during speech processing in normal and dyslexic readers using magnetoencephalography (MEG). We applied

the coherence (see section 3.4.2) and the mutual information (see section 3.4.5) analysis pipeline of Study 1 to characterize the *de-multiplexing* and the *encoding* mechanism in both groups. At present, Study 2 is the first study that evaluates the impact of the auditory deficits on the speech processing steps in dyslexic readers.

Neural response to amplitude-modulated noise in dyslexic readers

The auditory deficit in dyslexia is not limited to speech sounds (linguistic stimuli) and also affects the processing of non-linguistic stimuli. Numerous studies have shown that auditory regions respond differently to AM white noise in dyslexic readers compared to controls. These stimuli can be presented periodically to entrain neural oscillations at the modulation frequency specifically. Therefore, different neural groups involved in the *de-multiplexing* step can be stimulated independently. The processing of these stimuli is limited to the entrainment step, i.e., it does not involve *de-multiplexing* or *encoding*.

Psychophysical studies reported reduced perceptual sensitivity to slow AM white noise in dyslexic children (Lorenzi et al., 2000; Rocheron et al., 2002). Using MEG, Hämäläinen et al. (2012) reported impaired neural oscillatory entrainment to slow (at 2 Hz) AM white noise in the right hemisphere in dyslexic adults. These abnormalities have been associated to reduce sensitivity to prosodic and syllabic information in dyslexia. Dyslexic adults also present reduced neural sensitivity to faster frequency modulations (Menell et al. 1999; Poelmans et al., 2012). Abnormal entrainment to gamma AMs have been associated to reduce sensitivity to phonemic information in dyslexia. Using EEG, Poelmans and colleagues (2012) demonstrated that dyslexic adults presented deviant response compared to controls in response to speech weighted noise stimuli AM at 20 Hz. In the same vein, Menell et al., (1999) found that the scalp-evoked potentials were smaller in dyslexic adults compared to controls at AM rates of 10, 20, 40, 80 and 160 Hz. Lehongre and colleagues (2011) found reduced sensitivity to 30 Hz AMs in the left auditory regions of dyslexic adults. This deficit correlated with measures of phonological processing and rapid naming. Interestingly, the same study showed enhanced cortical entrainment at rates between 40 and 80 Hz in dyslexic adults in right auditory regions. Abnormal oversampling of the acoustic flow in dyslexia could indirectly affect phonological memory. Interestingly, after eight week of

remediation focused primarily on rapid auditory processing, phonological and linguistic training the children with developmental dyslexia showed significant improvements in language and reading skills, and exhibited activation for rapid relative to slow transitions in left prefrontal cortex (Gaab, Gabrieli, Deutsch, Tallal and Temple, 2007). More recently, Cutini and colleagues (2016) (using NIRS) did not found differences in the neural synchronization to fast AMs (40 Hz) between dyslexic and control children. Both groups presented bilateral response to fast AMs. Nevertheless, gamma neural oscillations are hardly detectable using the NIRS technique due to its low temporal resolution (~100 ms, see Figure 9).

Most of the studies which have looked at neural oscillations in dyslexia did not assess neural responses in the same dyslexic participants across the whole range of relevant frequencies for speech perception (i.e., delta, theta and gamma; Giraud and Poeppel, 2012a). Furthermore, the audio stimuli used to entrain neural oscillations slightly differ across studies.

In order to shed light on these inconsistencies, in Study 3, we measured neural entrainment in the delta (2 Hz), theta (4 Hz and 7 Hz), and gamma (low gamma, 30 Hz, high gamma, 60 Hz) bands in children and adults with and without dyslexia using MEG. We applied the phase locking analysis (see section 3.4.3) to estimate how consistently the phase of oscillatory MEG responses follows the AMs at different rates.

Functional brain changes related to reading experience

A comprehensive understanding of the "oscillatory" bases of developmental dyslexia should take into account how the deficit changes across development and with the amount of reading experience and exposure (Goswami et al., 2014).

In normal readers, phonological awareness skills develop in a predictable pattern similar across languages from larger to smaller sound units (e.g., rime to phoneme). Before learning to read, children are sensitive to the syllabic structure of words whereas phonemic awareness develops with reading acquisition (Liberman, Shankweiler, Fischer and Carter, 1974; Cossu, Shankweiler, Liberman, Katz and Tola, 1988; Harris and Hatano, 1999; Torgesen et al., 1999). The existence of this developmental sequence may be reflected in the neural

mechanisms involved in speech sampling and *encoding*. Low frequency sampling linked to syllabic stress may in fact be trained from birth (e.g., Curtin, 2010; Molnar et al., 2014) until the exposure of alphabetic principles, where an enhancement of neural entrainment to high frequencies should be observed (Minagawa-Kawai et al., 2011). The capacity of the neurons to sample the auditory stream at faster rates is important to obtain more detailed information about the input sounds. During speech listening, for example, the ability of neurons to track high frequency amplitude modulations could help to distinguish phonemes – i.e., the minimal contrasts between sounds.

In dyslexic readers, previous behavioral studies suggest that difficulties in the neural entrainment to slow and fast AMs are present in dyslexia throughout the lifespan (e.g., in children: Serniclaes et al., 2004; Goswami and Leong, 2013; in adults: Pennington et al., 1990; Soroli et al., 2010). However, all these studies focused on one age group (adults or children). Furthermore, the design used to measure neural entrainment and the characteristics of the stimuli presented to the participants differ across studies. Studies that directly compare both age groups with an identical paradigm and technique could provide additional evidence about the evolution of the trajectory of the phonological deficits in dyslexia (e.g., Lallier et al., 2009). Importantly, there is no previous study that analyzed the developmental modulation of typical and atypical auditory sampling in relation to that known to occur regarding phonological perceptual sensitivity (Ziegler and Goswami, 2005). It might be the case that neural entrainment difficulties to slow frequencies linked to prosodic and syllabic processing are similar in adults and children, in line with developmental data suggesting that phonological sensitivity to these speech rhythms is mastered before reading acquisition. Moreover, atypical neural entrainment to high frequencies linked to phonemic rate modulations could be stronger in dyslexic adults than in dyslexic children: Indeed, if phonemic rate processing is refined based on the amount of reading experience, larger gaps between dyslexic and skilled readers could be visible for the adult groups compared to the children groups.

In Study 2, we evaluated whether brain oscillations that synchronized to the rhythms present in continuous speech differ between age and reading groups. In

Study 3, we studied whether the neural entrainment to AM white noise at theoretically relevant frequencies (delta, theta, and gamma) changes between age and reading groups. Interestingly, in both experiments, groups were compared within an identical paradigm thus possibly providing additional evidence about the evolution of the trajectory of the phonological deficits in dyslexia and their neural oscillatory substrates (e.g., Lallier et al., 2009).

Structural brain changes related to reading experience

According to recent findings, the human brain does not reach full maturity until at least the mid-twenties (Giedd, 2004). Brain maturation is characterized by gray matter volume decreases and white matter volume increases from childhood through adulthood (Giedd et al., 1999; Sowell et al., 2003). Interestingly, brain structural changes due to maturation are sensitive to environmental influences, as well as, the acquisition of new skills during development, e.g. reading (Magnotta et al., 1999; Shaw et al., 2008). As a result, changes in myelination and pruning vary considerably across brain regions (Paxinos and Mai, 2004; Kanai and Rees, 2011), even between homologous regions in the left and right hemispheres (Geschwind and Levitsky, 1968). Such changes lead to hemispheric asymmetries in shape and size of brain regions. Several studies have shown macrostructural pro-left asymmetries in the size of the planum temporale in approximately 70% of adult and infant post-mortem brains (Witelson and Pallie, 1973). These asymmetries in the planum temporale contribute to reading abilities in children (Eckert, Lombardino, and Leonard, 2001). The degree of the left asymmetry (left area larger than right) correlates with reading and phonological skills in normal readers (Dalby, Elbro and Stødkilde, 1998).

Importantly, numerous studies have shown anatomical symmetry of the planum temporale in dyslexia, due to an enlarged planum in the right hemisphere in dyslexic individuals (Galaburda, 1985, 1989). Although some of the subsequent work analyzing the size of planum temporale with magnetic resonance imaging (MRI) confirmed Galaburda's findings (Larsen et al., 1990; Altarelli et al., 2014), there are studies that have failed to do so (Schultz et al., 1994; Leonard et al., 2001). Abnormal organization in the microcolumnar structure of the auditory cortex might be underlying the mentioned symmetries in temporal areas.

According to Giraud and Poeppel's model (2012a), two different neuronal populations specialized for sampling either slow or fast speech temporal structures in superficial layers (II/III) of the auditory cortex interact to encode stimulus-driven spiking activity coming from deeper layers (Giraud and Poeppel, 2012a, 2012b). Genetic factors associated with dyslexia could impair the neural migration of such populations of neurons toward other layers ("ectopias," Galaburda and Kemper, 1979) and compromise efficient interactions between the neural populations specialized for low and high frequency sampling (Caviness, Evrard and Lyon, 1978; Galaburda et al., 1985; Giraud and Ramus, 2013).

There are no previous studies that focused on how reading experience modulates brain structural changes in dyslexia. In Study 3, we collected structural MRI data from children and adults with and without dyslexia. We analyzed whether cortical thinning in temporal regions differs between normal and dyslexic readers. Interestingly, the participants included in this analysis also attended the MEG session (listening of AM white noise), which allowed us to investigate, for the first time, the links between the anatomy of the auditory cortex and its oscillatory responses in normal and dyslexic readers.

3 METHODS

In this section we will give an overview of the advanced instrumentation required to measure the magnetoencephalography (MEG) signals. Moreover, we will briefly introduce the principles of the source reconstruction that consists of estimation of the underlying cerebral sources from the measured magnetic fields on the scalp (Hämäläinen, Hari, Ilmoniemi, Knuutila and Lounasmaa, 1993; Hansen, Kringelbach and Salmelin, 2010). Finally, we will explain the mathematical basis of the electromagnetic signal analysis methods applied through the experiments (*i.e.* coherence, phase locking value (PLV), partial direct coherence (PDC), mutual information (MI) and lateralization index (LI)).

3.1 RELEVANCE OF THE MEG

One of the main advantages of electrocorticography (ECoG), electroencephalography (EEG) and MEG over functional magnetic resonance imaging (fMRI), near-infrared spectroscopy (NIRS) and positron emission tomography (PET) techniques is their excellent temporal resolution, of the order of milliseconds (Hämäläinen et al., 1993) (Figure 9). This high temporal resolution enables the investigation of fast variations in cortical activity, reflecting directly the ongoing neurophysiological processes (Hämäläinen et al., 1993).

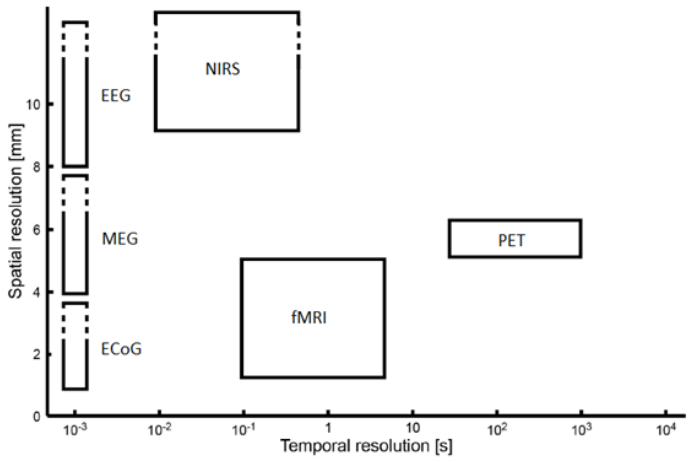

Figure 9. A comparison of different neuroimaging techniques based on temporal resolution and spatial resolution. EEG, electroencephalography,; MEG magnetoencephalography, NIRS, near-infrared spectroscopy; fMRI, functional magnetic resonance imaging; PET, positron emission tomography; ECoG, electrocorticography.

In addition, fMRI or PET measure indirect correlates of neural activity, such as the neurometabolic or neurobascular coupling, whereas ECoG, EEG and MEG techniques directly measure electromagnetic neural activity. Furthermore, EEG and MEG are non-invasive techniques and do not require seizure as in ECoG. In both EEG and MEG neurophysiological techniques the activity closest to the skull is most easily measured and deep source in the brain are roughly detected. EEG is sensitive to both currents flowing perpendicular (i.e. radial currents) and parallel (i.e. tangential currents) to the scalp, while MEG is insensitive to radial currents and mainly "sees" tangential currents, which are parallel to the scalp. Within this constraint, the MEG technique provides greater spatial resolution (few millimeters for focal cortical sources) than the EEG, as the magnetic fields don´t smear across the skull like the electric fields (Hämäläinen et al., 1993). In the present study, for the mentioned advantages, MEG has been considered as the technique of choice for the investigation of cortical activity during auditory processing.

3.2 WHAT DO WE MEASURE?

MEG signals recorded at the scalp are a reflection of the magnetic fields induced by synchronous electrical activity of tens of thousands of neurons. Electrical activity associated with neurons comes from action potentials and postsynaptic potentials (Figure 10).

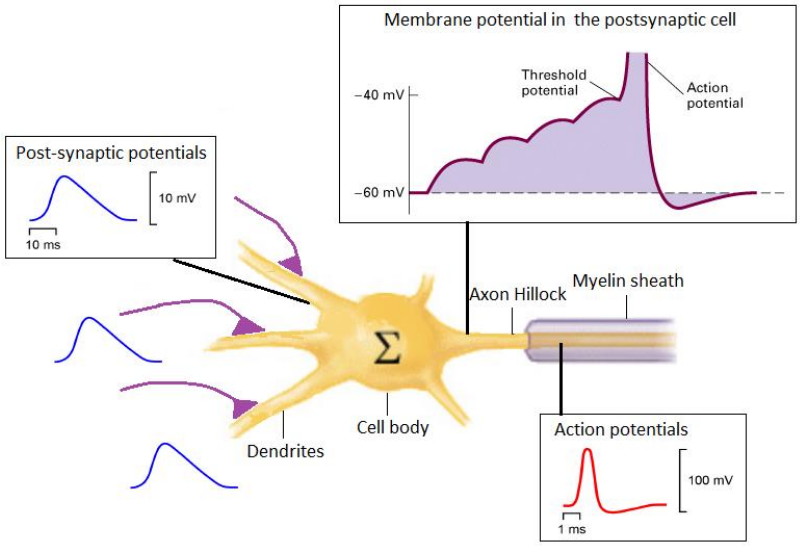

Figure 10. Summation of three excitatory post synaptic potentials to bring the membrane potential to threshold for an action potential.

An action potential is a discrete voltage spike that runs from the beginning to the terminal of the axon where the neurotransmitters are released. A postsynaptic potential is a voltage that occurs when neurotransmitters bind to receptors on the membrane of the postsynaptic cell. At a given moment, a neuron may receive postsynaptic potentials from thousands of other neurons. Whether or not threshold is reached, and an action potential generated, depends upon the spatial (i.e. from multiple neurons) and temporal (from a single neuron) summation of all inputs at that moment. Action potentials in the brain are typically not seen with MEG, because their duration (1 msec) is much shorter than that of postsynaptic potentials, and the patterns of axons currents during an action potential largely cancel out each other (Hämäläinen and Hari, 2002). MEG technique captures postsynaptic potentials of pyramidal neurons of the cerebral cortex that are lined-up along mainly tangential orientation. Temporal and spatial alignment allow postsynaptic potentials to summate (dipoles) rather than cancel each other out, and thus make it possible to record them at the scalp.

3.3 INSTRUMENTATION

Magnetic fields due to the activity of neurons in the brain are about one billion times smaller than the Earth´s static magnetic field. The only sensor that provides sufficient sensitivity to the cerebral magnetic fields is the Superconducting Quantum Interference Device (SQUID). To display its superconducting properties SQUID sensors need to be kept at very low temperature, typically below 20 Kelvin (-253°C). The most commonly employed coolant to achieve these very low temperatures is liquid helium, whose boiling point is 4.2 K or -269°C. Because of magnetic field decay with the source-sensor distance r (as r^{-2} for magnetometers and r^{-3} for gradiometers), sensors are place as close as possible to the head of the participant. Modern MEG systems use multiple SQUID sensors that uniformly cover the surface of a helmet. The helmet is immersed in a dewar full of liquid helium to maintain SQUID sensors in the superconducting state. The Elekta Neuromag system—used in this PhD thesis (Figure 11)—, is equipped with 102 sensor triplets containing one magnetometer and two orthogonal planar gradiometers. Magnetometers are sensitive to magnetic fields along the direction perpendicular to the surface of the pick-up coil. While

being very sensitive to nearby sources, such as neural currents in the brain, a magnetometer is sensitive also to deep sources. Planar gradiometers are insensitive to homogeneous fields (deep sources in the brain) but they give the maximal signal for sources right beneath them. Moreover, to attenuate the external noise, *e.g.* noise generated by electrical devices or moving magnetic objects, the MEG systems are enclosed in a magnetically shielded room.

Figure 11. The MEG system (Elekta-Neuromag, Helsinki, Finland) installed in BCBL.

3.4 MEG MEASUREMENTS

3.4.1 SOURCE RECONSTRUCTION

Before moving to the source space, the data was analyzed first at the sensor level. Significant effects from sensor space were localized within the brain using source reconstruction algorithms. MEG/EEG source reconstruction involves the estimation of the cortical current distribution, which gives rise to the externally measured electromagnetic field. It consists of solving forward and inverse problems. The forward problem is solved by starting from a given brain source configuration and calculating the magnetic fields at the sensors. These evaluations are necessary to solve the inverse problem which is defined as finding brain sources which are responsible for the measured fields at the MEG electrodes.

The forward model

The first step in solving the forward problem is to generate an individual volume conduction model of the patient's head. The most common models are the

spherical head model (Munk and Peters, 1993), which assumes that the brain is sphere-shaped, and the realistic head model that make use of geometric and electrical conductivity properties of the head tissues. The geometry information of the participant is provided by the structural images obtained using MRI. The conductivity values of different tissues are independent of the participants and are based on *in vivo* experiments. The advantage measuring the magnetic fields produced by neural activity is that they are likely to be less distorted by the anisotropic conductivities of tissues compared to the electric fields measured by EEG. There is a wide range of realistic head model approaches including the boundary element method (BEM) (Hämäläinen and Sarvas, 1989; Fuchs et al., 1998), the finite difference method (FDM) (Hallez et al., 2005) and the finite element method (FEM) (Thevenet, Bertrand, Perrin, Dumont and Pernier, 1991). Importantly, the MRI and the MEG techniques localize the head of the participants in different coordinate systems. Thus, before computing the forward model, multimodal information (structural (MRI) and functional (MEG) data) must be accurately aligned in on common spatial frame. The procedure of merging all acquired information into a common reference frame is called image registration and relies on sophisticated mathematical techniques (Modersitzki, 2004).

The leadfield L operator embodies all the mentioned anatomical and biophysical assumptions one need to account for in the forward model. The L links the current density J in the brain at location r_J with orientation θ_J to the magnetic field B measured at sensor location r. To define the location (x, y, z) of each current, it is necessary to segment the volume of the brain (often called the source spaced) in voxels of constant size (e.g. 5 × 5 × 5 mm voxels). The ε models an additive measurement noise at sensor location r, which is usually assumed to follow a Gaussian distribution with zero mean and a parameterized variance structure (Mattout, Phillips, Penny, Rugg and Friston, 2006).

$$B(r) = L(r, r_J, \theta_J)\, J\,(r_J, \theta_J) + \varepsilon(r) \quad . \tag{1}$$

Importantly, the magnetic field varies linearly with current amplitude and magnetic fields produced by several dipoles are simply additives, as consequence of the linearity of Maxell's equations. Therefore, if B is a $N_B \times 1$ vector containing the magnetic field measured in all N_B sensors, is a $N_\varepsilon \times 1$ vector containing the

noise measured in all N_ε sensors and J is a $N_J \times 1$ vector containing the amplitude of all N_J active sources, one can write

$$B = LJ + \varepsilon \quad , \tag{2}$$

where L is a $N_B \times N_J$ leadfield matrix.

The inverse model

One approach is to assume that the measured magnetic signal is generated by a single dipole, *e.g.* equivalent current dipole (ECD), which is characterized by a few parameters. Specifically, the position, orientation and amplitude of the ECD are interactively estimated to best explain the measured MEG signal. The main parameter assessing the certainty of an ECD model is the goodness of fit (g. o. f.), defined as:

$$g.o.f. = 1 - \frac{\|B - \hat{B}\|_2^2}{\|B\|_2^2} \quad , \tag{3}$$

with $\|x\|_2^2 = \sum_{i=1}^{n} x_i^2$ for any vector $x \in \mathbb{R}^n$. The g. o. f. quantifies the agreement between the measured MEG signals B and the $\widehat{B}$ signals that would be produced by this ECD at a given time.

Another approach to solve the inverse problem is to assume that the recorded MEG signal is generated by multiple sources distributed through the source space. One of the challenges for distributed inverse methods is that the number of currents (sources) by far exceeds the number of MEG sensors. Therefore, an infinite number of current distributions can explain the observed MEG signals. The non-uniqueness of the solution is a situation where an inverse problem is said to be ill-posed. Fortunately, this question has been addressed with the physics of ill-posedness and inverse modeling, which formalize the necessity of including additional mathematical and physical constrains in the model to find a unique solution. The assumption of different contextual information leads to a family of inverse solution methods, e.g. minimum norm (MN) and beamforming estimations.

In the case of beamforming approach (Van Veen, Van Drogelen, Yuchtman and Suzuki, 1997), it is assumed that all sources are uncorrelated. For that, a

weight vector $w(r_J)$ to apply to B is estimated through the following minimization problem

$$w(r_J) = \mathrm{argmin}_w\, E(\|wB\|_2^2) \quad \text{constrained to} \quad wL(r_J) = I\,. \tag{4}$$

In this minimization problem, the constraint ensures that the activity coming from the source located in r_J is reconstructed with unit gain, while minimizing the power from other sources. If C denotes the $N_B \times N_B$ covariance matrix of the magnetic field (B) and $L(r_J)$ the $N_B \times N_\theta$ leadfield matrix corresponding to sources at location r_J with N_θ orthogonal source orientations ($N_\theta \in \{1,2,3\}$),

$$w(r_J) = \left[L(r_J)^T C^{-1} L(r_J)\right]^{-1} L(r_J)^T C^{-1}\,. \tag{5}$$

By evaluating the activity in all sources positioned on a grid covering the brain, one can compute a tomographic map of current densities.

Source reconstruction algorithms project sensor space data to source space to localize neural activity within the brain. In this way, spatiotemporal maps of cerebral activity can be produced to visualize the brain regions involved in performing a specific task.

3.4.2 COHERENCE ANALYSIS

Coherence measures the degree of phase synchronization between two signals in the frequency domain. It is an extension of the Pearson correlation analysis, which determines the degree of coupling between two different signals $X = x(t)$ and $Y = y(t)$, providing a number between 0 (no linear dependency) and 1 (perfect linear dependency) for each frequency. If X(f)and Y(f)denote the Fourier transform of the segment of x(t) and y(t), by defining

$$P_{xx}(f) = \frac{1}{N}\sum_{n=1}^{N} X_n(f)X_n^*(f)\,, \tag{6}$$

$$P_{yy}(f) = \frac{1}{N}\sum_{n=1}^{N} Y_n(f)Y_n^*(f)\,, \tag{7}$$

$$P_{xy}(f) = \frac{1}{N}\sum_{n=1}^{N} X_n(f)Y_n^*(f)\,, \tag{8}$$

Where N is the number of averaged epochs, $P_{xy}(f)$ is the cross spectral density (CSD) between x(t) and y(t), and $P_{xx}(f)$ and $P_{yy}(f)$ the auto-spectral density of x(t) and y(t) respectively. Then, the coherence between x(t) and y(t) at frequency fcan be written as

$$C_{xy}(f) = \frac{|P_{xy}(f)|^2}{P_{xx}(f)P_{yy}(f)} \quad . \tag{9}$$

In a typical experimental design, brain related signals (e.g. x(t): MEG signals) are recorded and compared to a reference signal of interest (e.g. y(t): audio signal). In the present thesis (Study 1 and Study 2), coherence analysis was computed to obtain the correlation between the neural activity (e.g. x(t): MEG signals) and the speech envelope (e.g. y(t): audio signal) at different frequencies. In both cases, the coherence analysis is performed first at the sensor level. Then, the sensors and the frequencies (fs) where x(t) and y(t) signals presenting significant synchronization are identified. Finally, coherence at the source level is estimated using the beamforming inverse solution at the frequencies of interest (fs). Applying the beamformer in eq. 5 computed with the CSD matrix $C(f) = E(B(f)B(f)^*)$ instead of the covariance matrix to estimate coherence in the source space is a method known as dynamic imaging of coherence sources (DICS) (Gross et al., 2001). This method yields a coherence map that represents the synchronization degree between the reference signal and the neural activity from each source at a specific frequency.

In the present thesis, we computed coherence analysis and DICS to estimate the synchronization between the neural oscillations and the audio signals at different frequencies.

3.4.3 PHASE LOCKING VALUE ANALYSIS (PLV)

PLV is defined as the circular mean of the phase difference between two signals:

$$PLV(f) = \frac{1}{N}\left|\sum_{n=1}^{N} e^{i(\varphi_x(f)-\varphi_y(f))}\right| \quad , \tag{10}$$

Where $\varphi_x(f)$ and $\varphi_y(f)$ are the instantaneous phase of signal x(t) and y(t) respectively for frequency f. The phase can be estimated based on the Hilbert transform of band-passed signals or from the Fourier coefficient of the signals.

Just like the coherence, the phase locking value measures the phase synchronization but it removes the effects of signals amplitude. Indeed, the squared PLV is exactly equal to the coherence estimated after normalizing the Fourrier coefficients (that is for $X_n(f) \rightarrow X_n(f)/|X_n(f)|$ and $Y_n(f) \rightarrow Y_n(f)/|Y_n(f)|$). Indeed, doing so

$$P_{xx}(f) = P_{yy}(f) = 1 \quad , \tag{11}$$

and

$$Cxy\,(f) = P_{xy}(f) = \left|\frac{1}{N}\sum_{n=1}^{N}\frac{X_n(f)}{|X_n(f)|}\frac{Y_n^*(f)}{|Y_n^*(f)|}\right|^2 = \left|\frac{1}{N}\sum_{n=1}^{N} e^{i\varphi_x(f)}e^{-i\varphi_x(f)}\right|^2 = PLV_{xy}{}^2 \quad . \tag{12}$$

In the present thesis (Study 3), we computed PLV analysis to estimate how consistently the phase of the oscillatory activity in the MEG response follows the AMs at different rates (2, 4, 7, 30 and 60 Hz) across the recording. If the phase is perfectly aligned across trials the value is 1, and if the phase is perfectly random across trials the value is 0.

3.4.4 Partial direct coherence (PDC) analysis

The PDC quantifies the causal relationship between two signals in the frequency domain. PDC is based on the Granger Causality principle (Granger, 1969) and on vector autoregressive (VAR) modeling of the data. The VAR model of order p for a variable $X = x(t)$ is given by:

$$x(t)=\sum_{r=1}^{p} a(r)x(t-r) + \varepsilon(t) \quad , \tag{13}$$

$$\begin{pmatrix} x_1(t) \\ \vdots \\ x_N(t) \end{pmatrix} = \sum_{r=1}^{p} a_r \begin{pmatrix} x_1(k-r) \\ \vdots \\ x_N(k-r) \end{pmatrix} + \begin{pmatrix} \varepsilon_1(t) \\ \vdots \\ \varepsilon_N(t) \end{pmatrix} \quad , \tag{14}$$

where $x(t) = (x_1(t), x_2(t), \ldots, x_M(t))^T$ are the stationary N-dimensional simultaneously measured signals (e.g. number of sensors or brain sources); a(r)

are the N × N coefficient matrices of the model; and $\epsilon(t)$ is a multivariate Gaussian white noise process. The model order p was selected with the Schwartz Information Criterion. This criterion selects the model order that optimizes the goodness of fit of the model, while introducing a penalty depending on the complexity of the model.

In the frequency domain the version of Granger-causality is given by:

$$A(f) = I - \sum_{r=1}^{p} a(r) e^{-i2\pi fr/p} \quad . \tag{15}$$

The first term of the difference refers to the identity matrix (N-dimensional) and the second one to the Fourier transform of the VAR coefficients. Then, the PDC from the signal source j to source i is given by:

$$PDC_{j \to i}(f) = \frac{|A_{ij}(f)|}{\sqrt{\sum_k |A_{kj}(f)|^2}} \quad . \tag{16}$$

The PDC provides a measure of the linear directional coupling strength of x_j on x_i at frequency f. The PDC values vary between zero (no directional coupling) and one (perfect directional coupling). In the present thesis (Study 2), we computed PDC analysis to determine how different brain regions (Region 1: $x_1(t)$, Region 2: $x_2(t)$) interact during speech processing at a specific frequency band (f: delta band).

3.4.5 MUTUAL INFORMATION (MI) ANALYSIS

To understand what MI actually means, we first need to define entropy. The entropy of a discrete random variable X, denoted H(X), is a function which attempts to characterize the "uncertainty" of a random variable. If a random variable X takes on values in a set $X = \{x_1, x_2, \ldots, x_m\}$, and is defined by a probability distribution P(X), then we will write the entropy (Shannon and Weaver, 1949) as:

$$H(X) = -\sum_{x \epsilon X} P(x) \log P(x) \quad , \tag{17}$$

where log is natural logarithm.

Analogously, the joint probability H(X, Y) of two discrete random variables X and Y is defined as:

$$H(X, Y) = -\sum_{x\epsilon X}\sum_{y\epsilon Y} P(x, y) \log P(x, y) \quad , \qquad (18)$$

where $P(x, y)$ denotes the joint probability that X is in the state x_i and Y in state y_j (the number of states $X = \{x_1, x_2, \ldots, x_m\}$ and $Y = \{y_1, y_2, \ldots, y_n\}$ might differ).

Then, the MI(X, Y) between two random variables X and Y is defined as:

$$MI(X, Y) = H(X) + H(Y) - H(X,Y) \quad , \qquad (19)$$

Thus, MI(X;Y) quantifies the reduction in uncertainty about variable X given knowledge of variable Y. High MI indicates a large reduction in uncertainty; low MI indicates a small reduction; and zero MI between two random variables means the variables are independent.

In the present thesis (Study 1 and Study 2), MI was computed to analyze whether speech-entrained brain oscillations were hierarchically coupled across frequencies. More precisely, we examined whether phase of low-frequency oscillations (range 1-10 Hz) modulate the amplitude of higher frequency oscillations (range 4-80 Hz) (i.e., PAC).

3.4.6 Lateralization index (LI) analysis

In all the studies, brain hemispheric dominance for each measurement (coherence, phase-amplitude CFC or entropy) was determined by a measure called the laterality index (LI). The LI is calculated as:

$$LI = \frac{A_R - A_L}{A_R + A_L} \quad , \qquad (20)$$

where A_R and A_L expressed the corresponding measurement in each sensor (sensor level) or voxel (source level) of the right hemisphere and the symmetric voxel of the left hemisphere respectively.

4 STUDIES

We conducted three studies that examined behavioral, functional and structural brain data from children and adults with and without dyslexia:

In Study 1, we analyzed the neural mechanism underlying speech processing, i.e. *de-multiplexing* and *encoding* steps, in normal reader adults (12 female). Using magnetoencephalography (MEG) we recorded brain activity from twenty healthy adults while they were listening to speech (sentences). We performed coherence analysis (see section 3.4.2) between the MEG data and the amplitude of the speech signal to characterize the *de-multiplexing* step. We performed mutual information (MI) analysis (see section 3.4.5) between the phase of low frequency neural oscillations and the amplitude of high frequency neural oscillations to describe the *encoding* step.

In Study 2, we examined the neural mechanism underlying speech processing in children and adults with and without dyslexia. Forty participants took part in Study 2, including 20 skilled readers (10 females) and 20 dyslexic readers (11 females) matched one by one for age. Ten adult readers and 10 children at earlier stages of reading acquisition composed each group. As in experiment one, coherence and MI analysis were computed to characterize the *de-multiplexing* and *encoding* speech processing steps respectively. Furthermore, we computed a connectivity analysis (partial direct coherence (PDC)) to evaluate how different brain regions involved in speech processing interact in both groups.

In Study 3, we obtained a better acknowledge of the frequency bands where dyslexic readers present auditory perceptual deficits. Ten skilled reader children (five females) and 10 dyslexic children (four females) matched in age participated in the study. Eleven skilled reader adults (seven females) and 11 dyslexic reader adults (six females) matched in age. During the MEG recordings, participants listened to non-linguistic auditory signals that were amplitude modulated at different rates (2, 4, 7, 30 and 60 Hz). The modulation frequencies correspond to relevant phonological spectral components of speech. Dyslexics showed atypical brain synchronization also at syllabic (theta band) and phonemic (gamma band) rates. Furthermore, structural magnetic resonance imaging (MRI) was employed to

estimate structural anomalies (cortical thickness (CT)) in auditory cortex in dyslexia. Links between the anatomy of the auditory cortex and its oscillatory responses in normal and dyslexic readers were also studied in this experiment.

Importantly, in Study 2 and 3 we assessed both children and adults on similar tasks. This allowed us to provide an evaluation of the developmental modulation of typical and atypical auditory sampling.

4.1 STUDY 1: NEURAL MECHANISMS UNDERLYING SPEECH PROCESSING

In the present study, we recorded and analyzed MEG data from 20 skilled reader adults while hearing continuous speech. We were interested in characterizing the neural mechanisms underlying speech processing, i.e. *de-multiplexing* and *encoding* steps.

During the *de-multiplexing* process, we expected the prosodic and syllabic information to trigger neural oscillations at the phase of low frequencies (delta and theta) in fronto-temporo-parietal regions.

During the *encoding* process, we expected the entrainment to the phase of low frequencies to modulate the amplitude of faster neural oscillations. This second neural mechanism should be involved in the neural parsing of speech stream into linguistically relevant chunks.

Understanding the oscillatory mechanisms underlying speech processing in skilled readers will allow us to better characterize speech processing disorder in dyslexia (Study 2).

4.1.1 METHODS

4.1.1.1 Subjects

Twenty individuals (12 females) took part in the present study (age range: 8-43 yrs; M = 22; SD = 2.8). All participants were Spanish monolinguals and reported no hearing impairments and were right handed. The present experiment was undertaken with the understanding and written consent of each participant (or the legal tutor of each child below 18 years old). The Basque Center on Cognition Brain and Language (BCBL) ethical committee approved the experiment (following the principles of the Declaration of Helsinki) and all participants signed the informed consent.

4.1.1.2 Functional Data (MEG Recording)

Stimuli and procedure

The stimuli consisted of forty meaningful sentences ranging in duration from 7.42 to 12.65 s (M = 9.9; SD = 1.13). Sentences were uttered by a Spanish

native female speaker and digitized at 44.1 kHz using a digital recorder (Marantz PMD670). Audio files (*.wav) were segmented using the Praat software.

During MEG recording, sentences were presented auditorily to the participants at 75-80 decibel (dB) sound pressure level (SPL). Each trial began with a 1 sec long auditory tone (at 500 Hz tone) followed by a 2 sec-long silence before the sentence presentation. A comprehension question about the content of the last stimulus was presented auditorily 2 sec after the end of each sentence. During the sentence, participants were asked to fixate a white-color sticker on the screen that was switched off. Participants answered the question by pressing the corresponding button (Yes/No). After response, the next trial was presented. Response hands for Yes/No responses were counterbalanced across participants and the presentation order of the sentences was randomized. Participants were asked to avoid head movements and to try to blink only during time periods between sentences. Stimuli were delivered using Presentation software (http://www.neurobs.com/).

Data acquisition

MEG data were acquired in a magnetically shielded room using the whole-scalp MEG system (Elekta-Neuromag, Helsinki, Finland) installed at the BCBL: http://www.bcbl.eu/bcbl-facilitiesresources/meg/). The system is equipped with 102 sensor triplets (each comprising a magnetometer and two orthogonal planar gradiometers) uniformly distributed around the head of the participant. Head position inside the helmet was continuously monitored using four Head Position Indicator (HPI) coils. The location of each coil relative to the anatomical fiducials (nasion, left and right preauricular points) was defined with a 3D digitizer (Fastrak Polhemus, Colchester, VA, USA). This procedure is critical for head movement compensation during the data recording session. Digitalization of the fiducials plus ~100 additional points evenly distributed over the scalp of the participant were used during subsequent data analysis to spatially align the MEG sensor coordinates with T1 magnetic resonance brain images acquired on a 3T MRI scan (Siemens Medical System, Erlangen, Germany). MEG recordings were acquired continuously with a bandpass filter at 0.01-330 Hz and a sampling rate of 1 kHz. Eye-movements were monitored with two pairs of electrodes in a bipolar montage placed on the

external chanti of each eye (horizontal electrooculography (EOG)) and above and below right eye (vertical EOG).

Data pre-processing

To remove external magnetic noise from the MEG recordings, data were preprocessed off-line using the Signal-Space-Separation (SSS) method (Taulu and Kajola, 2005) implemented in Maxfilter 2.1 (Elekta-Neuromag). MEG data were also corrected for head movements, and bad channels were substituted using interpolation algorithms implemented in the software. Subsequent analyses were performed using Matlab R2010 (Mathworks, Natick, MA, USA). Heart beat and EOG artifacts were detected using Independent Component Analysis (ICA) and linearly subtracted from recordings. The ICA decomposition was performed using the Infomax algorithm implemented in Fieldtrip toolbox (Oostenveld, Fries, Maris and Schoffelen, 2011).

MEG measure computation

Coherence analysis

Sensor level coherence. Summary of the computed coherence analysis is described in Figure 12. Coherence between the MEG data (combination of gradiometer pairs) and the envelope (*Env*) of the audio signal was obtained in the 0.5-40 Hz frequency band with ~0.5 Hz (inverse of the epoch duration) frequency resolution (*Speech perception* coherence) (see also section 3.4.2). Signals from gradiometer pairs indexed by $r \in \{1{:}102\}$ ($g_{r,1}$ and $g_{r,2}$) were combined to estimate the signal of virtual gradiometers in the orientation $\theta \in [0;\pi]$:

$$g_{r,\theta}(t) = g_{r,1}(t)\cos\theta + g_{r,2}(t)\sin\theta, \tag{21}$$

Following Halliday et al. (1995) coherence based on the Fourier transform of artifact-free epochs was then computed between *Env* and $g_{r,\theta}$:

$$\mathrm{Coh}(r,f,\theta) = \frac{\left\|\langle \mathrm{Env}(f) g^{*}_{r,\theta}(f)\rangle\right\|^{2}}{\langle |\mathrm{Env}(f)|^{2}\rangle \langle \left|g_{r,\theta}(f)\right|^{2}\rangle} \tag{22}$$

where F = [0.5 - 40 Hz] and ⟨·⟩ the arithmetic mean. Thus, a coherence value for each (i) participant, (ii) MEG sensor (combination of gradiometer pairs) and (iii) frequency bin below 40 Hz was obtained. No effects in fact were expected at frequencies > 40 Hz (Bourguignon et al., 2013; Gross et al., 2013; Park, Ince, Schyns, Thut and Gross, 2015). The coherence spectra were obtained from 0.5 Hz to 40 Hz with a 0.5 Hz frequency resolution separately in each hemisphere for each participant. For each frequency bin, the difference between the maximum over all sensors (within each hemisphere) of *Speech perception* coherence value and the maximum over all sensors (in the respective hemisphere) of *Baseline* coherence value (coherence between the audio signals and resting state MEG signals) was calculated. The statistical significance of *Speech perception* coherence values (vs. *Baseline*) was determined at each frequency bin with a non-parametric permutation test (maximum statistic permutations, m.s.p., Nichols and Holmes, 2002) in both reading groups. The sampling distribution of the maximal difference of coherence values (maximum taken across all sensors) was evaluated using the exhaustive permutation test. Frequencies for which the non-permuted maximal difference exceeded the 95 percentile of this permutation distribution were defined as frequencies of interest, and the corresponding supra-threshold sensors were defined as sensors of interest for this frequency band. Contiguous significant frequencies were grouped in frequency "bands of interest". These frequency bands were selected to compute coherence analysis in the source space. Topographical sensor maps of the coherence were also computed to cross-validate the distribution of the source-level effects observed in the following analyses.

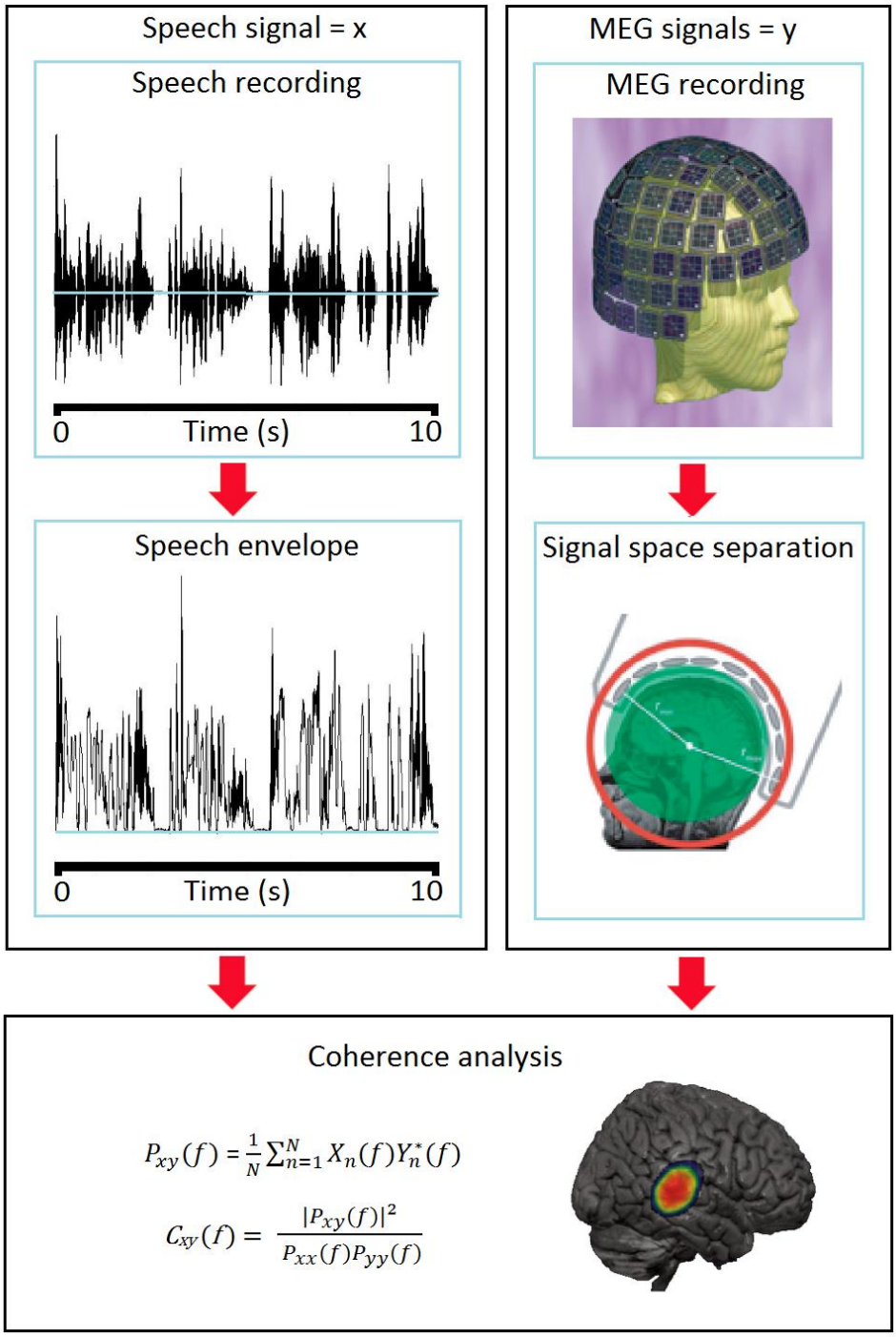

Figure 12. Summary of the computed coherence analysis. Upper Left. The amplitude *Env* of the speech signals was obtained from the Hilbert transformed broadband stimulus waveform. Upper Right. MEG signals are filtered using SSS method to correct for head movements and subtract external interferences. Bottom. Both signals are epoched to compute the individual coherence maps at the sensor l and the source level.

Source level coherence. The forward solution was based on the anatomical image (T1) of each individual participant. MRIs were segmented using Freesurfer software (Dale and Sereno, 1993; Fischl, Sereno and Dale, 1999). The forward model was based on a one-shell boundary element model of the intracranial space. It was computed for three orthogonal directions of sources, which were placed on a 5 mm grid covering the whole brain using MNE suite (Martinos Center for Biomedical Imaging, Massachusetts, USA). For each source (three directions), the forward model was then reduced to its two principal components of highest singular value, which closely correspond to sources tangential to the skull. Dynamic imaging of coherence sources (DICS) method (Gross et al., 2001) (see section 3.4.1) was used to identify brain areas showing relevant *Speech perception* synchronization. For integrating gradiometers and magnetometers in the source estimation, each sensor signal was normalized by its noise variance estimated from the continuous rest MEG data band-passed through 1-195 Hz. The cross-spectral density (CSD) matrix of MEG and the speech envelope signals was then computed for each frequency band of interest. Based on the forward model and the real part of the CSD matrix, brain coherence maps were produced using DICS algorithm (Gross et al., 2001) (see eq. 5).

A non-linear transformation from individual MRIs to the standard Montreal Neurological Institute (MNI) brain was first computed using the spatial-normalization algorithm implemented in Statistical Parametric Mapping (SPM8, Wellcome Department of Cognitive Neurology, London, UK). This was then applied to every individual coherence map.

PAC analysis

Sensor level PAC. Here we analyzed whether speech-entrained brain oscillations were hierarchically coupled across frequencies. More precisely, we examined whether phase of low-frequency oscillations (range 1-10 Hz) modulate the amplitude of higher frequency oscillations (range 4-80 Hz). First, MEG signals within each sensor were band pass filtered in the same frequency bands (fourth order Butterworth filter, forward and reverse, center frequency ±1 Hz (or ±5 Hz for frequencies above 40 Hz). Second, Hilbert transform was applied to the bandpass filtered data to compute phase or amplitude dynamics. Finally, MI (see

section 3.4.5) was calculated for all combination of phase (range 1-10 Hz) and amplitude (range 4-80 Hz) signals using the Information-Theory Toobox (Magri, Whittingstall, Singh, Logothetis and Panzeri, 2009). MI was quantified using the direct method with quadratic extrapolation for bias correction described in the Information-Theory Toolbox (Magri et al., 2009). Phase and amplitude signal dynamics were quantized into ten equi-populated bins to build marginal and joint probability distributions (Gross et al., 2013). This computation was performed for *Speech perception* and *Baseline* conditions. The statistical significance of *Speech perception* PAC values (vs. *Baseline*) was determined for each frequency combination with a non-parametric permutation test (maximum statistic permutations, m.s.p., Nichols and Holmes, 2002).

Source level PAC. Group phase-amplitude CFC effects between conditions were observed at the MEG sensor level between delta (0.5-1.5 Hz)-theta (5-7 Hz) and theta (5-7 Hz)-beta/gamma (20-40 Hz) frequency bands (Figure 15). Thus, further phase-amplitude CFC analyses at the source level for each participant were limited to these frequency bands. First, source time-series of both conditions were band pass filtered in the delta, theta and gamma frequency bands. Second, Hilbert transform was applied to the bandpass filtered signals to extract instantaneous phase or amplitude dynamics. Third, dependencies between delta-theta and theta-beta/gamma phase-amplitude signals respectively were obtained using the MI measurement for each condition. Finally, MI values obtained for both dipoles within each voxel were averaged and, as a result, we get a volumetric MI map for each condition, participant and frequency band combination (delta-theta and theta-beta/gamma bands). MI maps were spatially smoothed and transformed from individual MRIs to the standard MNI-Colin 27. Within the MNI space, we performed a dependent two-sample t-test with unequal variance to identify brain regions showing significant phase-amplitude CFC during *Speech perception* compared to *Baseline.* False discovery rate (FDR) test was applied over the t-score maps generated from the statistical analysis.

4.1.2 RESULTS

4.1.2.1 Functional Results

Coherence analysis

Sensor level coherence. We first analyzed the coherence spectra (0.5 to 40 Hz frequency band) in each MEG sensor for all the participants. Two bands of interest were identified in which coherence values were significantly higher for *Speech perception* than *Baseline* (i.e., the coherence computed for each participant between the speech signal and the MEG signal measured during resting state conditions). The first frequency band fell within the delta (0.5-1 Hz) band (sensor-level distribution in Figure 13, lower panels) and the second band within the theta (5.8-6.3 Hz) band (sensor-level distribution in Figure 13, lower panels). In both coherence peaks the effect was larger for the right lateralized sensors than the left lateralized sensors.

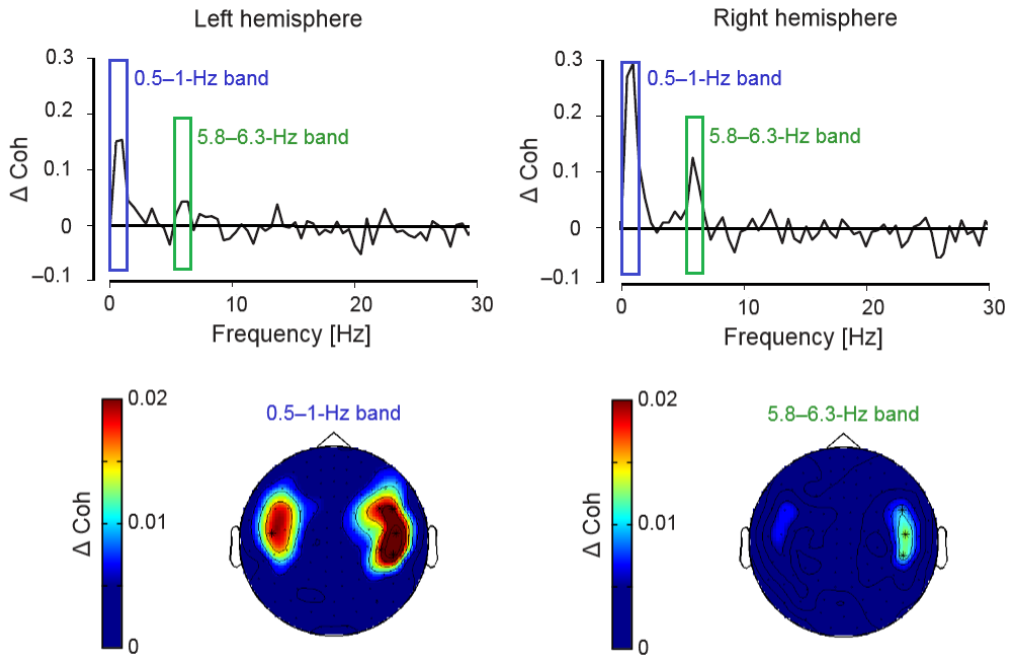

Figure 13. Sensor level analysis of coherence. Upper panel: Coherence spectra calculated from the difference between the *Speech perception* coherence (speech-brain coherence while listening) and the *Baseline* conditions (speech-brain coherence in resting state conditions) across all frequencies in the 0-30 Hz frequency range respectively in the left and the right lateralized sensors. After the permutation test, the frequency bands showing significantly larger *Speech perception* coherence compared to *Baseline* (p<0.05) are highlighted (delta (0.5-1 Hz) and theta (5.8-6.3 Hz)). Lower panel: Sensor-level maps of differential coherence (Speech perception vs. *Baseline*) for Controls and Dyslexic readers in the two frequency bands of interest. Sensors showing significant difference in coherence are represented with asterisks.

Source level coherence. The two frequency bands of interest (delta (0.5-1 Hz) and theta (5.8-6.3 Hz)) identified by the sensor-level analyses were further investigated with source reconstruction to highlight the brain regions that show increased coherence for *Speech perception* compared to *Baseline* for typical readers.

In the delta band, typical readers revealed a bilateral brain network with a rightward asymmetry as already seen in the sensor-level analyses (Figure 14). The set of brain regions whose oscillations synchronized with the speech in the delta band (p_{FDR}<0.05) were the right and the left auditory cortex, the right superior and middle temporal regions, the left superior temporal gyrus (STG) and the left inferior frontal regions.

In the theta band, source reconstruction for the same group revealed an effect (p_{FDR}<0.05) in right primary auditory areas, peaking in superior temporal regions (Figure 14). The present findings corroborate the sensor-level analyses presented above (Figure 13). The MNI coordinates of the coherence peaks falling within each region for the delta and theta bands are reported in Table 1.

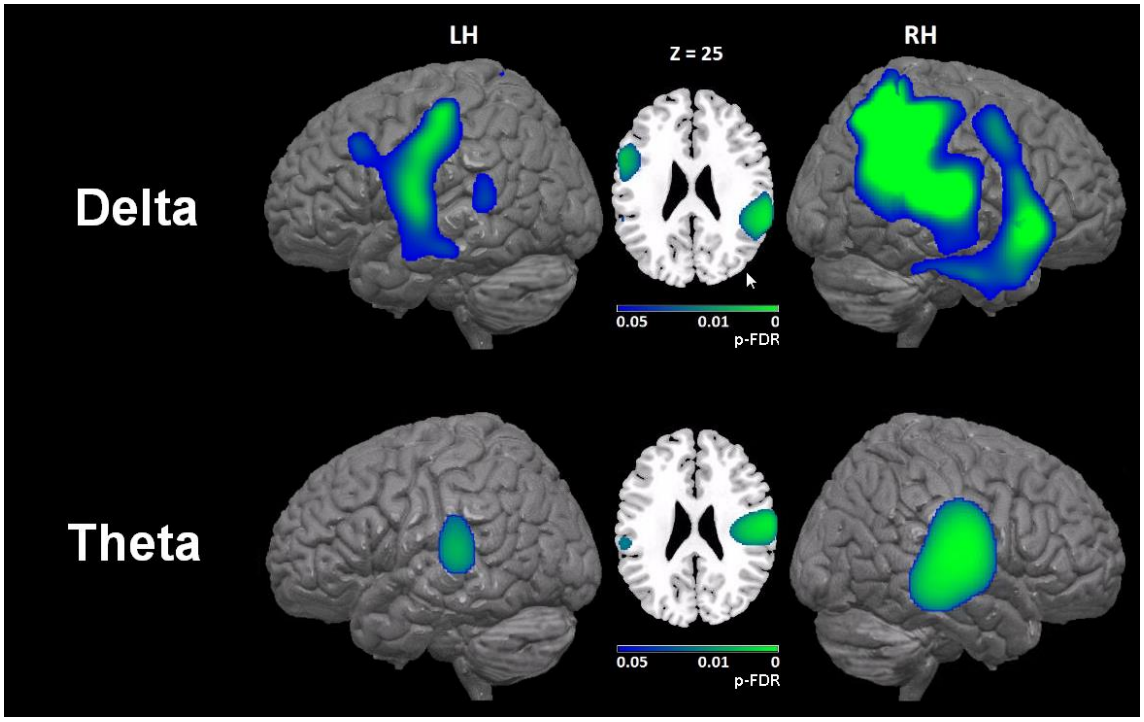

Figure 14. Source level analysis of coherence. Brain map (p-values) showing significantly increased coherence (p FDR<0.05, age corrected) for Speech perception compared to *Baseline* in the delta band and in the theta frequency band.

	Brain region	MNI Coordinates (x, y, z)
Delta coherence:		
	R Auditory Cortex	65 -42 18
	R Temporal	68 -31 -4
	L Inferior Frontal	-57 10 32
	L Auditory Cortex	-59 -42 19
	L Temporal	-58 1 -11
Theta coherence:		
	R Auditory Cortex	62 -14 11
	L Auditory Cortex	-62 -28 10

R,right; L,left

Table 1. MNI coordinates for the peaks of Speech perception coherence in the delta and theta frequency bands within each brain region.

PAC analysis

Sensor level PAC. We evaluated PAC at the sensor level computing MI all combinations of phase (range 0-10 Hz) and amplitude (range 4-80 Hz) for the *Speech perception* and the *Baseline* condition (see section 3.4.5). The statistical significance of *Speech perception* PAC values (vs. *Baseline*) was determined for each frequency combination with a non-parametric permutation test (maximum statistic permutations, m.s.p., Nichols and Holmes, 2001). Bilateral temporal sensors showed a significantly stronger ($p<0.05$) hierarchical PAC between delta (0.5-1.5 Hz)-theta (5-7 Hz) and theta (5-7 Hz)-beta/gamma (20-40 Hz) frequency bands for *Speech perception* condition compared to the *Baseline* (Figure 15).

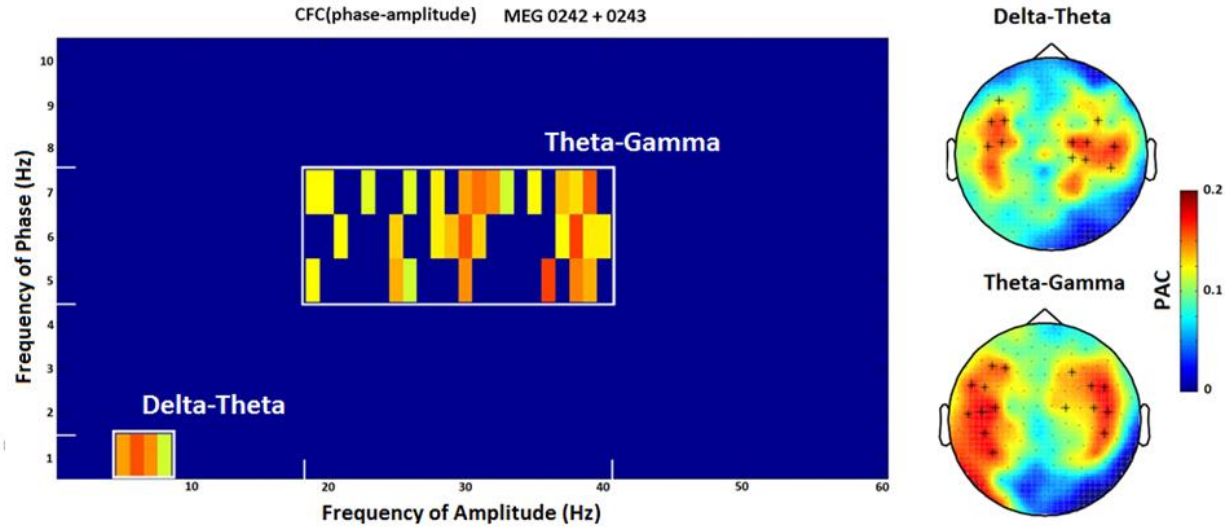

Figure 15. Sensor level analysis of PAC. On the left side, the significant MI values (*p*<0.05 FDR corrected) obtained for all combinations of phase (range 0-10 Hz) and amplitude (range 4-80 Hz) signals. On the right side, the sensor-level maps of the PAC (Speech perception vs. *Baseline*) between delta (0.5-1.5 Hz) - theta (5-7 Hz) and theta (5-7 Hz) - beta/gamma (20-40 Hz) frequency bands. Sensors showing significant difference in PAC are represented with asterisks.

Source level PAC. The source reconstruction analysis revealed a PAC enhancement between delta-theta and theta-beta/gamma frequency bands for *Speech perception* compared to *Baseline* in bilateral fronto-parietal and left temporal regions respectively (Figure 16) (p<0.05 FDR corrected). The MNI coordinates of the PAC peaks falling within each brain region are reported for the delta-theta and theta-beta/gamma bands in Table 2.

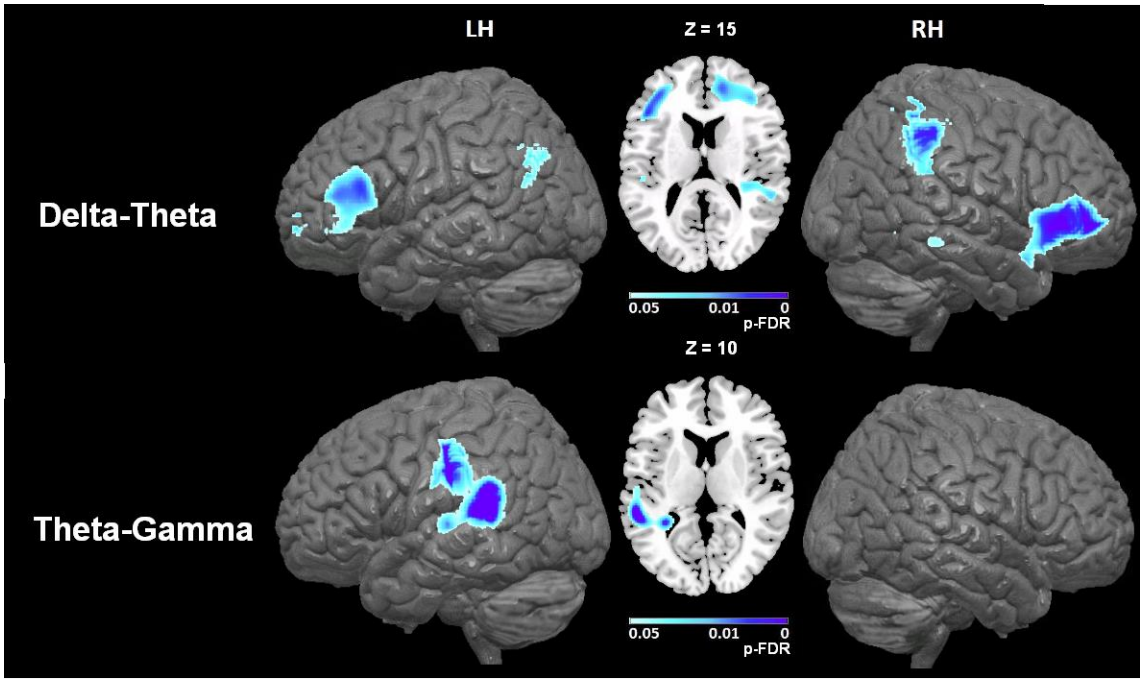

Figure 16. Source level analysis of the PAC. Brain map (p-values) showing significantly increased MI (p FDR<0.05, age corrected) between Delta (0.5-1.5 Hz) - Theta (5-7 Hz) and Theta (5-7 Hz) - Gamma (20-40 Hz) frequency bands for Speech perception compared to *Baseline*.

	Brain region	MNI Coordinates (x, y, z)
dleta-theta PAC:		
	R Supramarginal gyrus	48 -40 36
	R Middle frontal gyrus	42 39 -4
	L Angular gyrus	-35 -56 31
	L Inferior Frontal gyrus	-45 26 17
theta-beta/gamma PAC:		
	L Superior Temporal gyrus	-52 -41 17

R,right; L,left

Table 2. MNI coordinates for the peaks of delta-theta and theta-beta/gamma during Speech perception within each brain region.

4.1.3 DISCUSSION

Our results confirmed that neural oscillations represent an ideal medium through which the brain processes the incoming speech stream before extracting the meaning. We showed that neural oscillations within fronto-temporo-parietal regions deal with *de-multiplexing* (Coherence analysis) and *encoding* (MI analysis) steps.

Neural de-multiplexing mechanism

In the coherence analysis, we observed phase synchronization between low-frequency components of the speech envelope and neural activity in delta and theta frequency bands. Based on our results and previous findings, Figure 17 illustrates what occurs during the *de-multiplexing* step.

Numerous studies have shown that neural oscillations in theta band (4-7 Hz) track syllabic modulations (Greenberg, Carvey, Hitchcock and Chang, 2003; Greenberg, 2006), while slower activity in the delta band (<2 Hz) tracks prosodic modulations in speech envelope (Dauer, 1983). In line with previous MEG studies, no consistent phase synchronization was observed for frequencies higher than 7 Hz (Bourguignon et al., 2013). Previous studies found that speech envelope frequencies below 7 Hz are the most important for speech intelligibility (Elliot and Theunissen, 2009). Nevertheless, neural synchronization to higher frequency modulations in speech has been also reported. Studies using electrocorticography (ECoG) during speech listening found power synchronization also in the gamma frequency band (Morillon et al., 2012). The inconsistencies between the results from both techniques could be explained by the fact that ECoG measures the local neural activity while MEG measures local field potentials generated by a larger population of neurons.

Our results showed that neural synchronization in the theta and delta bands extended to different brain regions. Phase synchronization in the delta band was located in temporal and left frontal areas. These results are consistent with previous findings showing that temporal and frontal regions are perceptually sensitive to prosodic cues in speech (Friederici, 2011; Bourguignon et al., 2013; Gross et al., 2013). Moreover, we found that theta phase synchronization emerged

in bilateral temporal regions. Interestingly, studies have shown that delta and theta synchronization effects are significantly right lateralized in temporal areas (Bourguignon et al., 2013; Gross et al., 2013). Functional asymmetries during speech processing might be related simply to the time frames over which auditory stream is processed in each of the hemisphere. In line with Poeppel (2003), our results indicate that right hemisphere regions preferentially extract information from long integration windows (~150-1000 ms). Differences in the cytoarchitectonic (microstructural) organization between the right and left auditory cortices could explain the frequency dependent sensitivity asymmetries. Right auditory cortex contains smaller pyramidal cells in superficial cortical layers and exhibits smaller microcolumns (Hutsler and Galuske, 2003). Smaller pyramidal cells produce oscillations at slower rates. The smaller the cell the higher the membrane resistance and the slower the depolarization/repolarization cycle of the cell.

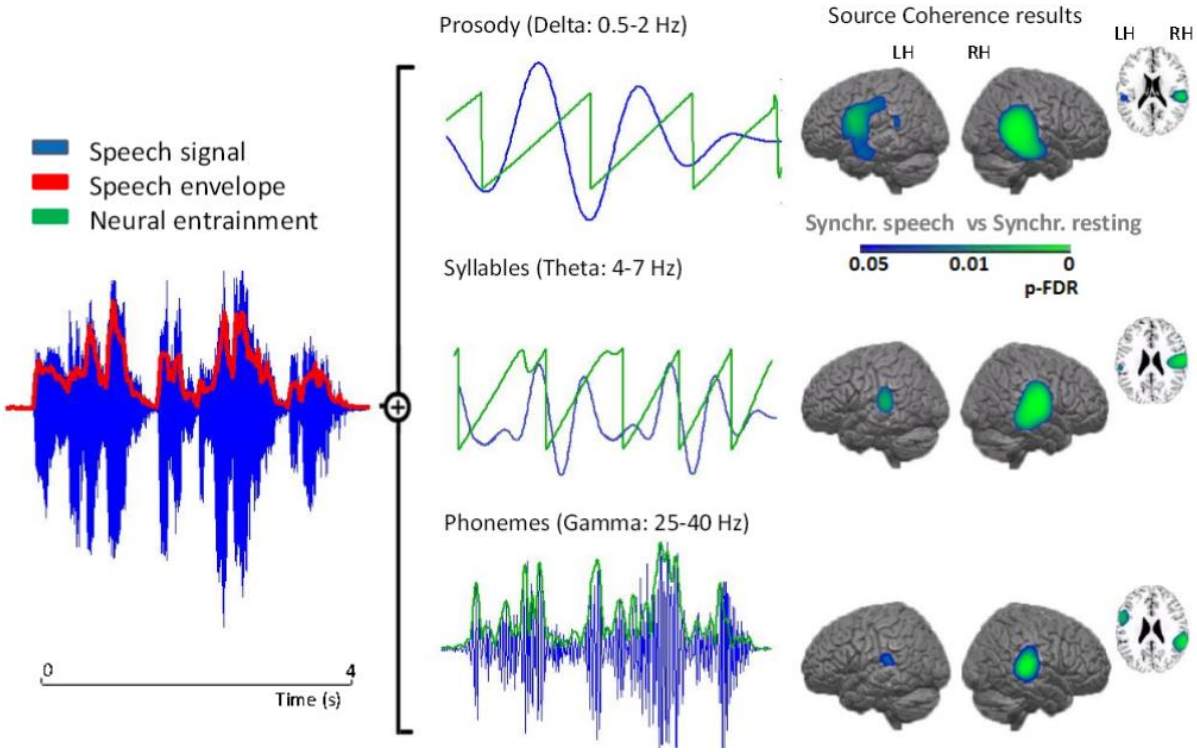

Figure 17. Diagram of the neural *de-multiplexing* mechanism. On the left side, the speech signal (blue) and the envelope of the speech signal are plotted. The speech signal represents a sentence of 4 seconds. On the right side, we showed how the prosodic and the syllabic amplitude modulations of the speech (blue) entrain the phase of delta and theta neural oscillations respectively. In addition, previous studies have shown that the phonemic amplitude modulations of the speech (blue) entrain the amplitude of gamma oscillations (Gross et al., 2013). We observed that

theta and gamma entrainment is limited to temporal regions while delta entrainment extends to frontal regions.

Overall, frequency division *de-multiplexing* mechanism enables the brain to process in parallel different frequency streams that compose complex sounds like speech. The parallel processing allows the activation of stable sensory representation in the presence of distortions of the audio signal and increases the *encoding* capacity of neural responses (Panzeri et al., 2010).

Neural encoding mechanism

Speech entrained brain oscillations at different frequency bands are hierarchically coupled for mediating the *encoding* of continuous speech in phonemic units (Gross et al., 2013; Hyafil et al., 2015). Based on our results and previous studies, Figure 18 summarizes the *encoding* step.

In the MI analysis that we computed we observed PA-CFC (Phase amplitude cross frequency coupling) between delta-theta and theta-gamma frequency bands during speech processing. In both cases, the phase of lower frequency oscillations modulated the amplitude of higher frequency oscillations. Here again, we showed that PA-CFC between delta-theta and theta-gamma covers different brain regions. Theta-gamma PA-CFC was limited to left temporal regions. Previous studies already reported theta-gamma PAC during intelligible speech processing in temporal regions (Lakatos et al., 2005; Gross et al., 2013). Theta-gamma PAC provides a plausible mechanism through which the phase dynamics of theta oscillations regulate the spiking of gamma neurons involved in phonemic processing (Hyafil et al., 2015). This result suggests that phonemic related gamma activity in left temporal regions can be segmented into discrete chunks, each of which contains phonemes that make up each syllable. In our results, delta-theta PA-CFC extended to bilateral fronto-parietal regions, although right hemisphere regions showed higher coupling values. Gross and colleagues (2013) also reported PA-CAP in fronto-parietal regions during continuous speech processing, but the effects where lateralized to the left hemisphere. The fronto-parietal network has been consistently associated with attentional control during speech processing (Hill and Miller, 2010). Attentional control is required to maintain serial order phonological information over time and to deploy attention to desired features

within the speech stream (Berthier and Ralph, 2014). Delta-theta PAC could be the neural mechanism through which phonological syllabic units are maintained for brief periods of time. Delta-theta PAC would allow grouping of syllabic phonological units into words and phrase structures for further processing steps. Bottom-up connections between temporal and fronto-parietal regions could facilitate the transmission of phonological syllabic units segmented by means of theta-gamma coupling.

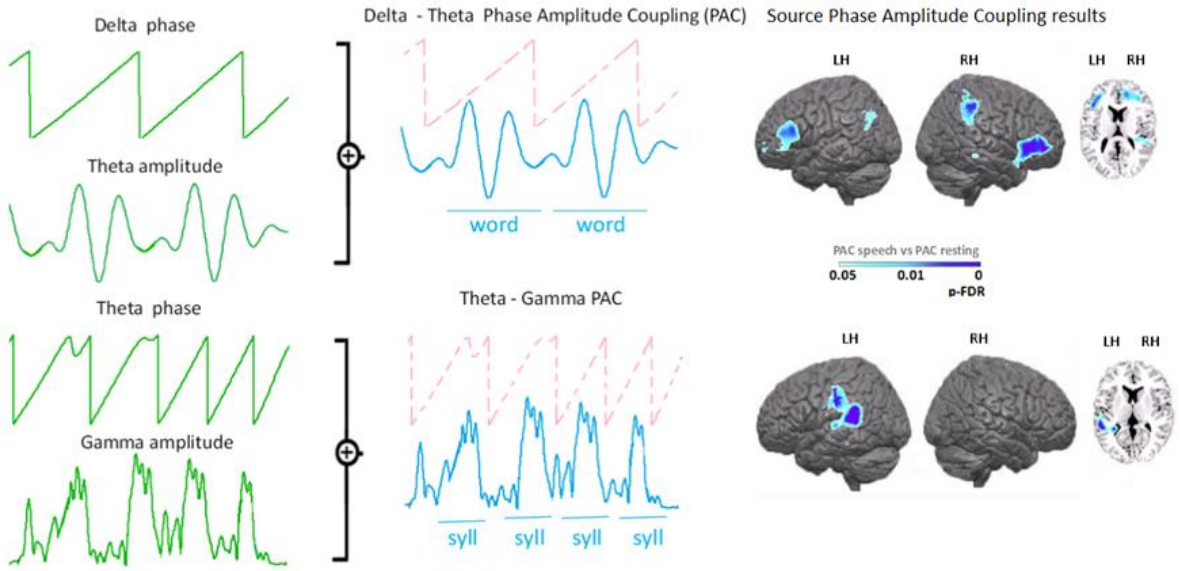

Figure 18. Parsing of the speech stream into different linguistic units. On the left side, we represent the neural entrainment to speech signal in delta, theta and gamma frequency bands (green) (*de-multiplexing* step). On the right side, we represent how the speech entrained neural oscillations are hierarchically coupled. In particular, we show how the phase of delta oscillations modulates the amplitude of theta oscillations in fronto-parietal regions. Delta-theta PAC could be the mechanisms through which syllables are grouped into words. Similarly, the phase of theta oscillations modulates the amplitude of gamma oscillations in left temporal regions. Theta-gamma PAC could be the mechanism through which phonemes are grouped into syllables.

At the same time, bottom-up connectivity from fronto-parietal to temporal regions permits the allocation of attentional resources to informative parts of the speech stream, e.g. speech edges. Gross and colleagues (2013) showed that edges in speech give rise to a phase synchronization enhancement of delta band oscillations in fronto-temporal regions. Edges in speech instantly reset the phase of ongoing delta oscillations, which effectively phase-lock the entire hierarchical structure of oscillatory activity to the stimulus. As a result of this delta phase resetting, theta-gamma PAC enhancement is observed mainly in left auditory

regions during salient speech events (Lakatos et al., 2005; Gross et al., 2013). Recent MEG studies suggest that low frequency (delta-theta) oscillations mediate the top-down connectivity (Park et al. 2015) between these regions. Although these results are very promising, further investigation is required to fully characterize the neural mechanism trough which different regions interact to process speech.

4.2 STUDY 2: OUT-OF-SYNCHRONY SPEECH ENTRAINMENT IN DEVELOPMENTAL DYSLEXIA

In the present study, we investigated the neural oscillatory correlates of temporal auditory processing in developmental dyslexia while listening to continuous speech. In particular, we wanted to determine whether the neural mechanisms involved in speech processing, i.e. *de-multiplexing* and *encoding*, are affected in dyslexia. We recorded MEG signals from 20 dyslexic readers (adults and children) and 20 age matched controls while they were listening to ~10 s long spoken sentences.

We hypothesized that neural entrainment to slow amplitude modulations in speech envelope would be disrupted in dyslexia (Goswami, 2011; Cutini et al., 2016). More precisely, we predicted that dyslexic readers would show atypical neural entrainment in the delta oscillatory band highlighted in Study 1 (0.5-1 Hz) in right auditory regions (Hämäläinen et al., 2012). Furthermore, we suggested that auditory perceptual deficits could affect subsequent processes (e.g attentional computations) involved in speech recognition. We expect that our results could help to clarify the specific frequency band that is impaired in dyslexic readers whilst listening to continuous speech and how these abnormalities could compromise phonological processing.

4.2.1 RESULTS

4.2.1.1 Behavioral results

Although adult participants exhibited an IQ > 100 on the WAIS battery, and all children an IQ > 100 on the WISC-R battery, an ANOVA with group (dyslexic, control) and age group (adults, children) as factors on IQ scores showed a main group effect ($p<0.01$), illustrating that the dyslexic participants exhibited lower IQ than their peers (Table 3). All further group analyses (group by age group) conducted on the whole sample were therefore controlled for IQ. First, the interaction between the two between subject factors considered never reached significance (neither at the behavioral nor at the neural level). Moreover, the dyslexic and the control group differed on all reading measures (for all group effects, $p<0.05$).

Phonological processing

The dyslexic and skilled readers performed similarly on both the phonemic and the semantic fluency tasks (Table 3).

	Dyslexic group				**Control group**			
	Adults(N=10)		Children(N=10)		Adults(N=10)		Children(N=10)	
Age (years)	29.75	(22.2-37.3)	11.08	(9.6-12.5)	32.5	(25.7-39.2)	11.6	(9.25-12.8)
IQ[1]	**115**	**(108.4-121.5)**	**109.8**	**(104.4-115.2)**	**125.4**	**(123.2-127.6)**	**114.8**	**(107.2-122.3)**
WM span	4.1	(3.2-4.9)	3.6	(2.6-4.6)	4.7	(3.7-5.6)	4.3	(3.6-5)
Word reading								
Accuracy (/40)	**38.2**	**(37-39.4)**	**33.2**	**(30-36.4)**	**39.8**	**(39.5-40.1)**	**39.7**	**(39.2-40.2)**
Time (sec)	**37.6**	**(29-46.2)**	**92.8**	**(51.8-133.8)**	**23.9**	**(20.8-27)**	**29.7**	**(24.2-35.2)**
Pseudoword reading								
Accuracy (/40)	**33.7**	**(30.9-36.5)**	**28**	**(24-32)**	**39**	**(38.3-39.7)**	**37.3**	**(36-38.6)**
Time (sec)	**64.6**	**(51.9-77.3)**	**122**	**(69.3-174.7)**	**39.1**	**(34.8-43.4)**	**52**	**(45.5-58.5)**
Phonological tasks								
Phonemic fluency (n. words)	18.6	(15.2-22)	12	(9.8-14.1)	20.4	(17.7-23.1)	13.5	(11.5-15.5)
Semantic fluency (n. words)	22.5	(19.2-25.8)	19.1	(14.9-23.3)	26.2	(22.3-30)	22.6	(18.8-26.3)
RAN (time in sec)								
- Color	25.4	(21.8-29)	51.1	(27.1-75.1)	19.8	(17.1-22.4)	29.3	(23.4-35.2)
- Picture	**32**	**(25.3-38.6)**	**46.1**	**(34-58.2)**	**24**	**(21.4-26.6)**	**28.8**	**(24.9-32.7)**
- Letter	15.3	(14-16.6)	20.6	(14.7-26.5)	11.9	(10.3-13.5)	17.3	(14-20.6)
- Digit	**14.3**	**(13.3-15.3)**	**19.8**	**(15.9-23.6)**	**11.5**	**(10-13.2)**	**13.9**	**(11.9-15.8)**
Pseudoword repetition (%)[2]	**78.6**	**(70.2-87.1)**	**79.4**	**(70.5-88.4)**	**90.6**	**(86-95)**	**84.6**	**(78.8-90.4)**
Phonemic deletion (%)[2]	**80**	**(66-94)**	**65.3**	**(40-90.7)**	**93**	**(85.3-100)**	**91.6**	**(85.2-98)**

p-values (one-tailed) were computed employing a univariate ANOVA controlling for IQ; U-Mann Whitney test in case of violation of sphericity.

[1] WAIS standard score for adults and WISC-R for children.

[2] missing values for three dyslexic participants and one control participant.

Table 3. Behavioral assessment for the Group factor (Dyslexic, Control) separated by Age Group (Adults, Children). Bold values highlight the tasks in which a significant difference between Controls and Dyslexic readers emerged. No interaction between Group and Age Group was observed.

The dyslexic group was slower at performing the RAN tasks on average compared to the controls; this effect was driven by the significantly slower performance for pictures and digits (all $p<0.05$).

On the pseudoword repetition task, dyslexic participants were less accurate overall ($p<0.05$). The qualitative analysis of the errors showed that the most common errors, for both dyslexic and control participants, were phonemic substitution errors. Lastly, on the task measuring phonological awareness (phonemic deletion), a significant group effect was observed on the accuracy measures ($p<0.01$).

Overall, both dyslexic adults and children exhibited phonological processing difficulties that were evident across various phonological constructs: phonological access and retrieval (RAN task), phonological short-term memory (pseudoword repetition), and phonemic awareness (phonemic deletion).

4.2.1.2 Functional results

Sensor level coherence

We first analyzed the coherence spectra (0.5 to 40Hz frequency band) computed separately in the left and the right hemisphere for normal and dyslexic readers (Figure 19, upper panels). In both groups, two bands of interest were identified in which coherence values were significantly higher for Speech perception than Baseline (i.e., the coherence computed for each participant between the speech signal and the MEG signal measured during resting state conditions).

The first frequency band fell within the 0.5-1 Hz range (i.e. the low delta range, sensor-level distribution in Figure 19, lower panels) and the second band within the 5.8-6.3 Hz range (theta, sensor-level distribution in Figure 19, lower panels). In both coherence peaks the effect was larger for the right lateralized sensors (Figure 19, upper panels) than the left lateralized sensors (Figure 19, upper panels). In the delta band, the coherence in those sensors was higher for the controls than the dyslexic readers ($p<0.05$). These analyses were further pursued at the brain-level.

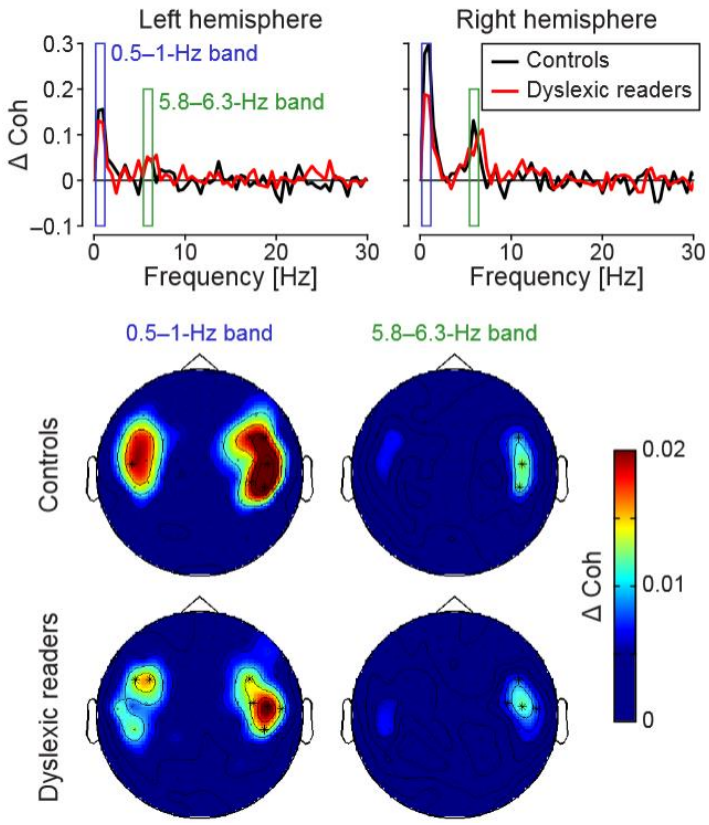

Figure 19. Sensor level analysis of coherence. Upper panel: Coherence spectra calculated from the difference between the *Speech perception* coherence (speech-brain coherence while listening) and the *Baseline* conditions (speech-brain coherence in resting state conditions) across all frequencies in the 0-30 Hz frequency range respectively in the left and the right lateralized sensors for Controls (black line) and Dyslexic readers (red line). After the permutation test, the frequency bands showing significantly larger *Speech perception* coherence compared to *Baseline* (p<0.05) are highlighted (delta (0.5-1 Hz) and theta (5.8-6.3 Hz)). Lower panel: Sensor-level maps of differential coherence (*Speech perception* vs. *Baseline*) for Controls and Dyslexic readers in the two frequency bands of interest. Sensors showing significant difference in coherence are represented with asterisks.

Source level coherence

The two frequency bands of interest (delta (0.5-1 Hz) and theta (5.8-6.3 Hz)) identified by the sensor-level analyses were further investigated with source reconstruction to highlight the brain regions that show increased coherence for Speech perception compared to Baseline for typical readers. In the delta band, typical readers revealed a bilateral brain network with a rightward asymmetry as already seen in the sensor-level analyses (Figure 20). The set of brain regions whose oscillations synchronized with the speech in the delta band (p FDR<0.05) were the right and the left auditory cortex (AC.R, AC.L), the right superior and middle temporal regions (Temp.R), the left temporal (Temp.L) and the left inferior

frontal gyrus (IFG.L). In the theta band, source reconstruction for the same group revealed an effect (p FDR<0.05) in right primary auditory areas, peaking in superior temporal regions (Figure 20). The present findings corroborate the sensor-level analyses presented above (Figure 19).

Group comparison (performed within the sources defined in controls, Figure 20; importantly, similar results were obtained when the mask was defined based on all participants) revealed increased coherence at the source level for the control compared to the dyslexic participants in the lower frequency band (delta, p FDR<0.05, including age of the participants and IQ as covariates, Figure 20 upper panel), while no difference emerged in the theta band. The reduced coherence in the delta range for dyslexic participants involved a subset of the brain regions identified above for the delta band: the AC.R (including a portion of the posterior superior temporal regions) and the pars opercularis of the IFG.L.

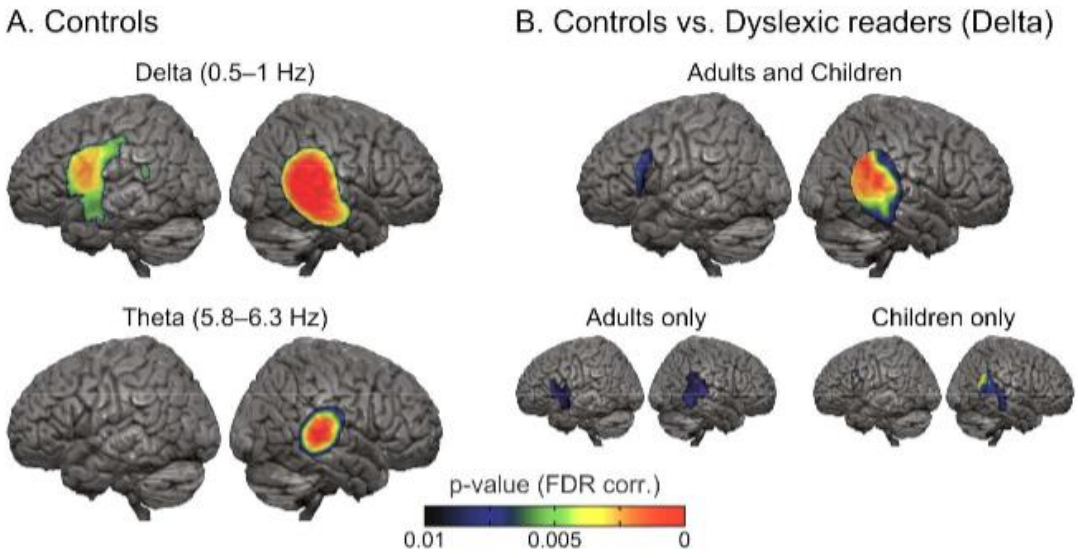

Figure 20. Source level analysis of coherence. Panel A: Brain map (p-values) showing significantly increased coherence (p FDR<0.05, age corrected) for *Speech perception* compared to *Baseline* in the delta (0.5-1 Hz) frequency band and in the theta (5.8-6.3 Hz) frequency band for typical readers. B. Brain map showing significantly increased *Speech perception* coherence (p FDR<0.05, age and IQ corrected) for control participants compared to dyslexic participants in the delta frequency band (upper panel). Below the same analysis is reported, performed separately for Adults and Children.

In addition, to test whether these group differences were modulated by development, we carried out further analyses for the adults and the children. The comparison between controls and dyslexic readers in the adult group showed

reduced coherence in right posterior temporal regions including the AC.R and the pars opercularis of the IFG.L for dyslexic readers (p FDR<0.05, age and IQ corrected, Figure 20). The child groups showed exactly the same trend: reduced coherence for dyslexic readers in right posterior temporal regions including portions of the AC.R and in the posterior portion of the IFG.L largely overlapping with the pars opercularis (p FDR<0.05, age and IQ corrected, Figure 20). Hence, the reduced speech-brain synchronization in dyslexic readers compared to normal readers appears preserved through the development from childhood to adulthood.

Sensor level PAC

Sensor level PAC. We evaluated PAC at the sensor level computing MI between all combinations of phase (range 0-10 Hz) and amplitude (range 4-80 Hz) for the *Speech perception* and the *Baseline* condition (see section 3.4.5). The statistical significance of *Speech perception* PAC values (vs. *Baseline*) was determined for normal and dyslexic readers for each frequency combination with a non-parametric permutation test (maximum statistic permutations, m.s.p., Nichols and Holmes, 2002).

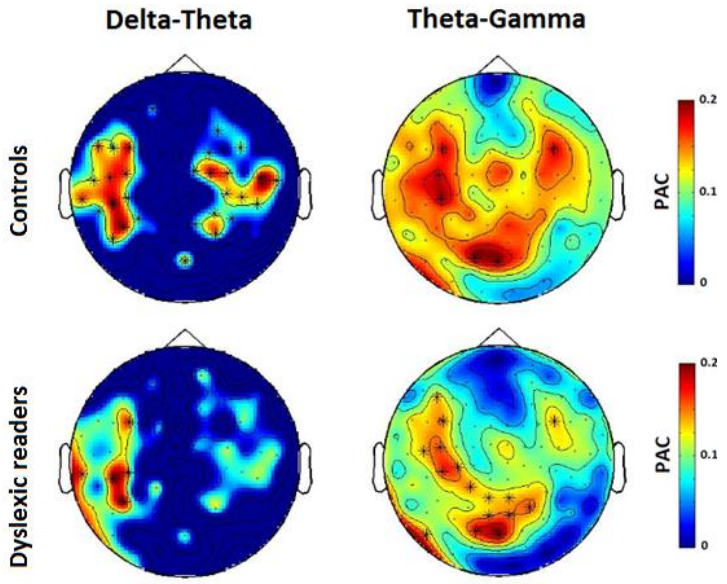

Figure 21. Sensor level analysis of PAC. Sensor-level maps of the PAC (Speech perception vs. *Baseline*) between delta (0.5-1.5 Hz) - theta (5-7 Hz) and theta (5-7 Hz) - beta/gamma (20-40 Hz) frequency bands in normal and dyslexic readers. Sensors showing significant difference in PAC are represented with asterisks.

Bilateral temporal sensors showed a significantly stronger (p<0.05) hierarchical PAC between delta (0.5-1.5 Hz)-theta (5-7 Hz) and theta (5-7 Hz)-

beta/gamma (20-40 Hz) frequency bands for *Speech perception* condition compared to the *Baseline* in both groups (Figure 21). No PAC differences between groups were obtained in delta-theta PAC or in theta-gamma PAC at the sensor level. Thus we did not continue with further analysis at the source space.

Source level PDC

The following analyses focused on the group effect found in the delta band at the source level. The cross-regional causal interactions within the network showing speech-brain coherence in the delta band were first evaluated for dyslexic readers and controls, separately controlling for age (compared to the connectivity pattern extracted from the resting state MEG recordings, p FDR<0.05). Following this analysis, a direct contrast between controls and dyslexic participants was performed.

Thus, we isolated a set of seed regions that synchronize with the delta frequency speech component within theoretically relevant brain regions: the left (IFG.L), bilateral temporal regions (Temp) and the primary AC (in line with Hickok and Poeppel, 2007, Table 4).

Figure 22 depicts the connectivity pattern of the brain regions involved in processing of delta oscillations in speech for the control group. The control group's network presents a larger number of significant connections and stronger coupling between the five seeds than the dyslexic group's network (Figure 22). We characterized the activity of the two nodes that revealed reduced regional coherence, i.e., the AC.R and the IFG.L.

	Brain region	MNI Coordinates (x, y, z)
Delta coherence:		
	R Auditory Cortex (AC.R)	65 -42 18
	R Temporal (Temp.R)	68 -31 -4
	L Inferior Frontal (IFG.L)	-57 10 32
	L Auditory Cortex (AC.L)	-59 -42 19
	L Temporal (Temp.L)	-58 1 -11
Theta coherence:		
	R Auditory Cortex	62 -14 11
	L Auditory Cortex	-62 -28 10

R,right; L,left

Table 4. MNI coordinates for the peaks of *Speech perception* coherence in the delta (0.5-1 Hz) and the theta (5.8-6.3 Hz) frequency bands for each of the Sources of Interest.

In Table 5 we report the connectivity profiles of each node based on two graph theory indices, i.e., Degree and Strength (considered separately for inward and outward connections, Brain Connectivity Toolbox, Rubinov and Sporns, 2010). 'Degree' is the number of connections to the node; 'Strength' is the sum of weights of the connections to the node. The AC.R has no outward connections and four inward connections in dyslexic readers, while the connectivity profile of the AC.R in controls is more balanced (see Degree values). Importantly, there is a pronounced difference between the two groups in the out-Strength profile of the AC.R, which is higher for control (1.79) than dyslexic readers (0). This confirms that the AC.R in dyslexic participants is not properly sending outward information to the rest of the network. The IFG.L has three inward connections and no outward connections in controls, while its connectivity profile in dyslexic readers is restrained to a single inward and outward connection.

The main group difference for the IFG.L resides in the inward strength profile of this region, which is higher for controls (1.91) compared to dyslexic participants (0.33). This suggests that the collection of information from other regions of the network by the IFG.L is operating more efficiently in the control than the dyslexic readers. After unraveling the brain network showing speech-neural entrainment in each group separately, we directly contrasted the causal dynamics between the control and the dyslexic groups.

	Control group				**Dyslexic group**			
	IN-degree	IN-strength	OUT-degree	OUT-strength	IN-degree	IN-strength	OUT-degree	OUT-strength
AC.R	**3**	**2.48**	**2**	**1.79**	**4**	**2.31**	**0**	**0**
Temp.R	*2*	*1.44*	*3*	*2.39*	*0*	*0*	*4*	*2.16*
AC.L	*3*	*2.24*	*3*	*2.02*	*1*	*0.67*	*1*	*0.56*
Temp.L	*1*	*1*	*4*	*2.87*	*1*	*0.57*	*1*	*0.64*
IFG.L	**3**	**1.91**	**0**	**0**	**1**	**0.33**	**1**	**0.52**

Table 5. Functional network dynamics of the five seeds considered in the PDC analyses performed for the 0.5-1 Hz frequency band of interest for control and dyslexic readers. Graph theory parameters (degree and strength) were separately computed for inward and outward connections. In bold values are highlighted the two seeds belonging to the brain regions showing differential regional coherence in delta band.

Statistical comparison between the networks of the two groups (p FDR<0.05, age and IQ corrected, Figure 22) revealed that dyslexic participants had significantly reduced connectivity between the AC.R and the IFG.L compared to controls (red arrow for controls in Figure 22). This connectivity impairment in the dyslexic group was in the feedforward direction from the AC.R to the IFG.L (AC.R→IFG.L). This group differential strength of connectivity was reliable for both adults and children, as represented in the histogram in Figure 22 (p<0.05 for both comparisons, age and IQ corrected).

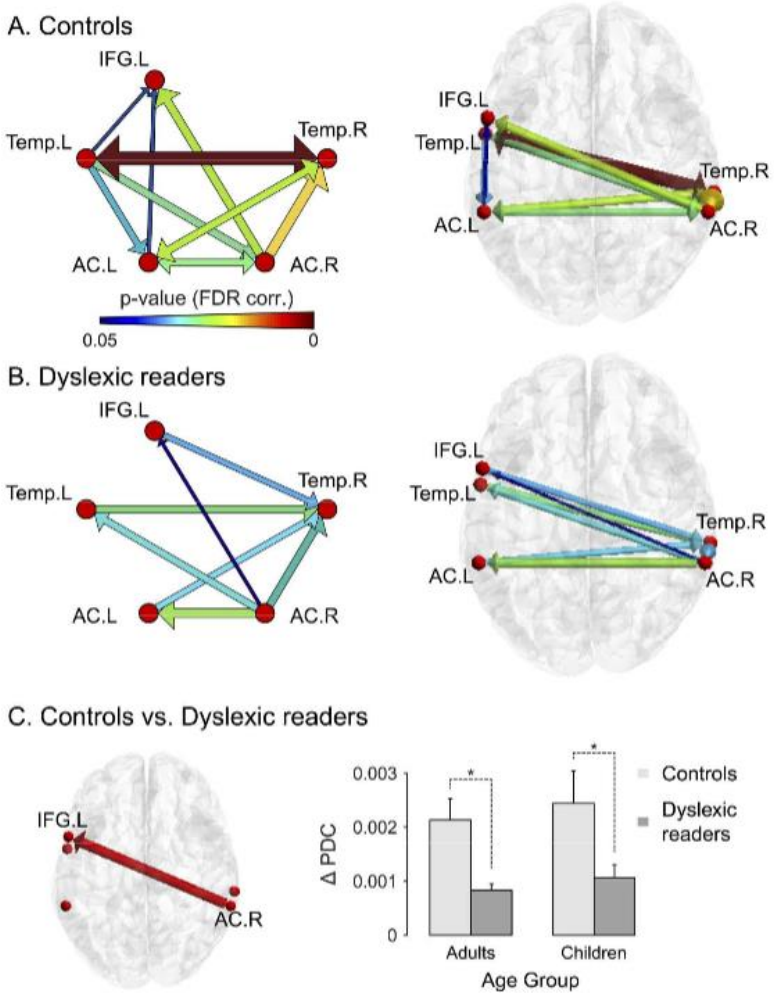

Figure 22. PDC analysis. Network dynamics for control (panel A) and dyslexic participants (B) among the five seeds in the delta (0.5-1 Hz) frequency band (during Speech perception compared to Baseline) plotted on both connectivity graphs and dorsal views of the brain renderings. Arrow orientation represents the causal direction of the observed coupling; arrow color and thickness represent the statistical strength of the connection (p-values). C: Left panel: Differential connection strength between control and dyslexic readers (p FDR<0.05, age and IQ

corrected). Right panel: Strength of RAC→LIFG connection (for dyslexic readers and their control peers) plotted separately for Adults and Children.

4.2.1.3 Correlations between reading, phonology and neural oscillations during Speech Perception

We considered MEG coherence (individual delta coherence values for AC.R and IFG.L) and inter-regional coupling (AC.R→IFG.L connectivity values) effects. We computed robust correlations (Pernet, Wilcox and Rousselet, 2013) between these physiological measures and the performance of each participant in reading and phonological tasks. Robust correlations (skipped Spearman rho) down-weight the role of outlier data, providing a better estimate of the true association with accurate false positive control and without loss of power. Table 6 presents the correlation values involving the measures, revealing significant group differences in reading (z-scores reflecting time values on the word and pseudoword reading lists) and phonological processing (accuracy in the phonological short term memory task, phoneme deletion accuracy and the average time required to perform the rapid automatized naming tasks). We evaluated these correlations independently for each group (control and dyslexic participants) correcting the p-values for multiple comparisons within each group (one-tailed probability FDR corrected). Significant correlations were further tested with partial correlations controlling for both the chronological age (Table 6) and IQ (given the group difference reported in Table 6).

In the control group no significant correlation emerged. In the dyslexic group, word reading time (positive z-scores reflect faster reading times) was significantly related to the regional coherence observed in the IFG.L ($r = 0.43$, $p<0.05$, plotted in Figure 23). Partial correlations confirmed this relation ($r = 0.44$, $p<0.05$). Within the same group, the AC.R→IFG.L connectivity strength positively correlated with accuracy measures in the phoneme deletion task ($r = 0.41$, $p<0.05$, plotted in Figure 23). Partial correlations further confirmed this positive relation ($r = 0.43$, $p<0.05$). To sum up, correlation analyses point to a relationship between (i) IFG.L coherence and reading and between (ii) AC.R→IFG.L coupling and phonological awareness.

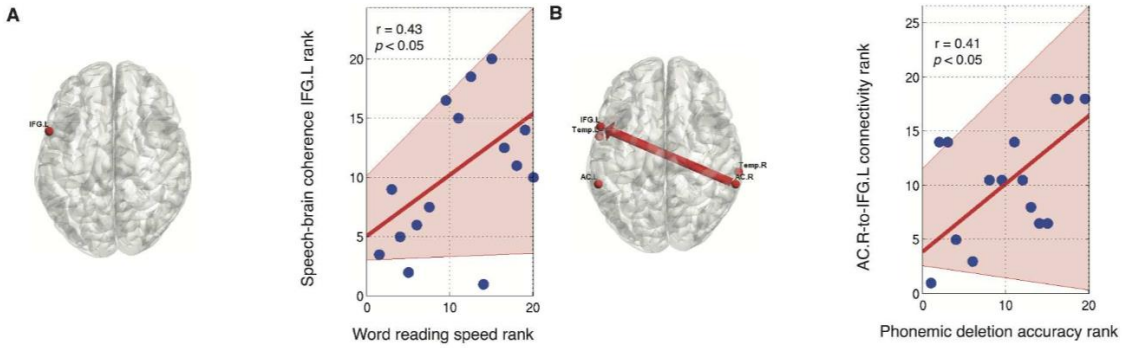

Figure 23. Robust correlations between speech-MEG coupling and behavioral assessments. Panel A: Correlation plot (and regression line) involving LIFG coherence values and z-scores of word reading time for dyslexic readers. B: Correlation plot (and regression line) involving accuracy in the phonemic deletion task and RAC→LIFG connection strength for dyslexic readers.

Control groups	RAC Coh	LIFG Coh	RAC-to-LIFG coupling
Word Reading Time (z-score)	0.14	0.31	0.03
Pseudoword Reading Time (z-score)	0.06	-0.12	-0.22
Pseudoword repetition (%)	0.12	-0.07	0.08
Phonemic deletion (%)	0.35	0.32	0.06
RAN (z-score)	-0.04	0.19	0.04
Dyslexic groups	RAC Coh	LIFG Coh	RAC-to-LIFG coupling
Word Reading Time (z-score)	-0.11	0.43	-0.02
Pseudoword Reading Time (z-score)	-0.23	0.04	0.14
Pseudoword repetition (%)	0.16	-0.22	-0.07
Phonemic deletion (%)	-0.2	0.27	0.41
RAN (z-score)	-0.05	-0.22	-0.17

Table 6. Correlations (Spearman Skipped rho indices) between behavioral (reading and phonological abilities) and physiological measures (local and interregional directed coherence) separately for the dyslexic and control group. Bold values represent statistically significant effects (one tailed, FDR corrected within groups).

4.2.2 METHODS

4.2.2.1 Subjects

Forty participants took part in the present study, including 20 skilled readers (10 males) and 20 dyslexic readers (9 males) matched one by one for age ($t(19) = 0.34$; see Table 4). All participants had Spanish as their native language and were not fluent in any other language. They had normal or corrected-to-normal vision and reported no hearing impairments. Ten adult readers and 10 children at earlier stages of reading acquisition composed each group (Table 4). The age of our children groups was 11.3 years old on average (from 8 to 14, SD = 2). We selected this time range for our group of children based on previous

neurophysiological evidence. Shaw and colleagues (2008) showed that in this time period the superior temporal regions are maturing. In fact, the age at which peak CT is reached (the point where increase gives way to decrease in CT, Magnotta et al. 1999) is 14.9 years old. Similarly, electrophysiological studies have observed that automatic grapheme-to-phoneme mapping is attained by this time period on average in healthy children (Froyen, Bonte, van Atteveldt and Blomert, 2009). The BCBL ethical committee approved the experiment (following the principles of the Declaration of Helsinki) and all participants signed the informed consent.

Our inclusion criteria for selecting dyslexic individuals were 1) self-reported childhood and/or reading difficulties at the time of testing, 2) intelligence quotient (IQ) superior to 80 on the Wechsler Adult Intelligence Scale (WAIS) or Wechsler Intelligence Scale Revised for children battery, 3) below-normal reading performance (-1.5 standard deviation below average) on item reading time and accuracy (pseudowords in particular) and 4) previous formal diagnosis of dyslexia. Exclusion criteria for the selection of the participants were the following: diagnosis of any other learning disability (Speech Language Impairment (SLI), Attention deficit hyperactivity disorder (ADHD), dyspraxia), a long absence from school for personal reasons, vision and/or audition problems history. Reading performance was evaluated with the word and pseudoword reading lists of the PROLEC-R battery (Cuetos, Rodríguez, Ruano and Arribas, 2007). Accuracy and total time to read the list were recorded and *z*-scores were computed. For children, we used the PROLEC battery's normative data that goes up to the age of 15-16 years old. For adults, *z*-scores were computed based on the performance of 46 skilled monolingual Spanish adults matched for age (M = 32.46; SD = 11.57) with the control ($t(54) = 0.72$, $P > 0.05$) and dyslexic ($t(54) = 0.06$, $P > 0.05$) groups of the present study.

All dyslexic participants, except for three, showed a deficit in pseudoword reading accuracy, whereas none of the control participants did. The three dyslexic participants with good pseudoword reading accuracy (accuracy: $z<1$) exhibited a deficit in pseudoword reading time ($z<-2$), and they were also impaired on word reading time ($z<-1.5$), a measure on which all control participants showed preserved performance.

4.2.2.2 Behavioral Data

Phonological processing

Verbal fluency (lexical phonological access).

- Lexical phonological access based on a phonemic cue: Participants were presented with the sound /t/ and had one minute to produce as many words as possible that started with this phoneme. The number of words produced was recorded.
- Lexical phonological access based on a semantic cue: Participants were presented with the semantic category of "animals" and had to produce as many words as possible *belonging to this category in 1 minute. The number of words produced was recorded.*

Rapid Automatized Naming (RAN) (lexical phonological access). We used the four RAN subtests of the Comprehensive Test of Phonological Processing (Wagner, Torgesen and Rashotte, 1999), measuring rapid picture, color, digit, and letter naming. For each of these tasks, six items were used. Each task was divided into two configurations, which were presented on separate sheets. Each configuration presented four rows of 9 items, for a total of 72 items per task. Participants were asked to name aloud each of the items as fast as they could, following the reading direction. The total time to name the 72 items for each of the four tasks was recorded (in seconds).

Pseudoword repetition (phonological short term memory). Participants listened to 24 pseudowords one after the other using headphones and were instructed to repeat them as accurately as possible. Items varied from 2 to 4 syllables (eight of 2, 3, and 4 syllables) and their structure followed Spanish phonotactic rules. They did not include the repetition of any phoneme. The number of correctly repeated pseudowords was recorded and converted into percentages. Phonemic errors were then analyzed, for example, phonemic addition (/ta*Ø*forbegun/ → /tas*f*orbegun/), phonemic substitution (/*t*alsomen/ → /*k*alsomen/), phonemic permutation (/mus*bol*ife/ → /mus*lob*ife/), and phonemic omission (/taforbegu*n*/ → /taforbegu*Ø*/). The total number of phonemic errors was recorded.

Phonemic deletion (phonemic awareness). Participants had to listen to pseudowords using headphones and were instructed to remove the first sound of the pseudoword and produce what remained. Twenty-four items were presented. These were two syllables-long and followed Spanish phonotactic rules. Half of the items started with a consonantal cluster (e.g., /tr/) and the remaining half with a simple consonant-vowel syllable (e.g., /pa/). The number of correct answers was recorded and converted into percentages. Then, errors were classified into the following categories: phoneme deletions errors (e.g., /*pl*adi/ → /adi/) and phonemic errors occurring outside of the deletion site (e.g., /*pl*adi/ → /lati/).

Data analysis for participant inclusion

Analyses of variance (ANOVAs) with group (dyslexic, control) and age group (adults, children) as the between subject factors were conducted on reading and phonological performance for each of the aforementioned task. Non-parametric tests (*U*-Mann Whitney, one-tailed, to assess group differences) were used in case of violation of the assumptions to run parametric tests. In order to examine the links between brain responses and both literacy and phonological skills, we conducted robust correlation analyses (Pernet et al., 2013) between these relevant variables (plus partial correlations controlling for age and IQ), within the dyslexic and control group separately (each n = 20).

4.2.2.3 Functional Data (MEG Recording)

Stimuli and procedure

The stimuli and the MEG procedure were the same as in study I.

Data acquisition

The MEG signals were recorded as in study I.

Data pre-processing

Data were preprocessed off-line using the Signal-Space-Separation method (Taulu and Kajola, 2005) implemented in Maxfilter 2.1 (Elekta-Neuromag) to subtract external magnetic noise from the MEG recordings. The MEG data were also corrected for head movements and bad channels were substituted using interpolation algorithms implemented in the software. The following analyses were performed using Matlab R2010 (Mathworks, Natick, MA, USA). Broadband

amplitude envelope (Env) of the audio signals was obtained from the Hilbert transformed broadband stimulus waveform (Drullman, Festen and Plomp, 1994). The preprocessed auditory stimuli and the corresponding MEG data were segmented into 2.048 ms-long epochs with 1.024 ms epoch overlap (Bortel and Sovka, 2007; Bourguignon et al. 2013). Epochs with EOG, MEG magnetometer and MEG gradiometer peak-to-peak amplitude larger than 200 μV, 4000 fT or 3000 fT/cm respectively were considered as artifact-contaminated and rejected from further analysis. On average, the percentage of epochs considered in further analyses was 73.2% (SD: 16.7%) and 74.1% (SD: 15.9%) for the control and the dyslexic participants respectively. These data were used in the following coherence analyses.

MEG measures computation

Coherence analysis

Sensor level coherence. The same procedure as in the sensor level coherence analysis of the Study 1 was applied for normal and dyslexic readers separately.

Source level coherence. Same procedure as in the source level coherence analysis of the Study 1 was applied for normal and dyslexic readers separately. After defining the coherence maps for each participant at the frequency bands of interest (delta and theta), sources of Interest (SOIs, the source space analogous of sensors of interest) were identified for the group of normal readers. SOIs were defined employing SPM with a FDR corrected $p<0.05$ threshold and both age and IQ of the participants as covariate. SOIs represented brain regions showing significantly higher coherence for the *Speech perception* compared to *Baseline* coherence for control participants. Within those SOIs (selected mask for further analyses), the between-group comparison (controls vs. dyslexic readers, p FDR<0.05) determined the grid points showing significant differential coherence values.

PDC analysis

Source level PDC. Source selection for connectivity analysis was based on the spatial overlap between statistical brain maps of coherence (Speech perception vs. Baseline coherence for control participants) in the frequency band of interest

and theoretically relevant regions identified by speech processing models (Scott and Johnsrude, 2003; Hickok and Poeppel, 2007). For each SOI we determined the source seeds showing maximal Speech perception coherence value averaged over the frequency band of interest. As in the source level analysis, source time-courses from these seeds were obtained with the DICS beamformer (see section 3.4.1). The CSD matrix of MEG data (gradiometers and magnetometers) was calculated for each frequency of the band of interest and the real part of the resulting CSDs were averaged. Finally, a single time-course was obtained for each source (which comprises two orthogonal tangential dipoles) by selecting the orientation of maximal power in the two-dimensional space spanned by the pair of dipoles. Effective connectivity analysis between source signals downsampled to 10 Hz was calculated during periods corresponding to sentence listening using PDC (see section 3.4.4). PDC analysis was performed using the Frequency-Domain Multivariate Analysis toolbox (FDMa, Freiburg Center for Data Analysis and University of Freiburg, Germany) and the model order was computed using algorithms developed in Multivariate Autoregressive Model Fitting (ARfit) software package (Schneider and Neumaier, 2001). In the PDC analysis, the frequency resolution (Δf) depends on the model order and on the sampling frequency (Δf = Fs/p). The model order varied between participants (M(p) = 11.7, SD(p) = 2.5) while the sampling frequency was invariably 10 Hz. Consequently, PDC and coherence were evaluated with a different frequency resolution. To evaluate the PDC in the 0.5-14Hz frequency band, we used the value at the frequency bin closest to the center frequency of this frequency band (M(f) = 0.89 Hz, SD(f) = 0.18 Hz).

The significance of the directional coupling between nodes of the neural networks activated by speech listening in the frequency band of interest - for each experimental group (control and dyslexic readers separately) - was assessed with FDR corrected statistics (age corrected). For each direction, PDC values obtained from Speech perception data were compared with those obtained from the Baseline data (resting state conditions). The same statistical analysis was employed for group comparison (control vs. dyslexic readers, age and IQ corrected). Connections showing significant differential coupling were further contrasted statistically for adults and children.

PAC analysis

Sensor level PAC. The same procedure as in the sensor level PAC analysis of Study 1 was applied for normal and dyslexic readers separately. Here again, significant delta-theta and theta-gamma PAC was observed in both groups. For each PAC map (delta-theta and theta-gamma) and participant, we obtained the maximum PAC value within all sensors. From these values, we computed a two tailed t-test comparing both groups.

4.2.3 DISCUSSION

Reading disorders in dyslexia have been associated with a deficit in *encoding* phonetic and phonological information in speech streams (Ramus and Szenkovits, 2008; Goswami, 2011). The present study provides, for the first time, evidence that both abnormal neural entrainment of the *Speech perception* network to natural speech signals and the consequently impaired connectivity within this network are associated with the phonological disorders in dyslexia. The reduced coherence values we observed for the dyslexic group compared to the control group emerged in a low-frequency speech component (delta, 0.5-1 Hz). This confirms that neural entrainment to the delta band component of the speech signal (speech envelope in the 0.5-4 Hz spectral domain) is relevant for speech recognition (Poeppel, Idsardi and Van Wassenhove, 2008; Ghitza, 2011; Ding, Chatterjee and Simon, 2014). Our results showing reduced auditory entrainment in the delta band for both adults and children with developmental dyslexia align with others reporting impaired processing of low-frequency spectral fluctuations in dyslexic adults (Hämäläinen et al., 2012; Lizarazu et al., 2015) and in children with poor reading skills (Abrams, Nicol, Zecker and Kraus, 2009; Lizarazu et al., 2015).

We also observed an extended brain network sensitive to the speech envelope in typical readers, involving peaks of activity in the auditory cortex (AC.R, Bourguignon et al., 2013) and middle temporal regions (Temp.R) of the right hemisphere. In the left hemisphere, significant coherence values were evident in the auditory cortex (AC.L), anterior temporal regions (Temp.L) and in the pars opercularis of the IFG (IFG.L, see MNI coordinates of peaks of coherence in Table 4). This regional pattern is in line with the speech processing brain network discussed by Giraud and Poeppel (2012a). Interestingly, in this cortical network,

dyslexic participants presented reduced coherence in the AC.R and in the IFG.L compared to typical readers. In the asymmetric sampling models (Poeppel et al., 2008; discussed by Giraud and Poeppel, 2012a), cytoarchitectonic differences between the two auditory cortices would cause entrainment in the AC.R to be mainly dominated by low-frequency oscillations (<10 Hz). Such low-frequency oscillations would serve as a chunking mechanism to properly sample high-frequency (phonemic) information from the auditory signal (Giraud and Poeppel, 2012a; Gross et al., 2013; Park et al., 2015). The successful coupling of low and high frequency speech signals would then provide the input for further language-related processes in higher-order regions (Hickok and Poeppel, 2007; Poeppel et al., 2008). The impaired entrainment to low-frequency in the AC.R in our dyslexic participants is consistent with the hypothesis that identifies the source of their phonological and reading problems in their entrainment to slow speech oscillatory components (Hämäläinen et al., 2012). This would, in turn, impair the binding between these low frequency speech contours and high frequency phonemic information (Goswami, 2011; Gross et al., 2013). The cross-frequency interactions reported by Gross and colleagues (2013: delta-theta and theta-gamma PAC) should not necessarily be affected per se in dyslexia. Atypical delta entrainment in dyslexia could in fact affect higher frequency oscillations just because the delta band is the first level within the hierarchical coupling. Indeed, no cross-frequency PAC differences were observed between normal and dyslexic readers, neither between delta-theta nor between theta and gamma.

The IFG.L also showed reduced coherence at the delta frequency band for the dyslexic group compared to the control group. In contrast to the AC.R, the left frontal region is involved in higher-order computations, such as predictive processing of speech information (Hickok and Poeppel, 2007; Park et al. 2015). Speech entrainment in this region may contribute to reading in dyslexics, as suggested by the significant correlation between the regional IFG.L coherence and the word reading speed in our dyslexic group (however, since it did not correlate with reading skills in normal readers it might not represent a general mechanism).

Accordingly, a large number of studies have reported the left inferior frontal cortex as contributing to phonological disorders in dyslexia (MacSweeney,

Brammer, Waters and Goswami, 2009; Kovelman et al., 2012), and some researchers have advanced the hypothesis that this region could be part of a larger brain network presenting abnormal functionality in dyslexic readers (Vandermosten et al., 2012; Boets et al., 2013). Effective connectivity analyses allow us to disentangle between whether the abnormal IFG.L activity in our dyslexic participants has back-propagated to the input auditory regions and caused the reduced coherence reported in the AC.R (cf. Boets et al., 2013), or, conversely, whether the reduced coherence in the AC.R causes the low coherence in the IFG.L (cf. Goswami, 2011). Our data support the second scenario (reduced AC.R→IFG.L connectivity). This result is in line with the auditory temporal sampling hypothesis (Goswami, 2011). The reduced connectivity found in our dyslexic participants may be caused by the fact that the AC.R does not properly entrain with low-frequency oscillatory components of the speech input. This effect would determine a chain reaction that affects all of the processing steps that followed, i.e., hampering the communication towards the IFG.L, thus impairing the oscillatory activity in the IFG.L itself. This conclusion is supported by studies reporting similar auditory entrainment effects with non-speech steady oscillatory signals (amplitude modulated white noise), showing abnormal phase synchronization for both low (Hämäläinen et al., 2012) and high (Lehongre et al., 2011; Lizarazu et al., 2015) frequency oscillations exclusively in the auditory cortices of dyslexic participants. From the anatomical point of view, this connection would be supported by first, the inter-hemispheric projections through the splenium of the corpus callusum (Vandermosten, Poelmans, Sunaert, Ghesquière and Wouters, 2013) and then, long-distance left-sided temporal-frontal white matter tracts such as the left arcuate fasciculus (Vandermosten et al., 2012; 2013; Saygin et al., 2013). This latter temporal-frontal projection supports the bi-directional communication (both feedforward and top-down) between anterior and posterior language regions. A number of studies have observed reduced white matter volume in dyslexic readers compared to healthy controls (Vandermosten et al., 2012; 2013; Saygin et al., 2013). Vandermosten and colleagues (2012) reported a significant relation between phonological awareness and the integrity of the left arcuate fasciculus. In our study, phonological awareness positively correlated with the strength of AC.R→IFG.L feedforward functional coupling in the dyslexic group.

Thus, it is possible that the integrity of the left arcuate fasciculus (possibly more so than the integrity of inter-hemispheric callosal auditory projections) contributed to the defective feedforward functional connectivity that we observed. It should be noted, however, that previous studies (Boets et al., 2013) did not report any relation between the integrity of the arcuate fasciculus and left frontal-temporal coupling measured with fMRI in dyslexia. It could be argued that the group effect we report is due to reading experience: because dyslexic participants read less, they train less their speech network. One way to address this issue is to compare dyslexic adults with a reading-matched control, i.e., the control children: interestingly, dyslexic adults present similar word reading skills as control children but worse phonological proficiency (as evidenced by pseudoword reading, pseudoword repetition and phonemic deletion, Table 3). Neurophysiological speech processing data go in the same direction, showing stronger AC.R→IFG.L connectivity for the control children than for the dyslexic adults (Figure 22). This suggests that reading experience does not interact with the impairment in the low-frequency acoustic entrainment here observed. Boets and colleagues (2013) also reported impaired functional connectivity within the phonological processing network of dyslexic readers. They observed reduced coupling between the left inferior frontal cortex and both the right auditory cortex and the left STG. They argue for the impaired access hypothesis (Boets, 2014; Ramus, 2014; Ramus and Szenkovits, 2008), since they assume an impaired feedback flow of information from inferior frontal to bilateral primary auditory regions (see Figure 1 in Ramus, 2014). However, because of methodological constraints, their study does not allow them to evaluate the directionality of the impaired (frontal-temporal) connectivity found in their dyslexic group. Conversely, our effective connectivity data involving the AC.R do not support the hypothesis of a deficit in feedback access to phonological representations in the auditory regions of the right hemisphere by the IFG.L (see also Park et al., 2015). Moreover, we did not find evidence for an impaired coupling between the IFG.L and the ipsilateral posterior temporal regions, as reported by Boets and colleagues (2013) in dyslexia. The definition of the delta speech-brain brain network in the present study highlighted a significant effect in the primary auditory regions (AC.L, Figure 20), but no effect in higher order associative auditory regions in the left posterior

temporal cortex (part of the phonological network, Giraud and Poeppel, 2012b; Fontolan, Morillon, Liegeois and Giraud, 2014) as in Boets and colleagues (2013). Crucially, Park and colleagues (2015) recently reported MEG evidence of top-down coupling in the delta band between left frontal regions and the left STG (beyond the AC.L considered in the present study) during continuous speech in a healthy population. These data were taken as evidence of dynamically updated predictions of incoming auditory information based on low-frequency speech information. Interestingly, they reported that slow oscillatory activity in left auditory cortex was also constrained by similar low frequency oscillations in posterior right temporal regions. In addition, no top-down signals constrained low-frequency entrainment in the right auditory cortex (Park et al., 2015). It is possible that in dyslexic readers, the IFG.L does not properly control in a top-down fashion the synchronization with the left superior temporal regions in the delta band. We hypothesize that while the functional frontal-to-temporal coupling (identified by Park et al., 2015) might function properly in dyslexia, the information arriving to the left frontal regions could already be defective. The consequence of such defective input could be the reduced ipsilateral left frontal-to-temporal coupling observed by Boets and colleagues (2013). In brief, for typical readers, low-frequency entrainment in the AC.R (driven by prosodic speech contours) would provide chunking cues that parse the speech signal and then facilitate efficient sampling of high frequency oscillatory speech information by the IFG.L. This would constrain the cross-frequency coupling (hierarchically involving delta-theta and theta-gamma oscillations as observed in Gross et al., 2013) of low and high frequency speech information obtained through the interaction between left frontal and posterior superior temporal regions. Successful matching would allow the phonological interpretation of the information processed in posterior temporal regions. Impaired entrainment to prosodic speech contours in the AC.R in dyslexic readers would hinder the following processing steps that we just described. It is possible that the damaged input arriving to the IFG.L (due to the defective incoming information from the AC.R) alters the acquisition of proper phonological processing, thus affecting the ability to identify and manipulate the sounds of the language stored in left posterior temporal regions and, possibly, consequently

affecting reading acquisition. Thus, the overall picture would still support the auditory temporal sampling hypothesis (Goswami, 2011).

The neural hierarchical coupling between different frequencies during speech processing hinders the possibility to isolate the neural entrainment effects associated to each linguistic unit (prosodic, syllabic and phonemic information). To solve this issue, we studied brain response to white noise (non-linguistic audio stimuli) amplitude modulated at frequencies that simulate prosodic, syllabic and phonemic fluctuations in speech. Compared to continuous speech, these stimuli are perfectly rhythmic and promote the neural oscillations of the auditory cortex at a single frequency. In the third study, we analyze neural entrainment to amplitude modulated white noise in normal and dyslexic readers. In addition, we structural analysis (based on CT) to better understand the links between the anatomy of the auditory cortex and its oscillatory responses in normal and dyslexic readers.

4.3 STUDY 3: DEVELOPMENTAL EVALUATION OF ATYPICAL AUDITORY SAMPLING IN DYSLEXIA: FUNCTIONAL AND STRUCTURAL EVIDENCE

The specific frequency bands at which dyslexic readers present atypical auditory neural entrainment is still under debate. In addition, whereas neuroanatomical alterations in auditory regions have been documented in dyslexic readers, whether and how these structural anomalies are linked to auditory sampling and reading deficits remains poorly understood. In the present experiment, behavioral, functional, and structural data were collected from two groups of skilled and dyslexic reader adults and children. From MEG recordings, we evaluated the synchronization (phase-locking value) of the oscillatory responses elicited in the left and the right auditory cortex by auditory signals (AM white noise) modulated at theoretically relevant frequencies (delta, theta, and gamma) (Lehongre et al., 2011; Hämäläinen et al., 2012). Furthermore, we calculated the LI that allowed us to better characterize the hemispheric dominance and asymmetry of the effects (Abrams et al., 2009; Lehongre et al., 2011). In addition, structural MRI was used to estimate CT of the auditory cortex of participants.

In Study 1, we showed that slow and fast cortical oscillations play an important role during speech processing. In Study 2, we showed that dyslexic readers present difficulties to track slow (delta band) AMs in speech, but not to follow faster AMs (in the theta band). Moreover, we could not observe neural entrainment to gamma band in either group. Gamma neural synchronization is hardly visible during speech processing using MEG. Neural oscillations during speech processing contain much more energy at low frequencies (delta/theta) compared to high frequencies (gamma). This makes low frequency neural oscillations to be more detectable than high frequency neural oscillations at the sensor level (better signal to noise ratio for low frequency oscillations compared to high frequency oscillations). In the present study, we use non linguistic stimuli that strongly modulate auditory cortical oscillations at a specific frequency (2 Hz, 4 Hz, 7 Hz, 30 Hz and 60 Hz). We expected differences in synchronization strength and hemispheric specialization to occur between dyslexic and skilled readers for both slow (delta, theta; Hämäläinen et al., 2012) and fast (gamma; Lehongre et al., 2011)

AM rates. Moreover, auditory sampling strength and hemispheric specialization were expected to be sensitive to chronological age: if phonemic sensitivity increases with the amount of reading exposure and experience (Anthony et al., 2005), adults should present stronger brain sensitivity (and stronger left hemispheric bias) to gamma modulations than children. However, the consistency of neural phase locking to slow rate AM noise that supports prosodic and syllabic processing should be similar in adults and children, in line with developmental data suggesting that phonological sensitivity to these speech rhythms should be mastered before reading acquisition. Moreover, atypical hemispheric asymmetry for auditory entrainment to phonemic rate modulations were expected to be stronger in dyslexic adults than in dyslexic children: Indeed, if phonemic rate processing is refined based on the amount of reading exposure, larger gaps between dyslexic and skilled readers should be visible for the adult groups compared to the children groups.

Lastly, structural analyses based on CT was expected to reveal a cortical thinning of the auditory cortex due to chronological age factors. After partialling out the cortical thinning effect due to chronological age, we predicted to observe a cortical thinning (synaptic pruning) in auditory regions due to the functional efficiency developed with reading experience. If phonemic sensitivity increases with reading experience and this is supported by an enhancement of phonemic rate AM tracking and synaptic pruning in auditory regions, a negative correlation between cortical thinning and synchronization strength to gamma modulations was expected, at least in skilled readers. On the other hand, this relation was not expected for the dyslexic participants, if reading impairment is associated with the atypical development of perceptual sensitivity to phonemic rate auditory information (Lehongre et al., 2011).

4.3.1 METHODS

4.3.1.1 Subjects

The present experiment was undertaken with the understanding and written consent of each participant (or the legal tutor of each child below 18 years old). Forty-two individuals took part in this study. Participants attending or having completed an education level superior to secondary school were assigned to the

adult group. Ten skilled reader children (five females) and 10 dyslexic children (four females) matched in age (t(18)51.01, P>0.05; age range: 8.0-14.3 years) participated in the study. Eleven skilled reader adults (seven females) and 11 dyslexic reader adults (six females) matched in age (t(20)50.37,P>0.05; age range: 17.3-44.9 yrs.) composed the adult group. All participants had Spanish as their native language and were not fluent in any other language. All participants had normal or corrected-to-normal vision and reported no hearing impairments and were right handed. All the dyslexic individuals taking part in this study reported reading and/or writing difficulties and had all received a formal diagnosis of dyslexia. None of the skilled readers reported reading or spelling difficulties or had received a previous formal diagnosis of dyslexia.

4.3.1.2 Behavioral data

Intelligence quotient- IQ

Children were administered the WISC-R (Wechsler, 1974), and adults were administered the WAIS batteries (Wechsler, 2008) to measure the intelligence quotient.

Reading

The reading performance of participants was evaluated with the word reading list and pseudoword reading list of the PROLEC-R battery (Cuetos et al., 2007). For each of the two lists, accuracy and total time to read the list were recorded.

Spelling aloud

Since Spanish is a transparent language, highly regular grapheme-to-phoneme conversion rules may help overcome reading problems in adults, particularly with increasing reading experience and age. To increase the sensitivity of a diagnosis of written language difficulties in the older group, we assessed phonological abilities bearing on visual word recognition but that do not directly tap reading activity and that have been shown to be impaired in dyslexic adult readers of transparent orthographies (Helenius, Salmelin, Cononolly, Leinonen and Lyytinen, 2002). Adult participants were presented with a spelling aloud task. In this task, they were presented with 15 Spanish words, one by one, and they had to

spell them aloud letter by letter. The words varied in frequency and length (2-5 syllables; 6-10 letters). Participants' responses were recorded.

Phonological processing

Pseudoword repetition (phonological short term memory). Same procedure as in study 2 (see section 4.2.1.2).

Phonemic deletion (phonemic awareness). Same procedure as in study 2 (see section 4.2.1.2).

4.3.1.3 Functional Data (MEG Recording)

Stimuli and Procedure

Auditory stimuli were obtained by modulating the amplitude of white noise sounds. The stimuli were generated at a sampling frequency of 44.1 kHz and modulated using Matlab R2010 (Mathworks, Natick, MA) functions. AM were applied at the following frequencies: 2, 4, 7, 30, and 60 Hz rates with 100% depth. In addition, one condition included non-modulated white noise. All stimuli lasted 10 s and appeared 25 times throughout the task. The order of the presentation of stimuli was pseudo-randomized across the experiment, with the only constraint that two stimuli modulated at identical frequency were never presented consecutively.

During the MEG recording, the participants sat comfortably in the magnetically shielded room watching a silent movie and hearing the stimuli. Participants were asked to pay attention to the movie and try to avoid head movements and blinks. Auditory stimuli were delivered to both ears using Presentation software (http://www.neurobs.com/) via plastic tubes. The volume levels were tuned (75-80 dB sound pressure level) to optimize the listening condition for all participants.

Data acquisition

MEG signals were recorded as in study I and II.

Data pre-processing

To remove external magnetic noise from the MEG recordings, data were preprocessed off-line using the Signal-Space-Separation method (Taulu and Kajola,

2005) implemented in Maxfilter 2.1 (Elekta-Neuromag). MEG data were also corrected for head movements, and bad channels were substituted using interpolation algorithms implemented in the software. Subsequent analyses were performed using Matlab R2010 (MathWorks). Heart beat and EOG artifacts were detected using ICA and linearly subtracted from recordings. The ICA decomposition was performed using the Infomax algorithm implemented in Fieldtrip toolbox (Bell and Sejnowski, 1995; Oostenveld et al., 2011). Raw data were segmented into epochs of duration corresponding to a two modulation cycles (1000, 500, 285, 66, and 33 ms long epochs for the 2, 4, 7, 30, and 60 Hz AM rates, respectively). Epochs with MEG peak-to-peak amplitude values exceeding 4000 ft (magnetometer) or 3000 ft/cm (gradiometer) were considered as artifact contaminated and rejected from the subsequent analyses. On average, the percentage of epochs retained in the final analyses were 67% (SD: 16%), 76% (12%), 83% (11%), 89% (9%), and 88% (13%) for the 2, 4, 7, 30, and 60 Hz modulation frequencies, respectively. There were no significant differences (P values>0.1) in the number of accepted trials between groups across all AM frequencies.

MEG measures computation

Phase locking value (PLV) analysis

Source level PLV. The forward solution was based on the anatomical MRI (T1) of each individual participant. MRI images were segmented using Freesurfer software (Dale and Sereno, 1993; Fischl et al., 1999). The MEG forward model was computed using a single shell boundary-element model using the MNE software (Gramfort et al., 2014) for pairs of orthogonal tangential current dipoles distributed on a 5 mm homogeneous grid source space covering the whole brain. The cross-spectral density matrix for all sensors was computed from the Fourier transformed artifact-free epochs at the AM frequency. Based on the forward model and the cross-spectral density matrix, dynamic imaging of coherent sources algorithm (Gross et al., 2001) was applied to obtain spatial filter coefficients for every source location and orientation (see section 3.4.1). Source activity at the AM frequency was then obtained as the matrix product of the spatial filter coefficients arranged in a row vector with each Fourier transformed epoch at the AM

frequency arranged in a column vector. Then, for each source the phase locking value (PLV) was calculated (see section 3.4.3). In this case, θ_n was the phase of the source activity for the *n*th epoch and the sum was performed across the N artifact-free epochs. Source data in both orientations were combined to obtain a single optimum orientation that maximizes the PLV. Thus, five PLV maps (one for each modulation rate: 2, 4, 7, 30, and 60 Hz) were obtained for each participant.

PLV maps for each frequency were transformed from individual MRIs to the standard MNI-Colin 27 brain using the spatial normalization algorithm implemented in SPM. Within the MNI space, brain regions showing significant PLVs across conditions (2, 4, 7, 30, and 60 Hz AM frequencies) and regardless of the group (skilled readers and dyslexics) were identified with a non-parametric permutation test (Nichols and Holmes, 2002). To do so, we first computed "surrogate" PLV maps, which were PLV maps computed with the condition-specific epoch length but using the data from the unmodulated noise condition. "Authentic" and surrogate maps were subtracted and further averaged across subjects (regardless of the group). Values from this contrast were then compared to their permutation distribution (permutation within subjects, performed over the label authentic and surrogate) built from a subset of 1000 permutations. Briefly, for each permutation, authentic and surrogate PLV maps from each individual were swapped with probability 0.5, the contrast map was then computed from these shuffled PLV maps, and the permutation distribution for that permutation was set to the maximal value (across all sources) of the contrast map. Sources with non-permuted PLV contrast above the 95-percentile of the permutation distribution were considered significantly ($p<0.05$) phase-locked to auditory stimulation. Bilateral STG (BA42), middle and posterior regions of the temporal sulcus (BA22), and the Heschl's s gyrus (BA41) showed robust PLV effects (Figure 24) (Giraud et al., 2000).

The statistical analysis was repeated for each frequency rate separately (Figure 25), and overall, these same regions were significantly activated (Table 7). Intracranial recordings found significant synchronization between neural oscillations and AM white noise regardless of the frequency rate in the same regions (stereoelectroencephalography; Bancaud and Talaraich, 1965; Liégeois-

Chauvel et al., 2004). Thus, we defined a region of interest (ROI) including the previously mentioned Brodmann areas (BA41, BA42, and BA22).

The mask defined by the ROI was applied to the corresponding PLV map for each participant and mean of the masked PLVs in the left hemisphere and right hemisphere was calculated separately. Brain hemispheric synchronization dominance for each frequency rate and participant was calculated using a laterality index (see section 3.4.6) In this case, A_R and A_L expressed mean of the masked PLVs in the right and left hemisphere respectively.

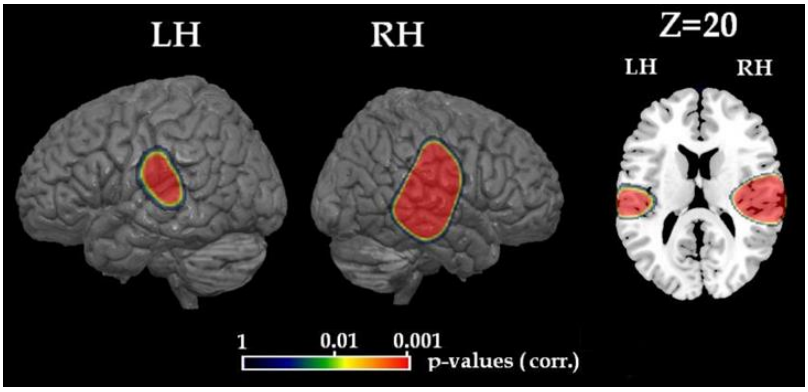

Figure 24. Statistical map (p-values) representing sources in the left (LH) and right (RH) hemispheres, that present stronger synchronization compared to the unmodulated condition across all frequencies and all participants. The brain slice in the axial plane at Z=20 (MNI coordinates) was used to better determine deeper sources.

AM frequency	Brain region	BA	MNI coordinates
2 Hz	R superior temporal sulcus	BA22	62 -10 11
2 Hz	L superior temporal gyrus	BA42	-61 -26 15
4 Hz	R superior temporal sulcus	BA22	63 -17 6
4 Hz	L inferior parietal	BA40	-59 -27 24
7 Hz	R superior temporal sulcus	BA22	62 -16 7
7 Hz	L superior temporal sulcus	BA22	-62 -25 8
30 Hz	R superior temporal sulcus	BA22	60 -24 6
30 Hz	L superior temporal sulcus	BA22	-57 -19 7
60 Hz	R superior temporal sulcus	BA22	59 -27 9
60 Hz	L superior temporal gyrus	BA22	-58 -30 16

R,right; L,left

Table 7. Brain source of maximum significance (minimum *P*-value) for each AM frequency and hemisphere.

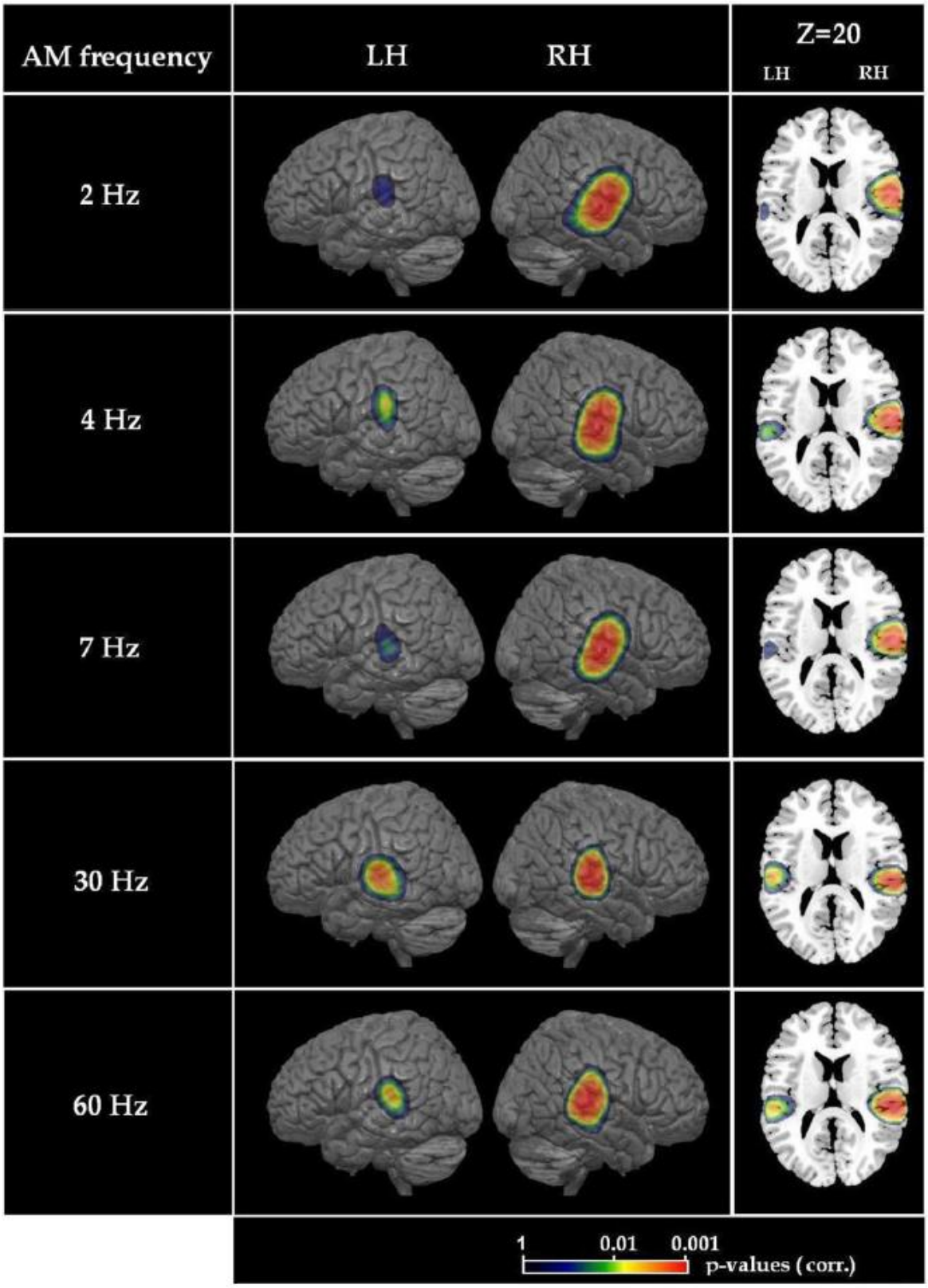

Figure 25. Statistical map (*P*-values) representing sources that present stronger synchronization compared to the unmodulated noise condition at each AM frequency across all participants. The brain slice in the axial plane at Z=20 (MNI coordinates) illustrates source deepness.

4.3.1.4 Structural data (MRI)

Data acquisition and pre-processing

All subjects underwent structural MRI scanning in a single session, using the same 3.0 Tesla Siemens Magnetom Trio Tim scanner (Siemens AG, Erlangen, Germany), located at the BCBL in Donostia-San Sebasti_an. A highresolution T1-weighted scan was acquired with a 3D ultrafast gradient echo (MPRAGE) pulse sequence using a 32-channel head coil and with the following acquisition parameters: FOV = 256; 160 contiguous axial slices; voxel resolution 1 mm × 1 mm × 1 mm; TR = 2300 ms, TE = 2.97 ms, flip angle = 9° . Cortical reconstruction and volumetric segmentation was performed with the Freesurfer image analysis suite, (http://surfer.nmr.mgh.harvard.edu/). Briefly, this processing includes motion correction, removal of non-brain tissue, automated Talairach transformation, segmentation of the subcortical white matter and deep gray matter volumetric structures, tessellation of the gray matter white matter boundary, automated topology correction, and surface deformation following intensity gradients to optimally place the gray/white and gray/cerebrospinal fluid borders at the location where the greatest shift in intensity defines the transition to the other tissue class (Dale, Fisch and Sereno, 1999; Fischl and Dale, 2000; Fischl et al., 2002; Ségonne et al., 2004).

MRI measures computation

CT analysis

A number of deformable procedures were performed automatically in the data analysis pipeline, including surface inflation and registration to a spherical atlas. This method uses both intensity and continuity information from the entire three-dimensional MR images in segmentation and deformation procedures to produce representations of CT, calculated as the closest distance from the gray/white boundary to the gray/CSF boundary at each vertex on the tessellated surface. These maps were not restricted to the voxel resolution of the original data and thus afford detection of submillimeter differences between groups. The CT analysis was restricted to the ROI defined in the MNI-Colin 27 space and was calculated separately for the right and left hemisphere. Finally, the cortical surface was resampled to each subject's space, and average CT data were obtained in each

hemisphere independently for each subject. LI values were also obtained. In this case, AR and AL reflect mean CT values restricted to the ROI in the right and left hemisphere, respectively.

4.3.1.5 Statistical analysis

Evaluation of the reading disorder in the dyslexic groups

Regarding the reading skills of children (Table 8), z-scores were computed based on the corresponding age norms (Cuetos et al., 2007). For adults, z-scores were computed based on the performance of 46 skilled monolingual Spanish adults matched for age (M = 32.46; SD = 11.57) with the control and dyslexic groups of this study (F<1). This norm was created and used for the purpose of this study since the PROLEC-R battery offers normative data up to the age of 15 - 16 years.

	Dyslexic group			Control group		
	M(SD)	**Range**	**z score**	**M(SD)**	**Range**	**z score**
Children (*n* = 20)						
		n = 10			*n* = 10	
IQ (Standard score)	113.9(10.0)	98-122	-	111.0 (8.0)	100-130	-
Word reading[a]		*n* = 10			*n* = 10	
Accuracy (/40)	34.3(6.0)	18-39	-7.0**	39.4(.08)	38-40	-0.05
Time (s)	73.4(48.2)	29-202	-3.7**	30.0(7.0)	20-48	0.60
Pseudoword reading[a]		*n* = 10			*n* = 10	
Accuracy (/40)	28.8(6.3)	16-34	-3.9**	37.0(1.4)	34-39	-0.25
Time (s)	95.7(59.1)	43-245	-2.7**	53.3(8.2)	43-60	0.34
Adults (*n* = 22)						
		n = 11			*n* = 11	
IQ (standard score)	118.5(4.5)	115-131		125.2(4.4)	115-127	
Word reading[b]		*n* = 11			*n* = 11	
Accuracy (/40)	38.4(1.6)	35-40	-4.2**	39.8(.038)	39-40	-0.15
Time (s)	37.2(11.7)	23-66	-4.6**	23.3(3.98)	19-27	-0.46
Pseudoword reading[b]		*n* = 11			*n* = 11	
Accuracy (/40)	34.(3.66)	28-40	-4.5**	39.0(.085)	37-40	0.04
Time (s)	63.0(16.4)	49-110	-7.8**	39.0(5.36)	32-50	-1.2
Spelling aloud[c]		*n* = 11			*n* = 11	
Accuracy (/15)	9.7(2.0)	8-12	-2.12*	14.45(.049)	14-15	0.0

a: z scores computed based on the PROLEC-R age-matched normative data
b: z-scores computed based on 46 skilled reader adults on the PROLEC-R reading lists.
c: tmodified statistics computed based on the mean performance of the control group.
*: p<0.05; **: p<0.01

Table 8. Characteristics of the four groups of participants regarding their IQ, reading and spelling skills.

In the absence of normative data for the spelling aloud task designed for this study, we used the t distribution method ($t_{modified}$, Crawford and Howell, 1998) to establish the presence of a deficit for each dyslexic adult as compared to the control group. This test has been shown to be robust in the case of small control groups (Crawford, Garthwaite, Azzalini, Howell and Laws, 2006). General IQ scores obtained by each participant were compared to 80 (only participants with a score superior to 80 were included in the study).

Group differences in phonological processing and brain measures

Independent ANOVAs with group (dyslexic vs. control) and age (adults vs. children) as between-subject factor were conducted on the measures obtained in the two phonological processing tasks. The number of participants that completed each phonological processing task is indicated in Table 9.

The analysis of the brain responses of participants during the passive listening task consisted in conducting mixed-design ANOVAs for each frequency condition separately (2 Hz, 4 Hz, 7 Hz, 30 Hz, and 60 Hz) on the mean of the masked PLVs, with hemisphere (left vs. right) as the within-subject factor and group and age as the between subject factor. Based on the observed significant effects of the between-subject factor, mean LI values were computed for the groups that significantly differed on PLVs. These LI values were tested against zero with a single t-test to determine a left or right significant lateralization for that specific frequency.

Lastly, a mixed-design ANOVA was conducted on CT with hemisphere as the within-subject factor, and group and age as the between-subject factor. The structural data of two participants was excluded from the analysis due to data acquisition problems in the MRI scanning. Thus, the CT of 20 dyslexic readers (10 children and 10 adults) and 20 normal readers (10 children and 10 adults) was calculated. For all ANOVAs, Bonferroni post hoc tests were used when appropriate and data transformation was performed when the assumptions to conduct ANOVA were violated.

Correlation analysis

Correlations between reading skills, phonological skills, and brain measures (LI of the PLVs at the frequencies showing significant group effects, and the LI of the CT) were conducted. Note that only reading time measures were used since accuracy scores were very high with little variance in the data (Table 8). In transparent orthographies, reading speed is known to be a stronger predictor of reading skills than reading accuracy. Data transformation was performed on reading times (1/x - corrected) to respect normality. Correlation analysis between the two brain lateralization indexes (structural - CT and functional - PLVs) were also computed.

4.3.2 RESULTS

4.3.2.1 Behavioral results

Table 9 presents the behavioral assessment for both dyslexic and skilled readers.

Phonological skills	**Dyslexic group**		**Control group**		
	M(SD)	**Range**	**M(SD)**	**Range**	**p**
Children (n = 20)					
Pseudoword repetition	*n* = 8			*n* = 10	
Accuracy (%)	78.6(6.7)	66.6-87.5	85.0(7.9)	70.8-100	< .005
Number of phonemic errors	6.5(2.2)	3-10	4.9(3.9)	0-13	< .05
Phonemic deletion	*n* = 9			*n* = 9	
Total Accuracy (%)	78.7(23.6)	25-100	91.1(8.9)	83.3-100	n.s
Number of deletion errors	3.7(4.8)	0-13	1.7(2.0)	0-7	0.23
Number of errors out of deletion site	2.8(3.6)	0-12	1.1(1.2)	0-3	0 .14
Adults (n = 22)					
Pseudoword repetition	*n* = 9			*n* = 11	
Accuracy (/40)	79.1(9.0)	66.6-91.6	91.8 (5.7)	79-100	< .005
Number of phonemic errors	5.8(2.0)	2-9	2.4(2.2)	0-7	< .05
Phonemic deletion	*n* = 11			*n* = 11	
Total Accuracy %)	82.9(15.2)	41.6-100	90.9(13.6)	62.5-100	n.s
Number of deletion errors	3.1(3.1)	0-12	2.2(3.2)	0-9	0.23
Number of errors out of deletion site	2.2(2.2)	0-8	0.4(0.9)	0-3	0.14

The P-value of the dyslexics vs.control comparison is provided in the last column. n = number of participants that took part in the task.

Table 9. Characteristics of the four groups of participants regarding their phonological skills.

Intelligence quotient- IQ

All participants obtained an IQ score superior to 80 on the WISC-R or WAIS tests, suggesting normal intelligence in all our participants. However, a main group effect was found ($F(1,38) = 4.34$, $P = 0.04$, $n_p^2 = 0.1$) suggesting that the dyslexic participants exhibited lower IQ than their control peers regardless of age ($F<1$) (Table 8). IQ was controlled for in further group comparisons and correlation analyses conducted within a sample including both dyslexic and control participants.

Reading and spelling aloud

Overall, both the group of dyslexic children and the group of dyslexic adults showed negative average *z*-scores, reflecting significantly impaired reading time and accuracy for both words and pseudowords (and spelling aloud for the dyslexic adults) compared to the age-matched norm. All corresponding averaged *z*-scores fell within the normal range for the two control groups (Table 8).

Phonological skills

A main effect of group ($F(1,33) = 10.6$, $P<0.01$, $n_p^2 = 0.24$) but not age ($F<1$) was found for total accuracy in the pseudoword repetition task, showing that dyslexic participants were worse at performing the task than control participants, regardless of the age ($F(1,33) = 1.46$, $P = 0.23$, $n_p^2 = 0.04$). Accordingly, dyslexic participants made more phonemic errors than their controls ($F(1,33) = 6.5$, $P<0.05$, $n_p^2 = 0.17$). Children tended to produce more phonemic errors ($M_{Ch} = 5.6$, $SD_{Ch} = 3.4$) than adults ($M_{Ad} = 4$, $SD_{Ad} = 2.8$) overall ($F(1,33) = 2.1$, $P = 0.15$, $n_p^2 = 0.06$). No interaction was found between the two factors ($F<1$). On the phonemic deletion task, no main effect or interaction was found on the total accuracy, the numbers of errors on the deletion site or outside of the deletion site (all *F*s<2.2). Still, it is noteworthy that dyslexic participants generally made more errors than their controls (Table 9).

4.3.2.2 Functional Results

PLV analysis

Source level PLV: No significant main effect of hemisphere, group or age or interaction between these factors was found on the PLVs for the 2 and 7 Hz frequency rates (all *F*s<3.1, *Ps*>0.8).

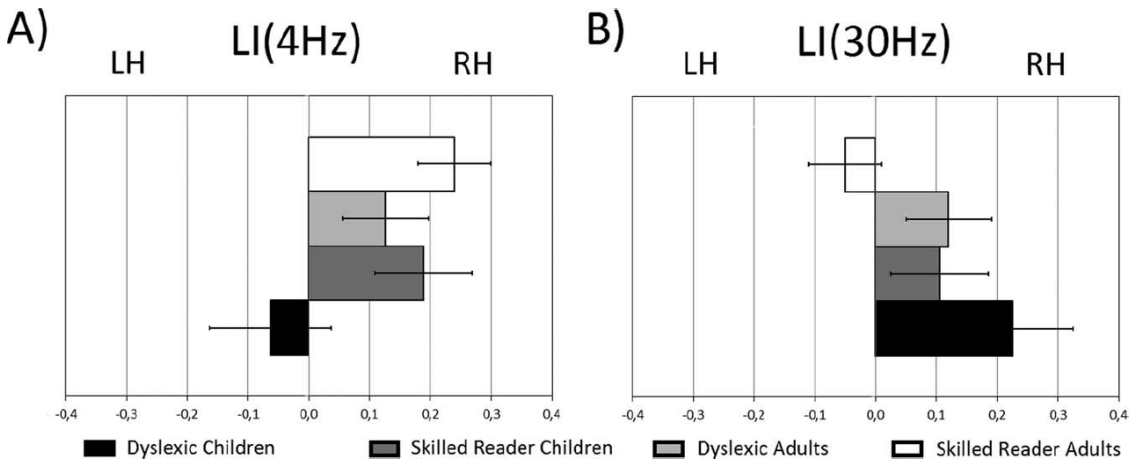

Figure 26. The mean and standard error of the LI at 4 Hz (A) and 30 Hz (B) in dyslexic children (black), skilled reader children (dark grey), dyslexic adults (light grey), and skilled reader adults (white) are represented (positive values indicate a rightward lateralization while negative values a leftward lateralization).

In Figure 26, we report the three main results emerging in the MEG analyses, as well as correlation of brain measures with reading and phonological measures.

Atypical Low Frequency (4 Hz) Synchronization Enhancement in Dyslexia Regardless of Age

We observed a significant group effect for the synchronization strength at the 4 Hz frequency rate ($F(1,37) = 4.8$, $P<0.05$, $n_p^2 = 0.1$) that was neither modulated by age or hemisphere (Fs<1.9). Overall, dyslexic participants presented stronger synchronization at 4 Hz ($M_{Dys} = 0.14$, $SD_{Dys} = 0.05$) compared to controls ($M_{Ctr} = 0.11$, $SD_{Ctr} = 0.05$). Hemispheric specialization patterns of LI values were assessed for the dyslexic and control groups separately. LI values showed a right hemispheric lateralization for brain synchronization at 4 Hz in the control group ($M_{Ctr} = 0.15$, $SD_{Ctr} = 0.33$, $P<0.05$), whereas this hemispheric dominance was not present for the dyslexic participants ($M_{Dys} = 0.09$, $SD_{Dys} = 0.34$, $P = 0.21$) (Figure 26).

Positive partial correlations (controlling for chronological age and IQ) were found between LI values and both word and pseudoword reading times (reciprocal transformation) in the control group, (Word: r = 0.54, P<0.01 (Figure 27 top panel); Pseudoword: r = 0.44, P<0.05 (Figure 27 bottom panel)) but not within the dyslexic group (P>0.7). In the control group, the faster the word and pseudoword reading, the more right lateralized the PLVs at 4 Hz.

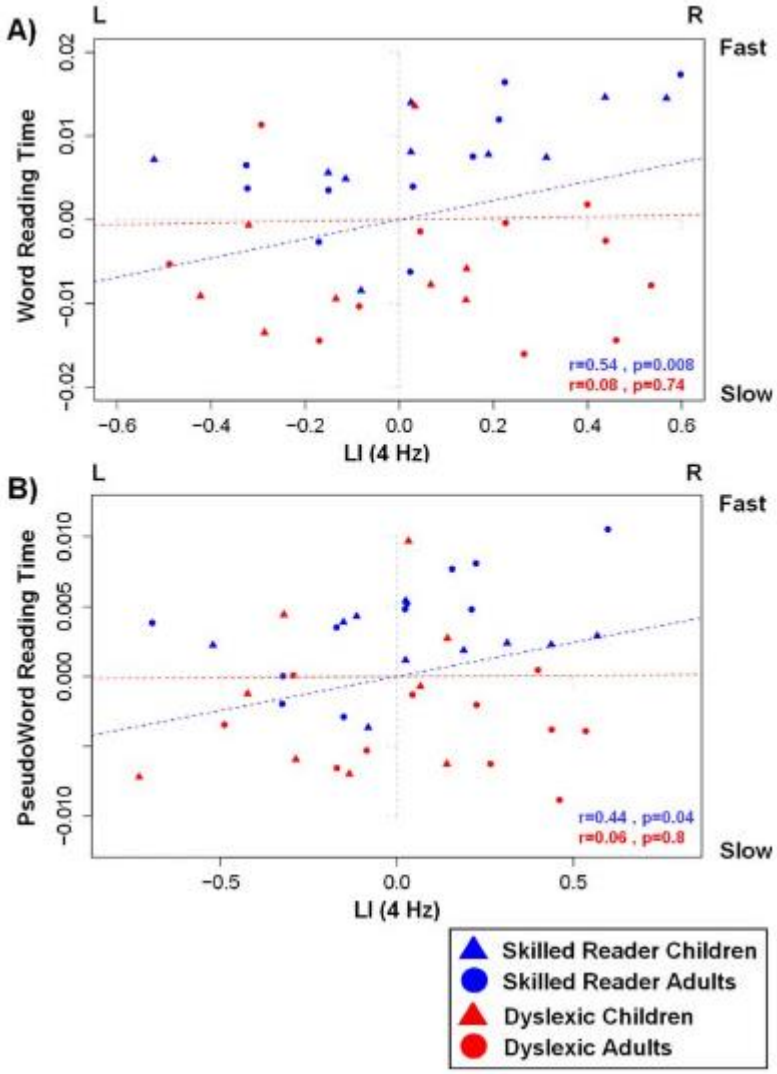

Figure 27. Correlation between the LI values at 4 Hz (LI(4Hz) on *x* axis; negative and positive values indicate left and right hemispheric dominance, respectively) and the residual values (age and IQ corrected) of the inverse of word (A) and pseudoword (B) reading times (*y* axis) within the group of skilled (children: blue triangle, adults: blue circle) and dyslexic (children: red triangle, adults: red circle) readers.

High Frequency (30-60 Hz) Synchronization Enhancement with Age Regardless of the Group

An age effect was found for the synchronization strength for both conditions of gamma frequency (30 Hz: $F(1,37) = 10.2$, P<0.01, $n_p^2 = 0.21$; 60 Hz: $F(1,37) = 11.44$, $P<0.01$, $n_p^2 = 0.23$). Adults showed stronger neural synchronization to the AM noises (30 Hz: $M_{Ad} = 0.06$, $SD_{Ad} = 0.02$; 60 Hz: $M_{Ad} = 0.05$, $SD_{Ad} = 0.05$) than children (30 Hz: $M_{Ch} = 0.03$, $SD_{Ch} = 0.02$; 60 Hz: $M_{Ch} = 0.015$, $SD_{Ch} = 0.01$). Hemispheric specialization patterns of LI values at 30 Hz and 60 Hz were assessed for children and adults separately. LI values at 30 Hz reflected a rightward hemispheric lateralization of the PLVs in children ($M_{Ch} = 0.17$, $SD_{Ch} =$

0.32, P = 0.03), but not in adults (M_{Ch} = 0.02, SD_{Ch} = 0.29, P = 0.72) (Figure 26). No hemispheric asymmetry in the PLVs was found for AM noise at 60 Hz, in either of the groups. When individual chronological age and IQ were partialled out, the number of errors at repeating pseudowords and LI values at 30 Hz showed a significant positive relationship in adults (r = 0.51, P = 0.02) but not in children (r = 0.1, P = 0.7) indicating that adults with the strongest leftward hemispheric lateralization for AM noise at 30 Hz were the most accurate in repeating pseudowords (Figure 28).

Right-Lateralized Neural Entrainment to AM Noise at 30 Hz in Adults and Children with Dyslexia

Interestingly, a hemisphere by group interaction was observed for the synchronization strength at 30 Hz (F(1,37) = 4.13, P<0.05, $n_p^2 = 0.1$), which was not modulated by age (F(1,37) = 0.53). Post hoc analysis showed that PLVs were higher in the dyslexic group than the control group in the right hemisphere (P<0.05; M_{Dys} = 0.06, SD_{Dys} = 0.03; M_{Ctr} = 0.04, SD_{Ctr} = 0.02), whereas no group difference was found in the left hemisphere (P>0.5; M_{Dys} = 0.04, SD_{Dys} = 0.02; M_{Ctr} = 0.04, SD_{Ctr} = 0.03). Moreover, greater PLVs were found in the right compared to the left hemisphere in the dyslexic group (P = 0.02) indicating an asymmetry toward the right hemisphere. In controls, no difference was found between the two hemispheres (P = 0.68), suggesting bilateral sensitivity to 30 Hz modulations. Analyses of the LI values confirmed that dyslexic participants presented a significant rightward hemispheric lateralization for the neural synchronization to AM modulations at 30 Hz (M_{Dys} = 0.17, SD_{Dys} = 0.27, P<0.01), while controls showed no hemispheric bias (M_{Ctr} = 0.02, SD_{Ctr} = 0.29, P = 0.72) (Figure 26).

No correlation was found between the LI values at 30 Hz and reading, phonemic awareness, or phonological short-term memory measures after controlling for IQ and chronological age (all rs<0.34, Ps>0.14).

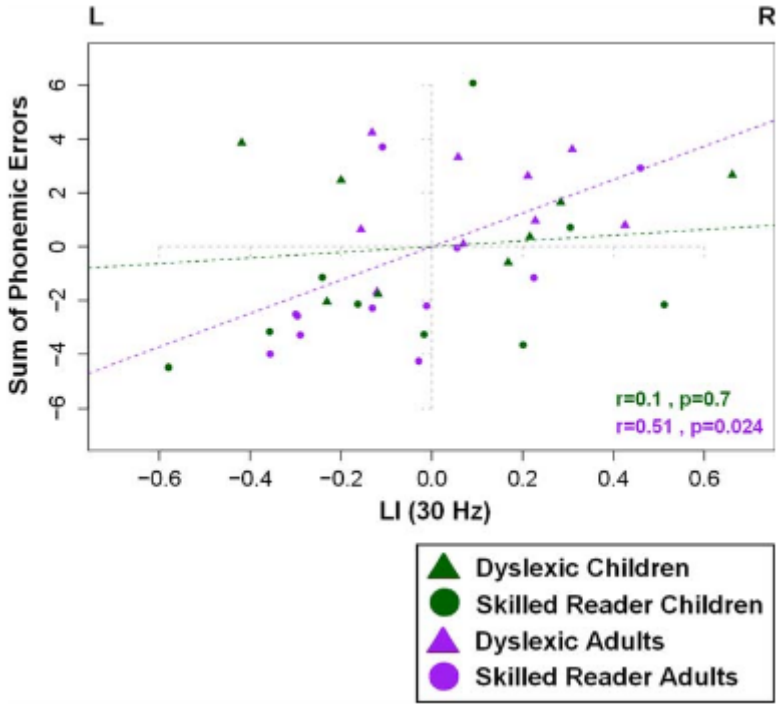

Figure 28. Correlation between the LI values at 30 Hz (LI(30 Hz) on *x* axis; negative and positive values indicate left and right dominance, respectively) and the residual values (age and IQ corrected) of the sum of phonemic errors in the phonological short term memory task (*y* axis) within the group of children (dyslexic: green triangle, control: green circle) and adults (dyslexic: purple triangle, control: purple circle) readers.

4.3.2.3 Structural Results

CT analysis

An age effect on CT was found ($F(1,35) = 33.3$, $P<0.01$, $n_p^2 = 0.48$), which also interacted with hemisphere ($F(1,35) = 5.6$, $P<0.05$, $n_p^2 = 0.14$). Post hoc analysis revealed that the auditory cortex was thinner in adults ($M_{RH} = 2.7$, $SD_{RH} = 0.15$; $M_{LH} = 2.7$, $SD_{LH} = 0.18$) than children ($M_{RH} = 2.9$, $SD_{RH} = 0.13$; $M_{LH} = 3$, $SD_{LH} = 0.11$) in both right ($P<0.001$) and left ($P<0.01$) hemispheres. Moreover, the right auditory cortex was thinner than the left auditory cortex in children ($P<0.01$) but not in adults ($P = 0.64$) (Figure 29). Analyses of the LI of CT confirmed that children show a significant rightward asymmetry of the auditory cortices (P50.04) that was not present in adults ($P = 0.46$). No main effect or interaction effect involving the factor group was found (Fs<2.44).

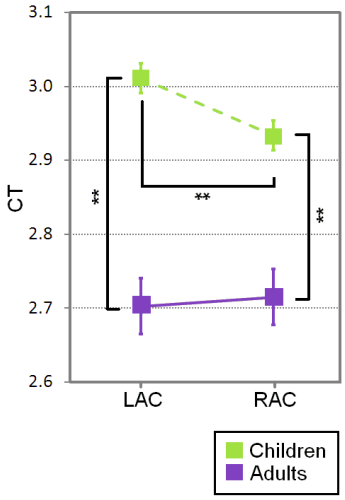

Figure 29. Mean and standard error of the CT in the left (LAC) and right (RAC) auditory cortex in adults (purple) and children (green) (P<0.01).**

4.3.2.4 Relation between Functional (PLVs) and Structural (CT) Results

Because both CT and PLVs at 4 Hz and 30 Hz played a significant role in both the age and group differences presented above, we performed partial correlation analyses, controlling for chronological age and IQ, between the functional and structural LI measures within the control group and the dyslexic group as well as in the child group and the adult group. For the 4 Hz frequency rate, we observed a positive correlation between LI of both CT and PLVs at 4 Hz in the dyslexic group (r = 0.5, P = 0.01). A lateralized bias in the neural synchronization to AM noise at 4 Hz to the right hemisphere was associated with a left hemispheric bias for cortical thinning. No such correlation emerged within the control group (r = 0.2, P = 0.2) (Figure 30 top panel).

When considering the 30 Hz frequency rate, LI of CT and PLVs correlated negatively within the whole control group (r = 20.4, P<0.05), indicating that an asymmetry of neural synchronization to AM noise at 30 Hz toward the left hemisphere was associated with cortical thinning bias towards this same left hemisphere. No such correlation was found within the dyslexic group (r = 0.15, P = 0.27) (Figure 30 bottom panel).

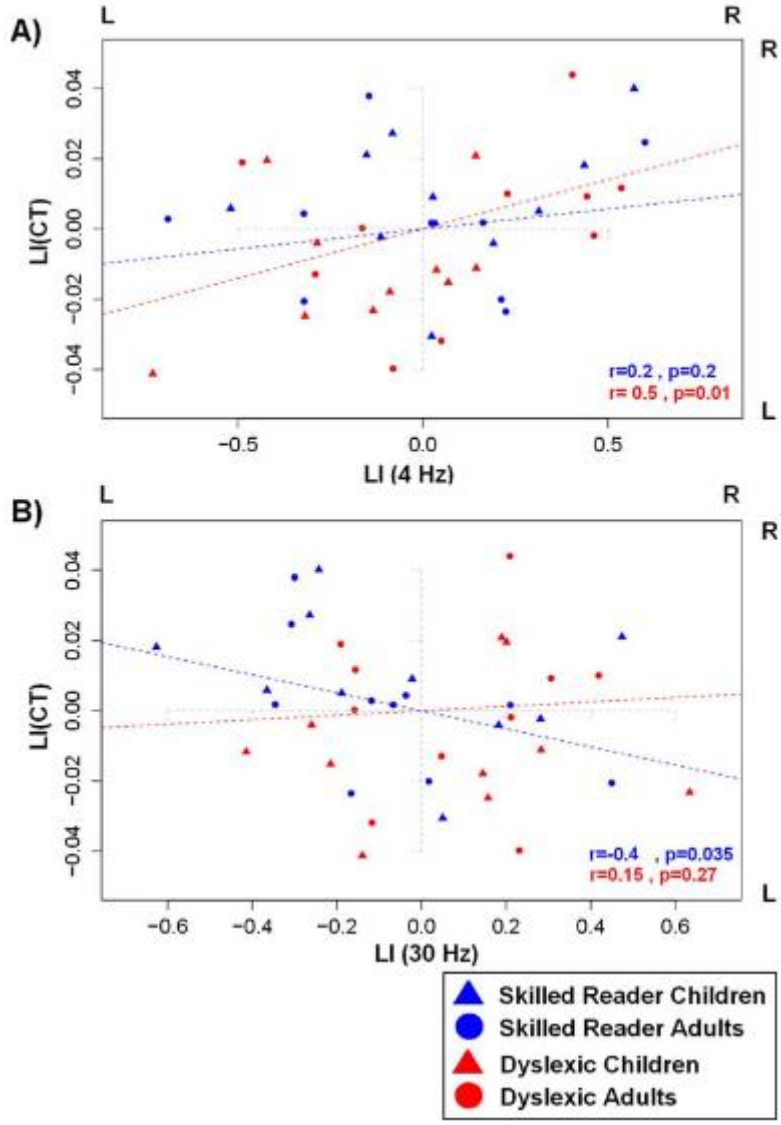

Figure 30. (A): Correlation between the LI at 4 Hz (LI(4 Hz) on the *x* axis; negative and positive values indicate left and right dominance respectively) and the LI of the CT (LI(CT)) (*y* axis; negative and positive values indicate thicker CT in the left (relative to the right) and right (relative to the left) auditory cortex respectively) within skilled (*n*520, blue) (children: blue triangle, adults: blue circle) and dyslexic (children: red triangle, adults: red circle) readers. (B): Correlation between the LI at 30 Hz (LI(30 Hz)) and LI(CT) in skilled (children: blue triangle, adults: blue circle) and dyslexic (children: red triangle, adults: red circle) readers.

4.3.3 DISCUSSION

This study adds important evidence to support the idea that atypical neural sampling of auditory signals at slow or/and fast frequency bands underlies developmental dyslexia (Lehongre et al., 2013; Power, Mead, Barness and Goswami, 2013). Children and adults were tested for the first time with a similar paradigm, allowing us to examine whether the neural sampling deficit in developmental dyslexia is modulated by developmental changes. Importantly, we

used MEG recordings in association with the structural brain images of the participants to provide insights on the neural sources of the sampling deficit found in dyslexia. Our results showed atypical neural synchronization to both syllabic- and phonemic-rate modulations in the dyslexic group compared to their control peers. Models of typical *Speech perception* show that neuronal activity from the right auditory cortex is optimized for sampling speech information occurring at low frequencies (at delta-theta) (Abrams et al., 2009), while high frequencies are processed bilaterally (Boemio et al., 2005; Vanvooren et al., 2014) or with a left hemispheric bias (Poeppel, 2003). Consistent with this literature, both skilled reader adults and children showed a rightward asymmetric specialization for sampling slow AM noise (4 Hz) and a bilateral synchronization for faster AM noise (30 Hz). Dyslexic children and adults showed the opposite pattern, that is, an absence of significant rightward lateralization for low frequencies (4 Hz), and a rightward lateralization for high frequencies (30 Hz). Abnormal sensitivity and lateralization patterns for neural synchronization to low frequency temporal features present in non-speech and speech signals have previously been associated with reading impairments (Hämäläinen et al., 2012; Power et al., 2013). Accordingly, we found a significant relationship between synchronization asymmetries at 4 Hz and reading speed within the control group, showing that stronger rightward asymmetric synchronization was associated with faster pseudoword and word reading. Contrary to what was observed for hemispheric asymmetry, the overall strength of synchronization for AM noise processing at 4 Hz did not seem to contribute to normal reading. In fact, PLVs were stronger in the dyslexic group than in the control group in both hemispheres. This unexpected high neural synchronization to the auditory stimuli in our dyslexic sample may indicate a greater reliance on sampling auditory information at the syllabic-rate in these participants compared to their skilled reader peers. Interestingly, sensitivity to the phonological syllabic rate (4 Hz) is of special relevance for Spanish, which falls within the rhythmic class of syllable-timed languages (Ramus, Nespor and Mehler, 1999). The high availability of syllabic-rate information in Spanish may have led our dyslexic participants to compensate by relying more strongly on temporal modulations at this rate, possibly to cope with their impaired right hemispheric specialization. Cross-linguistic differences in phonological parameters

could also explain why we did not observe any group difference at the lowest rate (2 Hz). According to the temporal sampling theory of dyslexia (Goswami, 2011), atypical temporal sampling within both the delta (2 Hz) and theta (4 Hz) ranges should contribute to reading disorders, since they relate to the *encoding* of syllabic-relevant speech rates (e.g., syllabic stress and syllable, respectively; Goswami, 2015). Supporting evidence has been reported for speech (Power et al., 2013) and non-speech (Hämäläinen et al., 2012) stimuli in English individuals. Contrary to Spanish, English is a stress-timed language and stress might be especially prominent and relevant for speech segmentation and phonological development in this language. Rhythm variations between Spanish and English might therefore have an impact on the strength of the sampling deficits observed at delta in dyslexia (and possibly theta, as proposed earlier). This deficit in the delta range might also be less strong for stimuli that do not directly tap into language, like those in the present study, so we cannot yet rule out the possibility that an atypical speech sampling at delta has a role to play in dyslexia, even in syllable-timed languages (see Bourguignon et al., 2013 for the importance of the delta band for speech processing in French).

Regarding phonemic-rate conditions (30 Hz and 60 Hz), we observed a rightward synchronization asymmetry for the dyslexic group, driven by an atypical synchronization enhancement in the right auditory cortex to the low gamma rate (30 Hz). In fact, the same atypical hemispheric lateralization pattern for speech sampling in the low gamma range has been reported in dyslexic adults (Lehongre et al., 2013) and pre-readers with high hereditary risk for dyslexia (Vanvooren et al., 2014). Right hemispheric bias has been linked to inattentive speech and non-speech processing (Scott, Rosen, Beaman, Davis and Wise, 2009) which, in the case of this study, may indicate that dyslexic individuals suffer from a limitation in the resources allocated to the processing of stimuli occurring at phonemic-relevant rates. Interestingly, the neurophysiological oscillatory anomalies observed in our dyslexic group were not modulated by the chronological age of participants, neither at syllabic nor at phonemic- rates (4 Hz and 30 Hz, respectively). Dyslexic adults therefore showed a deficit even when compared to younger skilled readers with “more comparable” reading experience, which supports a possible causal link between the sampling deficit and the reading difficulties of our dyslexic

participants. Regarding syllabic-rate processing, the size of the deficit of the dyslexic group was not modulated by developmental changes. Interestingly, all our participants had possibly already reached the highest developmental point in terms of their sensitivity to, and rightward asymmetries for, the processing of syllabic-rate units (low frequencies: 4 Hz). This is in line with studies showing that this specific oscillatory sampling mechanism may be achieved before reading is acquired, in normal pre-readers, as well as pre-reader children with high hereditary risk for dyslexia (Vanvooren et al., 2014). Regarding phonemic-rate neural auditory synchronization, adults showed stronger synchronization values than children for both the 30 Hz and 60 Hz conditions. This sensitivity enhancement to high frequencies was associated to better phonemic processing in adults only (who have greater reading experience than children, as illustrated by fewer phonemic errors in adults than children in the pseudoword repetition task). This higher phonemic sensitivity goes hand in hand with the acquisition of reading expertise (Castles and Coltheart, 2004). In addition, whereas adults did not show any hemispheric specialization for synchronizing their neural response to these stimuli, a rightward hemispheric asymmetry was observed in children (see also Vanvooren et al., 2014 in pre-readers). Following the rationale discussed earlier, this right hemisphere asymmetry in children might stem from the allocation of fewer (or less tuned) attentional resources to phonemic-rate stimuli (Scott et al., 2009). Thus, the rightward lateralization is present in the early stages of reading acquisition but vanishes with reading experience, moving toward a symmetric sensitivity for phonemic-rate auditory processing. To move from this rightward asymmetry to a symmetric sensitivity, the left hemisphere should be more actively involved in entrainment to fast frequency modulations (30 Hz) relative to the right hemisphere. Studies using tonal judgment tasks suggest that left and right hemisphere regions respond differently if the stimuli provide the possibility to access linguistic information (Klein, Zatorre, Milner and Zhao, 2001). Indeed, right hemisphere regions would be specialized in pitch discrimination (Zatorre and Evans, 1992) while left hemisphere regions are required for a linguistic categorization of the pitch (Gandour et al., 1998). The stronger involvement of the left auditory cortex in processing high frequency (phonemic) rates could explain why adults present better performance in categorizing phonemes compared to

children (Hazan and Barrett, 2000). In line with these observed age effects, an age-related improvement in phonemic-rate sensitivity was observed in the dyslexic adults compared to the dyslexic and skilled reader children. The dyslexic adults (some of whom had received training and remediation throughout life) may therefore have kept on improving their sensitivity to phonemic speech information throughout development, like their age-matched controls. Nonetheless, this enhancement did not allow them to catch up with their peers in their reading and phonological skills.

Regarding anatomical variations, we observed that CT in the auditory cortex of participants was modulated by their age group, independently of their reading level status. In particular, the auditory cortex in both the left and the right hemispheres was thinner in adults than in children. These data are consistent with research reporting developmental changes in cortical thinning in these regions (Magnotta et al., 1999; Shaw et al., 2008). In spite of the evidence provided by studies showing that auditory regions are typically larger in the left hemisphere than the right hemisphere (Geschwind and Levitsky, 1968; Galaburda et al., 1978; Rademacher, Caviness, Steinmetz and Galaburda, 1993; Penhune et al., 1996; Shapleske et al., 1999; Altarelli et al., 2014), this structural asymmetry was only obtained in our group of children. No structural differences between skilled readers and dyslexics were thus found in the left and right auditory cortex (Schultz et al., 1994). Nevertheless, we observed variations between the dyslexic and the control groups regarding the links between structural and functional asymmetries. After controlling for nonverbal IQ and chronological age (i.e., controlling for cortical thinning due to maturation; Magnotta et al., 1999; Shaw et al., 2008), we observed that the CT asymmetries and pruning were linked to a stronger phonemic-rate (30 Hz) sensitivity in skilled readers, but to a stronger syllabic-rate (4 Hz) sensitivity in dyslexic readers. Thus, the left auditory regions might be specialized for processing phonological units of different sizes (phoneme vs. syllable) in skilled and dyslexic readers. This relation between the CT pruning and the specialization to process high frequency oscillations might be a critical factor in improving phonological processing at the phonemic-level and adequate reading development. The lack of this relation in our dyslexic participants suggests that they may rely on syllabic units (large grain) for phonological analysis, whereas

skilled readers may preferentially use smaller units such as phonemes. This result is also in line with the synchronization enhancement observed at 4 Hz in the dyslexic group compared to the group of skilled readers.

Lastly, the impaired phonological sampling highlighted here in our dyslexic participants may also stem from a perturbation of the streams of information propagation (bottom- up, top-down) between lower and higher-level auditory regions. In fact, genetic factors (ectopias, Galaburda and Kemper, 1979) in dyslexia have been proposed to alter the neural interactions (gamma-theta) within the auditory cortex (Giraud and Ramus, 2013) involved in speech coding. Nevertheless, since we used non-linguistic stimuli (AM white noise), our study of the temporal sampling deficits in developmental dyslexia was constrained to the evaluation of the atypical neural responses within auditory primary areas. Future studies should be conducted to better characterize how an atypical auditory sampling in dyslexics hinders the following processing steps in higher level areas (i.e., left IFG) during *Speech perception*.

5 GENERAL DISCUSSION

In this section, we discuss the implications of the results obtained from our three studies. Firstly, we clarify the role of auditory cortical oscillations at different frequency bands in the processing of continuous speech. Secondly, we specify which cortical oscillations are disrupted in dyslexia in response to continuous speech perception and the consequences of such atypical speech sampling on the speech network, phonological and reading skills. Thirdly, we propose a structural explanation of atypical auditory oscillatory entrainment in dyslexia. Finally, we discuss how our work can lead to propose new ways to remediate reading difficulties in dyslexia, through music and rhythm interventions.

Before moving to the discussion of the results, in Table 10 we summarized the overlap of the participants across the three studies. From all the participants (normal readers) included in Study 1, 61% was included in Study 2 and in Study 3. From all the participants (normal and dyslexic readers) included in Study 2, 81 % of the normal readers and 67% of the dyslexic readers were included in Study 3. This strong overlapping allows us to compare results across studies and make a strong claim about the neural entrainment deficits in dyslexia.

	Study 1	**Study 2**	**Study 3**
Study 1	_	61% _	61% _
Study 2	61% _	_	81% 67%
Study 3	61% _	81% 67%	_

Table 10. Overlapping of the participants across studies. Red cells represent the percentages for dyslexic readers and blue cell represent the percentages for normal readers.

The role of neural oscillations during speech processing in normal readers

Speech comprises hierarchically organized rhythmic components that represent prosody (delta band), syllables (theta band) and phonemes (gamma band). During speech processing steps, cortical oscillations at different frequency bands track these quasi-rhythmic modulations. It is assumed that two critical processing steps

need to be carried out before extracting meaning from speech: a *de-multiplexing* step, the parallel analysis of different phonological components, and an *encoding* step, i.e., the segmentation of the speech stream into linguistically relevant chunks that can be individually processed (Stevens, 2002; Poeppel, 2003; Ghitza, 2011).

In Study 1, we computed a coherence analysis between the speech envelope and brain oscillations to better understand the frequency *de-multiplexing* neural mechanism. Coherence analysis was performed to determine correlations between magnetoencephalography (MEG) activity and the phonological components of the speech envelope. We observed neural entrainment to prosodic (delta) and syllabic (theta) components in different brain regions (Gross et al., 2013). Delta entrainment was observable in bilateral temporal and frontal regions, as well as in parietal areas (Bourguignon et al., 2013, Gross et al., 2013) whereas theta entrainment was more localized in temporal regions. In addition, we computed mutual information (MI) to analyze whether speech-entrained brain oscillations were hierarchically coupled across frequencies. In line with previous results (Gross et al., 2013), we found delta-theta and theta-gamma coupling within different brain regions (Figure 14). Delta-theta coupling emerged in bilateral fronto-parietal areas while theta-gamma coupling was localized in left temporal regions.

Regarding the latter coupling, it has been proposed that speech entrained theta oscillations control the spiking of gamma neurons involved in phonemic processing (Hyafil et al., 2015). The theta-gamma phase amplitude coupling (PAC) could be the neural mechanism through which phonemic related gamma activity is grouped into syllabic chunks for further processing. Delta-theta PAC was more distributed and extended to fronto-parietal regions. Fronto-parietal regions are linked to the maintenance of verbal sequences and higher cognitive processes, e.g. attentional control (Majerus, 2013; Ekman, Fiebach, Mezler, Tittgemeyer and Derrfuss, 2016). Studies from short term memory research have implicated bilateral fronto-parietal regions as being critical for buffering phonological representations during continuous speech processing. Indeed, we proposed that delta-theta coupling could be the neural mechanism through which syllabic units

are put together to build larger elements of language, such as word and phrase structures.

Speech processing models associate perceptual processes to neural computations in temporal regions, while higher-order processes are linked to frontal-parietal regions (Temple et al., 2003; Peelle et al., 2010; Peyrin et al., 2012; Wild et al., 2012). In Study 3, we evaluated the neural entrainment to amplitude modulated (AM) white noises at frequencies that correspond to the rhythmic components of speech. As previously shown (Hämäläinen et al., 2012), the processing of these non-linguistic stimuli is limited to auditory perceptual regions in our data, too (Figure 25). Interestingly, the regions that showed significant entrainment to AMs at 4, 7, 30 and 60 Hz (temporal areas) overlapped with the brain regions that showed theta entrainment and theta-gamma coupling during speech processing (Figure 16). This means that neural oscillations in theta and gamma frequency bands could underlie pure perceptual operations during speech processing. Nevertheless, the brain regions that showed neural entrainment to AMs at 2 Hz in Study 3 (temporal areas; Figure 25) differed from the brain regions showing delta entrainment and delta-theta coupling (fronto-temporo-parietal areas) during speech processing in Study 1 (Figure14 and Figure 16). These differences suggest that neural oscillations in the delta band are involved not only in perception but also in higher order cognitive operations, e.g. attention mechanisms (Lakatos et al., 2008).

It is known that during speech processing, perceptual and attentional computations interact, even before extracting meaning from the speech (Alsius, Navarra, Campbell and Soto, 2005). This means that functional connectivity between temporal, frontal and parietal regions is critical (Rauschecker and Scott, 2009; Peelle et al., 2010; Hickok and Poeppel, 2004). Recent studies suggest that slow brain oscillations facilitate communication between distant neural networks (Kopell, Ermentrout, Whittington and Traub, 2000; Jacobs and Kahana, 2010). In the connectivity analysis (partial direct coherence) of Study 2, we showed that slow (delta) neural oscillations facilitate the communication between temporal and fronto-parietal regions. Interestingly, we found that the right hemispheric phase locking to speech in the delta band modulated neural oscillations in frontal

areas, e.g. the left inferior frontal region (Figure 22). We postulated that low-frequency oscillations mediate bottom-up input streams through which perceptual information is transferred to left frontal areas where attentional processes are carried out (Wild et al., 2012). Similarly, we suggested that top-down processes would facilitate the allocation of attentional resources to informative parts of the speech, e.g. speech onsets. On this line, Park and colleagues (2015) showed that the strength of top-down modulations between fronto-parietal and temporal regions increases before the arrival of a speech onset. Top-down modulations reset the phase of ongoing delta oscillations in temporal regions, which effectively phase-lock the entire hierarchical structure of oscillatory activity to the stimulus (Gross et al., 2013). As a result of this delta phase resetting, theta-gamma PAC enhancement is observed mainly in left auditory regions during salient speech events (Lakatos et al., 2005; Gross et al., 2013).

Altogether, these results highlight the importance of delta neural oscillations during speech processing. We showed that delta cortical oscillations are associated with perceptual operations during speech processing, but also play an important role in attentional mechanisms. Furthermore, delta oscillations facilitated the communication within the brain network (fronto-temporo-parietal) involved in speech processing.

The auditory sampling deficit in dyslexia

Some appealing theories of dyslexia attribute a causal role to auditory atypical oscillatory neural activity, suggesting it generates some of the phonological problems in dyslexia (Goswami, 2011; Giraud and Ramus, 2013). These theories propose that auditory cortical oscillations of dyslexic individuals do not synchronize with prosodic, syllabic and phonemic cues in speech that are critical to properly process phonological information. The results of the present work contribute to refine these hypotheses.

In the coherence analysis of Study 2, we showed that dyslexic readers (as normal readers) presented significant brain-to-speech synchronization in the delta and theta frequency bands. As previously mentioned, speech-brain synchronization in the delta and theta bands is important to extract prosodic and syllabic information from speech (Poeppel, 20013). Importantly, in the delta band

(0.5-1 Hz), reduced speech-brain synchronization in dyslexic readers compared to normal readers emerged in both the right auditory cortex and the left inferior frontal gyrus (IFG). Entrainment differences in delta were maintained through development, as we did not observe differences between adults and children. Previous studies already reported atypical auditory entrainment in the delta band in dyslexia (Goswami, 2011; Hämäläinen et al., 2012). Interestingly, in Study 3, we did not found any differences between groups in the neural entrainment to AM noise at 2 Hz (delta band) in auditory regions. Although these results between Study 2 and Study 3 may seem contradictory, it is important to note that we did not observed speech-to-brain synchronization at 2 Hz in Study 2. This suggests that auditory entrainment to low-delta (0.5-1 Hz) amplitude fluctuations may be more important for speech processing (in Spanish), than neural entrainment to high-delta modulations (2 Hz). Furthermore, we showed that the brain sources showing synchronization to both nonverbal (Study 3) and speech (Study 1) auditory oscillations in the delta band were different and hardly comparable (Figure 14 and Figure 25). Again, this suggests that delta entrainment during speech processing involves perceptual and higher order computations, e.g. attention, during speech processing. Reduced auditory entrainment to delta fluctuation might cause deficits for processing slow fluctuations (prosodic contours) in speech (Goswami, 2011; Hämäläinen et al., 2012).

Regarding theta neural entrainment, in Study 2, no difference between groups was found in the brain-to-speech synchronization within the theta (5.8-6.3 Hz) band. Likewise, we did not find differences between the dyslexic and the control groups in the neural entrainment to AM noise at 7 Hz (high-theta) in Study 3. Nevertheless, differences emerged for AM noises at 4 Hz (low-theta): dyslexic readers (children and adults) presented stronger synchronization for AM noise processing at 4 Hz. Study 2 showed that brain-to-speech synchronization at high-theta (5.8-6.3 Hz) was important for speech processing, since both groups showed significant entrainment (second experiment). However, none of the groups showed significant brain-to-speech synchronization in the low-theta range (4Hz) compared to resting (Figure 13). This suggests that the speech signal may not contain essential syllabic information at 4 Hz and an enhancement of synchronization to speech at this frequency in dyslexia would not lead to any processing benefit

during speech processing (in Spanish). Furthermore, Study 3 showed that dyslexic readers presented reduced right hemispheric synchronization for sampling low frequency AMs (Poeppel, 2003) compared to normal readers. Importantly, rightwards lateralization for sampling syllabic-rate stimuli is likely to contribute to reading performance (see Abrams et al., 2009 for similar results) since we showed that stronger rightwards asymmetric synchronization to syllabic-rate AM noises was associated with faster word and pseudoword reading times in Study 3 (Figure 27).

No significant speech-to-brain synchronization was observed for frequencies above 7 Hz (Bourguignon et al., 2012) in normal readers, nor in dyslexics in Study 2 (Figure 13). However, when listening to AM white noise stimuli (Study 3), we observed that both groups showed significant entrainment at 30 and 60 Hz (Figure 25). It is likely that AM white noise stimuli entrained neural oscillations at high frequencies more efficiently than speech because of their perfect periodicity. In line with previous studies (Lehongre et al., 2013; Vanvooren et al., 2014), we showed that dyslexic participants (children and adults) exhibited reduced bilateral response for stimuli presented at 30 Hz (Poeppel, 2003), which also was reflected by a stronger right lateralized synchronization to phonemic-rate stimuli in the dyslexic groups (Figure 28). Right hemispheric lateralization has been linked to inattentive speech and non-speech processing (Scott et al., 2009) which, in the case of the present study, may indicate that dyslexic readers suffer from a limitation in the resources allocated to the processing of stimuli occurring at phonemic relevant rates. In fact, left-hemisphere lateralization for 30 and 60 Hz AMs correlated with the sum of phonemic errors in the phonological short term memory task.

Figure 31 summarizes the main results obtained across the three Studies. Overall, we showed that dyslexic readers presented stable atypical auditory entrainment to delta (prosodic), theta (syllabic) and gamma (phonemic) frequency bands across development. Furthermore, we demonstrated that neurophysiological oscillatory anomalies in dyslexia altered the asymmetric temporal sensitivity in auditory cortex observed in normal readers who exhibited a preferential processing of slower modulations by right auditory cortex, and bilateral processing for faster modulations.

Interestingly, we did not find significant difference in the PAC values between normal and dyslexic readers, neither in the delta-theta nor in the theta-gamma coupling. This leads us to suggest that the *encoding* mechanism *per se* may not affected in dyslexia, but that reduced delta speech-neural entrainment in dyslexia could affect higher frequency oscillations by the simple fact that delta is the first level within the spectral hierarchical coupling. Concretely, reduced delta entrainment in left frontal regions could disturb delta-theta coupling within these regions, and consequently, theta-gamma coupling in temporal regions. Abnormalities in the modulating frequency (delta) could lead to jitters in the segmentation of syllabic information, which in turn would cause distorted phonological representations in dyslexia.

Furthermore, we showed that in normal readers, delta oscillations controlled top-down and bottom up processes that facilitate the communication between fronto-temporo-parietal regions involved in speech processing. Reduced delta entrainment in dyslexia could affect bottom-up and top-down processes during speech processing. Interestingly, we found that the connectivity from the right auditory cortex to the left IFG was weaker in the dyslexic group than in the skilled reader group (both in children and adults). In other words, our results suggest that bottom-up processes that facilitate the transfer of phonological information towards higher cognitive processes are impaired in dyslexia. Moreover, abnormal delta entrainment in left frontal regions could compromise further top-down processes that drive attention towards relevant information within the speech, e.g. edges in the speech. Indeed, dyslexic readers present difficulties in the auditory processing of amplitude envelope rise time in speech (Goswami, 2007).

Together these results suggest that auditory entrainment to delta (0.5-1 Hz), theta (4 Hz) and gamma (30 Hz). Importantly, we suggested that atypical auditory entrainment to delta AMs in dyslexia could i) reduced the sensitivity to detect prosodic contours in speech, ii) disrupted the *encoding* of syllabic and phonemic information during speech processing and ii) compromised higher order operations involved in speech processing (e.g. attention).

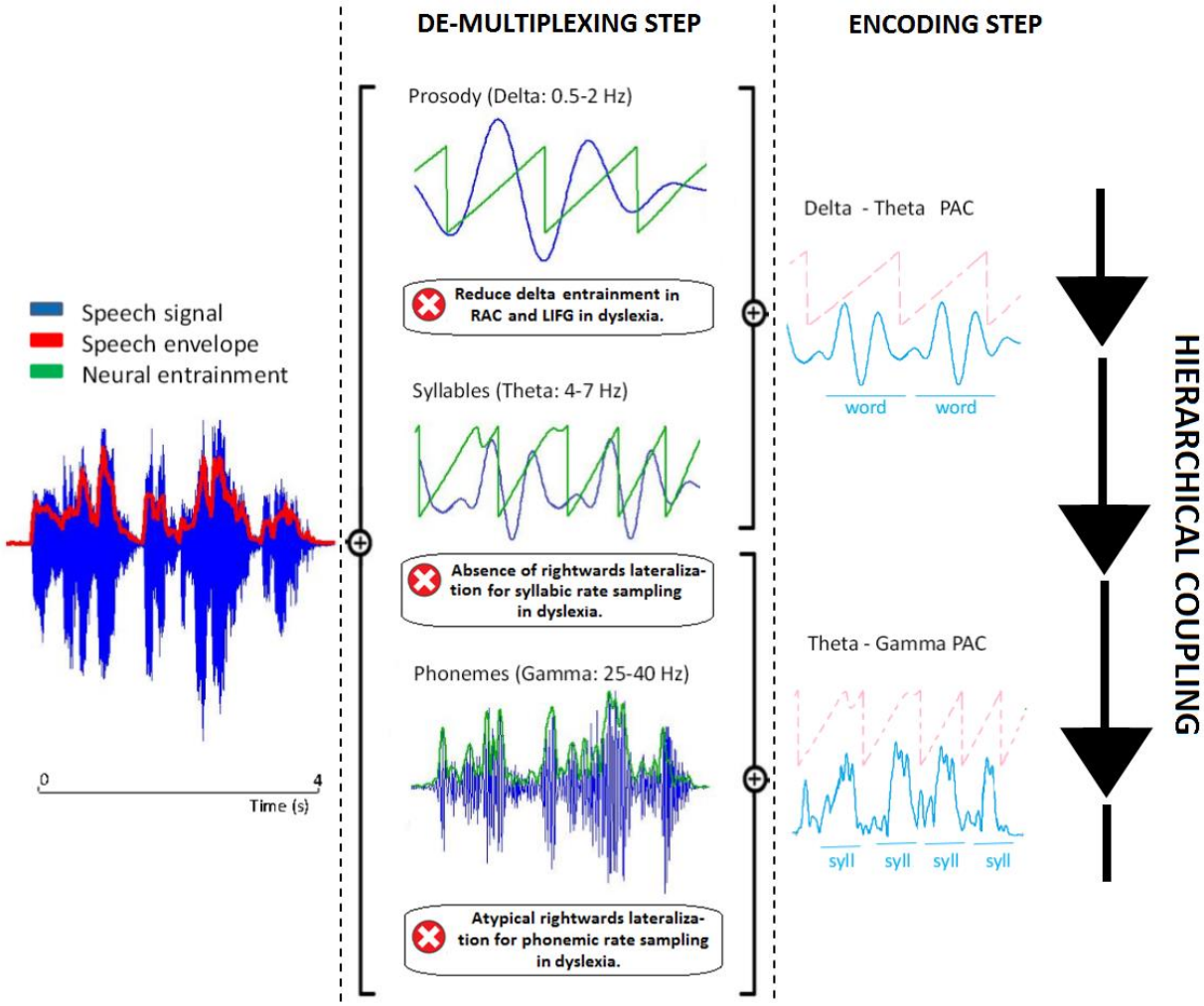

Figure 31. The figure summarizes the neural mechanisms involved in speech processing. Based on our results, we highlighted the steps where dyslexic readers showed atypical neural responses. On the left side, we represent the speech signal (blue) and the speech envelope (red). On the middle part of the figure, we show that the speech envelope contains linguistic information at multiple time-scales. The information on slow time scales, in the delta (0.5 – 2 Hz) and theta (4 – 7 Hz) band, corresponds to prosodic and syllabic information. The information at faster time rates, in the gamma (25 – 40 Hz) band, corresponds to phonemic information. Neural oscillations in different brain regions align their endogenous oscillations at mentioned frequencies with matching temporal modulations in the speech envelope. During the *de-multiplexing* step, the phase of delta and theta brain oscillations tracks prosodic and syllabic fluctuations (green signal). Similarly, the amplitude of gamma brain oscillations synchronizes to phonemic modulations (green signal). Atypical entrainment by dyslexic participants to prosodic, syllabic (Goswami 2011; Leong and Goswami 2014) and phonemic (Lehongre et al., 2013) rhythms of speech signal could be related to difficulties in the *de-multiplexing* step and affect subsequent processing steps (*encoding*). In Study 2, we showed that our dyslexic group presented difficulties tracking prosodic rhythms (delta) of speech. In Study 3, we determined atypical neural entrainment to sample slow (theta) and fast (gamma) AMs. On the right part of the figure, we illustrate how speech entrained brain oscillations are hierarchically coupled for mediating the *encoding* of phonological units. In Study 1, we highlighted PAC between delta-theta and theta-gamma frequency bands during speech processing.

The underlying anatomical correlates of the auditory deficits in dyslexia

In Study 3, besides MEG data, we collected structural MRI data to estimate cortical thickness (CT) of the auditory cortex of participants (children and adult with and without dyslexia).

By focusing on structural data, we observed that CT in bilateral auditory cortex of participants was modulated by their age group, independently of their reading level status. This data is consistent with research reporting a cortical pruning in these regions due to increased experience with auditory (or speech) stimuli (Magnotta et al., 1999; Shaw et al., 2008). Importantly, no CT differences between normal and dyslexic readers were found in the left and the right auditory cortex (Schultz et al., 1994; Eckert et al., 2003). However, we observed variations between dyslexic and normal readers regarding the links between CT and neural entrainment asymmetries.

Interestingly, having structural and functional data within the same participants allowed us to better characterize the links between the anatomy of the auditory cortex and its oscillatory responses. We showed that a leftwards hemispheric lateralization in CT (thinner cortex in the left hemisphere than the right hemisphere) was related to a stronger left hemispheric lateralization of neural entrainment to stimuli presented at the phonemic rate (30 Hz) in normal readers. In contrast, the same anatomical index was related to a stronger rightwards hemispheric lateralization for neural entrainment to stimuli presented at the syllabic rate (4 Hz) in dyslexic readers. This relation between CT pruning and the specialization to process high frequency oscillations might be a critical factor in developing phonemic awareness in normal readers. The lack of this relation in our dyslexic group could affect the way in which the phonological awareness skill develops progressing from larger to smaller units of sound. The relation between CT pruning and the specialization to processes low frequency oscillations in dyslexia could indicate that dyslexic readers developed stronger syllabic than phonemic sensitivity to process auditory stimuli, and remained anchored at a coarse grain level, which impairs grapheme-to-phoneme conversion. This result is also in line with the synchronization enhancement observed at 4 Hz in the dyslexic group compared to the group of controls.

Is it possible to improve neural entrainment in dyslexia?

Our results suggest that dyslexic readers present auditory entrainment deficits to slow fluctuations that could affect multiple neural mechanisms involved in speech processing. This said, how could synchronization to speech rhythms be enhanced in dyslexia?

In one of our recent studies we tested whether priming speech sentences with their amplitude envelope low-pass filtered at 8 Hz would improve the perception of this sentence (Ríos, Molnar, Lizarazu, and Lallier, under review). This task was used to entrain the perceptual and attentional auditory system with the structure of speech before listening to the target speech signal. We hypothesized that the priming would facilitate the extraction of the low frequency components in the target sentence, upon which higher linguistic processes involved in speech perception will rely. Accordingly, children were more accurate to recognize a pseudoword within a sentence presented in quiet or multi-talker babble noise, when the sentence was primed by its amplitude envelope (<8 Hz) compared to when it was preceded by an un-modulated white noise. Interestingly, the priming benefit (pseudoword identification accuracy of the primed versus non-primed sentence) was related to the reading skills of the children. Poorest readers were the ones that exhibited the highest benefit from the speech envelope prime. Our study is in line with research showing that repetition of speech helps cognitive and neural resources to focus on finer grain acoustic information in the repeated speech segments (Deutsch, Lapidis, and Henthorn, 2008; Tierney, Dick, Deutsch, and Sereno, 2013).

Interestingly, repetition is a fundamental component of music. Indeed, musical rhythmic patterns are periodic, which allows the perceptual and attentional auditory systems to predict when the next beat is going to occur. Psychological and neuroscientific research demonstrated that musical training positively affects cognitive development (Miendlarzewsks and Trost, 2013). It has been shown that children who undergo musical training have better verbal memory, second language pronunciation accuracy and reading ability. Therefore, it is not surprising that the research in dyslexia is now focusing on the potential beneficial effects of music on phonological and reading development. The right

auditory cortex, like in speech processing, is crucial for perceiving some aspect of slow rhythms during music listening. Furthermore, the connectivity between the right auditory cortex and frontal regions facilitate the development of musical skills (Albouy et al., 2013; Peretz, 2013; Peretz, Vuvan, Lagrois and Armony, 2015). This strikingly echoes the results of the Study 2, reporting that the connectivity between the right auditory and the left frontal regions in the delta frequency band was strongly related to phonological and reading skills.

The relation between speech rhythm, music rhythm and reading is also reflected in data showing that sensitivity to rise time is associated with sensitivity to musical rhythmic parameters, which furthermore predicts phonological awareness and reading development (Huss, Verney, Fosker, Mead and Goswami, 2011). If we can confirm that music training programs positively impact the development of reading and reading related skills (Thomson, Leong and Goswami, 2013; Chobert, François, Velay and Besson, 2014), music should become a significant part of educational and health practice, since it can improve durably the life of the dyslexic population.

6 CONCLUSIONS

Overall, the present work strengthens proposals assuming that the impaired perception of speech sounds (prosodic, syllabic and phonemic cues) affects phonological processing in dyslexia at the early (children) and later (adults) stages of reading development. Importantly, we showed that atypical neural entrainment to delta modulations in dyslexic readers could affect multiple neural mechanisms involved in speech processing, i.e. *de-multiplexing*, *encoding* and connectivity processes. Furthermore, we showed for the first time that atypical specialization of the CT thickness to slow and fast AMs in dyslexia underlie the acoustic sampling deficit experienced in dyslexia.

Overall, the present work opens a framework to develop new tools for the early detection of dyslexia. We hope that running longitudinal experiments in pre-reader children could help determine whether some of the oscillatory neuromarkers highlighted across our studies are able to predict which child will suffer from dyslexia even before they start to learn to read.

For example, the task in Study 3 does not required attention nor any reading skills, but could be used to evaluate the child's ability to entrain to relevant frequencies (delta, theta, and gamma). This could provide insights of the ability to segment the speech stream of each child with respect to its peers. We expect that children at risk of developing dyslexia will present the lowest synchronization values to delta rates. Furthermore, we hypothesize that these children show reduced neural synchronization to syllabic and phonemic rates compared to children and adult literates, as the sensitivity to syllabic and phonemic structures of words still has to develop with reading acquisition.

7 REFERENCES

Abrams, D. A., Nicol, T., Zecker, S., & Kraus, N. (2009). Abnormal cortical processing of the syllable rate of speech in poor readers. The Journal of Neuroscience, 29(24), 7686-7693.

Adams, M. J. (1994). Beginning to read: Thinking and learning about print. MIT press.

Ahissar, E., Nagarajan, S., Ahissar, M., Protopapas, A., Mahncke, H., & Merzenich, M. M. (2001). Speech comprehension is correlated with temporal response patterns recorded from auditory cortex. Proceedings of the National Academy of Sciences, 98(23), 13367-13372.

Aitkin, L. M., & Webster, W. R. (1972). Medial geniculate body of the cat: organization and responses to tonal stimuli of neurons in ventral division. Journal of Neurophysiology.

Albouy, P., Mattout, J., Bouet, R., Maby, E., Sanchez, G., Aguera, P. E., ... & Tillmann, B. (2013). Impaired pitch perception and memory in congenital amusia: the deficit starts in the auditory cortex. Brain, 136(5), 1639-1661.

Alsius, A., Navarra, J., Campbell, R., & Soto-Faraco, S. (2005). Audiovisual integration of speech falters under high attention demands. Current Biology, 15(9), 839-843.

Altarelli, I., Leroy, F., Monzalvo, K., Fluss, J., Billard, C., Dehaene-Lambertz, G., ... & Ramus, F. (2014). Planum temporale asymmetry in developmental dyslexia: revisiting an old question. Human brain mapping, 35(12), 5717-5735.

Altarelli, I., Leroy, F., Monzalvo, K., Fluss, J., Billard, C., Dehaene-Lambertz, G., ... & Ramus, F. (2014). Planum temporale asymmetry in developmental dyslexia: revisiting an old question. Human brain mapping, 35(12), 5717-5735.

Amitay, S., Ahissar, M., & Nelken, I. (2002). Auditory processing deficits in reading disabled adults. Journal of the Association for Research in Otolaryngology, 3(3), 302-320.

Anthony, J. L., & Francis, D. J. (2005). Development of phonological awareness. Current Directions in Psychological Science, 14(5), 255-259.

Arvaniti, A. (2009). Rhythm, timing and the timing of rhythm. Phonetica, 66(1-2), 46-63.

Baccalá, L. A., & Sameshima, K. (2001). Partial directed coherence: a new concept in neural structure determination. Biological cybernetics, 84(6), 463-474.

Bancaud, J., & Talairach, J. (1965). La stéréo-électroencéphalographie dans l'épilepsie: informations neurophysiopathologiques apportées par l'investigation fonctionnelle stéreotaxique, par J. Bancaud, J. Talairach et [leurs collaborateurs] A. Bonis [et al.]. Masson.

Bartlett, E. L. (2013). The organization and physiology of the auditory thalamus and its role in processing acoustic features important for speech perception. Brain and language, 126(1), 29-48.

Bell, A. J., & Sejnowski, T. J. (1995). An information-maximization approach to blind separation and blind deconvolution. Neural computation, 7(6), 1129-1159.

Bendor, D., & Wang, X. (2007). Differential neural coding of acoustic flutter within primate auditory cortex. Nature neuroscience, 10(6), 763-771.

Berthier, M. L., & Ralph, M. A. L. (2014). Dissecting the function of networks underpinning language repetition. Dissecting the function of networks underpinning language repetition, 5.

Binder, J. R., Rao, S. M., Hammeke, T. A., Yetkin, F. Z., Jesmanowicz, A., Bandettini, P. A., ... & Hyde, J. S. (1994). Functional magnetic resonance imaging of human auditory cortex. Annals of neurology, 35(6), 662-672.

Blumstein, S. E., Cooper, W. E., Zurif, E. B., & Caramazza, A. (1977). The perception and production of voice-onset time in aphasia. Neuropsychologia, 15(3), 371-383.

Boatman, D., Lesser, R. P., & Gordon, B. (1995). Auditory speech processing in the left temporal lobe: an electrical interference study. Brain and language, 51(2), 269-290.

Boemio, A., Fromm, S., Braun, A., & Poeppel, D. (2005). Hierarchical and asymmetric temporal sensitivity in human auditory cortices. Nature neuroscience, 8(3), 389-395.

Boets, B. (2014). Dyslexia: reconciling controversies within an integrative developmental perspective. Trends in cognitive sciences, 18(10), 501-503.

Boets, B., de Beeck, H. P. O., Vandermosten, M., Scott, S. K., Gillebert, C. R., Mantini, D., ... & Ghesquière, P. (2013). Intact but less accessible phonetic representations in adults with dyslexia. Science, 342(6163), 1251-1254.

Bortel, R., & Sovka, P. (2007). Approximation of statistical distribution of magnitude squared coherence estimated with segment overlapping. Signal Processing, 87(5), 1100-1117.

Bourguignon, M., De Tiege, X., de Beeck, M. O., Ligot, N., Paquier, P., Van Bogaert, P., ... & Jousmäki, V. (2013). The pace of prosodic phrasing couples the listener's cortex to the reader's voice. Human brain mapping, 34(2), 314-326.

Bowers P. (1989). Naming speed and phonological awareness: Independent contributors to reading disabilities. National Reading Conference Yearbook, 38, 165-172.

Bowers, P. G., & Wolf, M. (1993). Theoretical links among naming speed, precise timing mechanisms and orthographic skill in dyslexia. Reading and Writing, 5(1), 69-85.

Bradley, L., & Bryant, P. E. (1978). Difficulties in auditory organisation as a possible cause of reading backwardness. Nature.

Brady, S., Shankweiler, D., & Mann, V. (1983). Speech perception and memory coding in relation to reading ability. Journal of experimental child psychology, 35(2), 345-367.

Breier, J. I., Gray, L., Fletcher, J. M., Diehl, R. L., Klaas, P., Foorman, B. R., & Molis, M. R. (2001). Perception of voice and tone onset time continua in children with dyslexia with and without attention deficit/hyperactivity disorder. Journal of experimental child psychology, 80(3), 245-270.

Brodmann, K. (1909). Vergleichende Lokalisationslehre der Groshirnrinde. Barth.

Brown, W. E., Eliez, S., Menon, V., Rumsey, J. M., White, C. D., & Reiss, A. L. (2001). Preliminary evidence of widespread morphological variations of the brain in dyslexia. Neurology, 56(6), 781-783.

Brugge, J. F., Nourski, K. V., Oya, H., Reale, R. A., Kawasaki, H., Steinschneider, M., & Howard, M. A. (2009). Coding of repetitive transients by auditory cortex on Heschl's gyrus. Journal of Neurophysiology, 102(4), 2358-2374.

Bryant, P. (1998). Sensitivity to onset and rhyme does predict young children's reading: a comment on Muter, Hulme, Snowling, and Taylor (1997). Journal of Experimental Child Psychology, 71(1), 29-37.

Butler, B. E., & Lomber, S. G. (2015). Functional and structural changes throughout the auditory system following congenital and early-onset deafness: implications for hearing restoration. The effect of hearing loss on neural processing.

Canolty, R. T., & Knight, R. T. (2010). The functional role of cross-frequency coupling. Trends in cognitive sciences, 14(11), 506-515.

Castles, A., & Coltheart, M. (2004). Is there a causal link from phonological awareness to success in learning to read?. Cognition, 91(1), 77-111.

Catts, H. W., Fey, M. E., Zhang, X., & Tomblin, J. B. (2001). Estimating the Risk of Future Reading Difficulties in Kindergarten ChildrenA Research-Based Model and Its Clinical Implementation. Language, speech, and hearing services in schools, 32(1), 38-50.

Catts, H. W., Adlof, S. M., Hogan, T. P., & Weismer, S. E. (2005). Are specific language impairment and dyslexia distinct disorders?. Journal of Speech, Language, and Hearing Research, 48(6), 1378-1396.

Caviness Jr, V. S., Evrard, P., & Lyon, G. (1978). Radial neuronal assemblies, ectopia and necrosis of developing cortex: a case analysis. Acta neuropathologica, 41(1), 67-72.

Chan, A. M., Dykstra, A. R., Jayaram, V., Leonard, M. K., Travis, K. E., Gygi, B., ... & Cash, S. S. (2014). Speech-specific tuning of neurons in human superior temporal gyrus. Cerebral Cortex, 24(10), 2679-2693.

Chiappe, P., Stringer, R., Siegel, L. S., & Stanovich, K. E. (2002). Why the timing deficit hypothesis does not explain reading disability in adults. Reading and Writing, 15(1-2), 73-107.

Chobert, J., François, C., Velay, J. L., & Besson, M. (2014). Twelve months of active musical training in 8-to 10-year-old children enhances the preattentive processing of syllabic duration and voice onset time. Cerebral Cortex, 24(4), 956-967.

Cogan, G. B., & Poeppel, D. (2011). A mutual information analysis of neural coding of speech by low-frequency MEG phase information. Journal of neurophysiology, 106(2), 554-563.

Compton, D. L. (2003). Modeling the relationship between growth in rapid naming speed and growth in decoding skill in first-grade children. Journal of Educational Psychology, 95(2), 225.

Cossu, G., Shankweiler, D., Liberman, I. Y., Katz, L., & Tola, G. (1988). Awareness of phonological segments and reading ability in Italian children. Applied psycholinguistics, 9(01), 1-16.

Crawford, J. R., & Howell, D. C. (1998). Comparing an individual's test score against norms derived from small samples. The Clinical Neuropsychologist, 12(4), 482-486.

Crawford, J. R., Garthwaite, P. H., Azzalini, A., Howell, D. C., & Laws, K. R. (2006). Testing for a deficit in single-case studies: Effects of departures from normality. Neuropsychologia, 44(4), 666-677.

Cuetos, F., Rodríguez, B., Ruano, E., & Arribas, D. (2007). Batería de evaluación de los procesos lectores. Revisada (PROLEC-R). Madrid: TEA.

Curtin, S. (2010). Young infants encode lexical stress in newly encountered words. Journal of experimental child psychology, 105(4), 376-385.

Cutini, S., Szűcs, D., Mead, N., Huss, M., & Goswami, U. (2016). Atypical right hemisphere response to slow temporal modulations in children with developmental dyslexia. NeuroImage.

Dalby, M. A., Elbro, C., & Stødkilde-Jørgensen, H. (1998). Temporal Lobe Asymmetry and Dyslexia: Anin VivoStudy Using MRI. Brain and Language, 62(1), 51-69.

Dale, A. M., & Sereno, M. I. (1993). Improved localizadon of cortical activity by combining EEG and MEG with MRI cortical surface reconstruction: a linear approach. Journal of cognitive neuroscience, 5(2), 162-176.

Dale, A. M., Fischl, B., & Sereno, M. I. (1999). Cortical surface-based analysis: I. Segmentation and surface reconstruction. Neuroimage, 9(2), 179-194.

Dauer, R. M. (1983). Stress-timing and syllable-timing reanalyzed. Journal of phonetics.

De Martino, S., Espesser, R., Rey, V., & Habib, M. (2001). The “temporal processing deficit” hypothesis in dyslexia: New experimental evidence. Brain and cognition, 46(1), 104-108.

Denckla, M. B., & Rudel, R. G. (1976). Rapid ‘automatized’naming (RAN): Dyslexia differentiated from other learning disabilities. Neuropsychologia, 14(4), 471-479.

Deutsch, G. K., Dougherty, R. F., Bammer, R., Siok, W. T., Gabrieli, J. D., & Wandell, B. (2005). Children's reading performance is correlated with white matter structure measured by diffusion tensor imaging. Cortex, 41(3), 354-363.

Deutsch, D., Lapidis, R., & Henthorn, T. (2008). The speech-to-song illusion. Journal of the Acoustical Society of America, 124(4), 2471.

Ding, N., Chatterjee, M., & Simon, J. Z. (2014). Robust cortical entrainment to the speech envelope relies on the spectro-temporal fine structure. Neuroimage, 88, 41-46.

Doelling, K. B., Arnal, L. H., Ghitza, O., & Poeppel, D. (2014). Acoustic landmarks drive delta–theta oscillations to enable speech comprehension by facilitating perceptual parsing. Neuroimage, 85, 761-768.

Dole, M., Hoen, M., & Meunier, F. (2012). Speech-in-noise perception deficit in adults with dyslexia: Effects of background type and listening configuration. Neuropsychologia, 50(7), 1543-1552.

Drullman, R., Festen, J. M., & Plomp, R. (1994). Effect of reducing slow temporal modulations on speech reception. The Journal of the Acoustical Society of America, 95(5), 2670-2680.

Eckert, M. A., Lombardino, L. J., & Leonard, C. M. (2001). Planar asymmetry tips the phonological playground and environment raises the bar. Child development, 72(4), 988-1002.

Ehri, L. C., Nunes, S. R., Willows, D. M., Schuster, B. V., Yaghoub-Zadeh, Z., & Shanahan, T. (2001). Phonemic awareness instruction helps children learn to read: Evidence from the National Reading Panel's meta-analysis. Reading research quarterly, 36(3), 250-287.

Ekman, M., Fiebach, C. J., Melzer, C., Tittgemeyer, M., & Derrfuss, J. (2016). Different roles of direct and indirect frontoparietal pathways for individual working memory capacity. The Journal of Neuroscience, 36(10), 2894-2903.

Eliez, S., Rumsey, J. M., Giedd, J. N., Schmitt, J. E., Patwardhan, A. J., & Reiss, A. L. (2000). Morphological alteration of temporal lobe gray matter in dyslexia: an MRI study. Journal of Child Psychology and Psychiatry, 41(05), 637-644.

Elliott, T. M., & Theunissen, F. E. (2009). The modulation transfer function for speech intelligibility. PLoS comput biol, 5(3), e1000302.

Fan, P., Manoli, D. S., Ahmed, O. M., Chen, Y., Agarwal, N., Kwong, S., ... & Shah, N. M. (2013). Genetic and neural mechanisms that inhibit Drosophila from mating with other species. Cell, 154(1), 89-102.

Fawcett, A. J., Nicolson, R. I., & Dean, P. (1996). Impaired performance of children with dyslexia on a range of cerebellar tasks. Annals of Dyslexia, 46(1), 259-283.

Fine, J. G., Semrud-Clikeman, M., Keith, T. Z., Stapleton, L. M., & Hynd, G. W. (2007). Reading and the corpus callosum: An MRI family study of volume and area. Neuropsychology, 21(2), 235.

Fischl, B., Sereno, M. I., & Dale, A. M. (1999). Cortical surface-based analysis: II: inflation, flattening, and a surface-based coordinate system. Neuroimage, 9(2), 195-207.

Fischl, B., & Dale, A. M. (2000). Measuring the thickness of the human cerebral cortex from magnetic resonance images. Proceedings of the National Academy of Sciences, 97(20), 11050-11055.

Fischl, B., Salat, D. H., Busa, E., Albert, M., Dieterich, M., Haselgrove, C., ... & Montillo, A. (2002). Whole brain segmentation: automated labeling of neuroanatomical structures in the human brain. Neuron, 33(3), 341-355.

Fontolan, L., Morillon, B., Liegeois-Chauvel, C., & Giraud, A. L. (2014). The contribution of frequency-specific activity to hierarchical information processing in the human auditory cortex. Nature communications, 5.

Foundas, A. L., Leonard, C. M., Gilmore, R., Fennell, E., & Heilman, K. M. (1994). Planum temporale asymmetry and language dominance. Neuropsychologia, 32(10), 1225-1231.

France, S. J., Rosner, B. S., Hansen, P. C., Calvin, C., Talcott, J. B., Richardson, A. J., & Stein, J. F. (2002). Auditory frequency discrimination in adult developmental dyslexics. Perception & psychophysics, 64(2), 169-179.

Friederici, A. D. (2011). The brain basis of language processing: from structure to function. Physiological reviews, 91(4), 1357-1392.

Froyen, D. J., Bonte, M. L., van Atteveldt, N., & Blomert, L. (2009). The long road to automation: neurocognitive development of letter–speech sound processing. Journal of Cognitive Neuroscience, 21(3), 567-580.

Fuchs, M., Wagner, M., Wischmann, H. A., Köhler, T., Theißen, A., Drenckhahn, R., & Buchner, H. (1998). Improving source reconstructions by combining bioelectric

and biomagnetic data. Electroencephalography and clinical neurophysiology, 107(2), 93-111.

Gaab, N., Gabrieli, J. D. E., Deutsch, G. K., Tallal, P., & Temple, E. (2007). Neural correlates of rapid auditory processing are disrupted in children with developmental dyslexia and ameliorated with training: an fMRI study. Restorative neurology and neuroscience, 25(3-4), 295-310.

Galaburda, A. M. (1989). Ordinary and extraordinary brain development: Anatomical variation in developmental dyslexia. Annals of Dyslexia, 39(1), 65-80.

Galaburda, A. M. (1999). Developmental dyslexia: A multilevel syndrome. Dyslexia, 5(4), 183.

Galaburda, A. M., LeMay, M., Kemper, T. L., & Geschwind, N. (1978). Right-left asymmetrics in the brain. Science, 199(4331), 852-856.

Galaburda, A. M., & Kemper, T. L. (1979). Cytoarchitectonic abnormalities in developmental dyslexia: a case study. Annals of neurology, 6(2), 94-100.

Galaburda, A., & Sanides, F. (1980). Cytoarchitectonic organization of the human auditory cortex. Journal of Comparative Neurology, 190(3), 597-610.

Galaburda, A. M., Sherman, G. F., Rosen, G. D., Aboitiz, F., & Geschwind, N. (1985). Developmental dyslexia: four consecutive patients with cortical anomalies. Annals of neurology, 18(2), 222-233.

Gandour, J., Wong, D., & Hutchins, G. (1998). Pitch processing in the human brain is influenced by language experience. Neuroreport, 9(9), 2115-2119.

Geschwind, N., & Levitsky, M. (1968). Human brain: left-right asymmetries in temporal speech region. Science, 161, 186-187.

Geschwind, N., & Galaburda, A. M. (1985). Cerebral lateralization: Biological mechanisms, associations, and pathology: I. A hypothesis and a program for research. Archives of neurology, 42(5), 428-459.

Ghitza, O. (2011). Linking speech perception and neurophysiology: speech decoding guided by cascaded oscillators locked to the input rhythm. Frontiers in psychology, 2, 130.

Ghitza, O., & Greenberg, S. (2009). On the possible role of brain rhythms in speech perception: intelligibility of time-compressed speech with periodic and aperiodic insertions of silence. Phonetica, 66(1-2), 113-126.

Giedd, J. N. (2004). Structural magnetic resonance imaging of the adolescent brain. Annals of the New York Academy of Sciences, 1021(1), 77-85.

Giedd, J. N., Blumenthal, J., Jeffries, N. O., Castellanos, F. X., Liu, H., Zijdenbos, A., ... & Rapoport, J. L. (1999). Brain development during childhood and adolescence: a longitudinal MRI study. Nature neuroscience, 2(10), 861-863.

Gillon, G. T. (2007). Phonological awareness: From research to practice. Guilford Press.

Giraud, A. L., Lorenzi, C., Ashburner, J., Wable, J., Johnsrude, I., Frackowiak, R., & Kleinschmidt, A. (2000). Representation of the temporal envelope of sounds in the human brain. Journal of Neurophysiology, 84(3), 1588-1598.

Giraud, A. L., & Poeppel, D. (2012a). Speech perception from a neurophysiological perspective. In The human auditory cortex (pp. 225-260). Springer New York.

Giraud, A. L., & Poeppel, D. (2012b). Cortical oscillations and speech processing: emerging computational principles and operations. Nature neuroscience, 15(4), 511-517.

Giraud, A. L., & Ramus, F. (2013). Neurogenetics and auditory processing in developmental dyslexia. Current opinion in neurobiology, 23(1), 37-42.

Gogtay, N., Giedd, J. N., Lusk, L., Hayashi, K. M., Greenstein, D., Vaituzis, A. C., ... & Rapoport, J. L. (2004). Dynamic mapping of human cortical development during childhood through early adulthood. Proceedings of the National academy of Sciences of the United States of America, 101(21), 8174-8179.

Goswami, U. (1998). The role of analogies in the development of word recognition. Word recognition in beginning literacy, 41-63.

Goswami, U. (2011). A temporal sampling framework for developmental dyslexia. Trends in cognitive sciences, 15(1), 3-10.

Goswami, U. (2015). Sensory theories of developmental dyslexia: three challenges for research. Nature Reviews Neuroscience, 16(1), 43-54.

Goswami, U., & Bryant, P. (1990). Phonological skills and learning to read (No. Sirsi) i9780863771507). Hove: Lawrence Erlbaum.

Goswami, U., Thomson, J., Richardson, U., Stainthorp, R., Hughes, D., Rosen, S., & Scott, S. K. (2002). Amplitude envelope onsets and developmental dyslexia: A new hypothesis. Proceedings of the National Academy of Sciences, 99(16), 10911-10916.

Goswami, U., & Leong, V. (2013). Speech rhythm and temporal structure: converging perspectives. Lab. Phonol, 4(1), 67-92.

Goswami, U., Power, A. J., Lallier, M., & Facoetti, A. (2014). Oscillatory "temporal sampling" and developmental dyslexia: toward an over-arching theoretical framework. Frontiers in human neuroscience, 8.

Gould, J. H., & Glencross, D. J. (1990). Do children with a specific reading disability have a general serial-ordering deficit?. Neuropsychologia, 28(3), 271-278.

Gramfort, A., Luessi, M., Larson, E., Engemann, D. A., Strohmeier, D., Brodbeck, C., ... & Hämäläinen, M. S. (2014). MNE software for processing MEG and EEG data. Neuroimage, 86, 446-460.

Granger, C. W. (1969). Investigating causal relations by econometric models and cross-spectral methods. Econometrica: Journal of the Econometric Society, 424-438.

Greenberg, S., Carvey, H., Hitchcock, L., & Chang, S. (2003). Temporal properties of spontaneous speech—a syllable-centric perspective. Journal of Phonetics, 31(3), 465-485.

Greenberg, S. (2006). A multi-tier framework for understanding spoken language. Listening to speech: An auditory perspective, 411-433.

Gross, J., Kujala, J., Hämäläinen, M., Timmermann, L., Schnitzler, A., & Salmelin, R. (2001). Dynamic imaging of coherent sources: studying neural interactions in the human brain. *Proceedings of the National Academy of Sciences*, *98*(2), 694-699.

Gross, J., Hoogenboom, N., Thut, G., Schyns, P., Panzeri, S., Belin, P., & Garrod, S. (2013). Speech rhythms and multiplexed oscillatory sensory coding in the human brain. PLoS Biol, 11(12), e1001752.

Gütig, R., & Sompolinsky, H. (2009). Time-warp–invariant neuronal processing. PLoS Biol, 7(7), e1000141.

Hackett, T. A., Stepniewska, I., & Kaas, J. H. (1998). Subdivisions of auditory cortex and ipsilateral cortical connections of the parabelt auditory cortex in macaque monkeys. Journal of Comparative Neurology, 394(4), 475-495.

Hallez, H., Vanrumste, B., Van Hese, P., D'Asseler, Y., Lemahieu, I., & Van de Walle, R. (2005). A finite difference method with reciprocity used to incorporate anisotropy in electroencephalogram dipole source localization. Physics in medicine and biology, 50(16), 3787.

Hansen, P., Kringelbach, M., & Salmelin, R. (2010). MEG: an introduction to methods. Oxford university press.

Hämäläinen, M. S., & Sarvas, J. (1989). Realistic conductivity geometry model of the human head for interpretation of neuromagnetic data. IEEE transactions on biomedical engineering, 36(2), 165-171.

Hämäläinen, M., Hari, R., Ilmoniemi, R. J., Knuutila, J., & Lounasmaa, O. V. (1993). Magnetoencephalography—theory, instrumentation, and applications to noninvasive studies of the working human brain. Reviews of modern Physics, 65(2), 413.

Hämäläinen, M., & Hari, R. (2002). Magnetoencephalographic characterization of dynamic brain activation: Basic principles and methods of data collection and source analysis. Brain mapping: The methods, 227-254.

Hämäläinen, J. A., Rupp, A., Soltész, F., Szücs, D., & Goswami, U. (2012). Reduced phase locking to slow amplitude modulation in adults with dyslexia: an MEG study. Neuroimage, 59(3), 2952-2961.

Harris, M., & Hatano, G. (1999). Learning to read and write: A cross-linguistic perspective (Vol. 2). Cambridge University Press.

Hasan, K. M., Molfese, D. L., Walimuni, I. S., Stuebing, K. K., Papanicolaou, A. C., Narayana, P. A., & Fletcher, J. M. (2012). Diffusion tensor quantification and cognitive correlates of the macrostructure and microstructure of the corpus callosum in typically developing and dyslexic children. NMR in Biomedicine, 25(11), 1263-1270.

Hazan, V., & Barrett, S. (2000). The development of phonemic categorization in children aged 6–12. Journal of phonetics, 28(4), 377-396.

Helenius, P., Salmelin, R., Connolly, J. F., Leinonen, S., & Lyytinen, H. (2002). Cortical activation during spoken-word segmentation in nonreading-impaired and dyslexic adults. The Journal of neuroscience, 22(7), 2936-2944.

Hickok, G., & Poeppel, D. (2004). Dorsal and ventral streams: a framework for understanding aspects of the functional anatomy of language. Cognition, 92(1), 67-99.

Hickok, G., & Poeppel, D. (2007). The cortical organization of speech processing. Nature Reviews Neuroscience, 8(5), 393-402.

Hill, K. T., & Miller, L. M. (2009). Auditory attentional control and selection during cocktail party listening. Cerebral cortex, bhp124.

Huss, M., Verney, J. P., Fosker, T., Mead, N., & Goswami, U. (2011). Music, rhythm, rise time perception and developmental dyslexia: perception of musical meter predicts reading and phonology. Cortex, 47(6), 674-689.

Hutsler, J., & Galuske, R. A. (2003). Hemispheric asymmetries in cerebral cortical networks. Trends in neurosciences, 26(8), 429-435.

Hyafil, A., Giraud, A. L., Fontolan, L., & Gutkin, B. (2015). Neural cross-frequency coupling: connecting architectures, mechanisms, and functions. Trends in neurosciences, 38(11), 725-740.

Jacobs, J., & Kahana, M. J. (2010). Direct brain recordings fuel advances in cognitive electrophysiology. Trends in cognitive sciences, 14(4), 162-171.

Jensen, O., & Lisman, J. E. (1996). Theta/gamma networks with slow NMDA channels learn sequences and encode episodic memory: role of NMDA channels in recall. Learning & Memory, 3(2-3), 264-278.

Joanisse, M. F., Manis, F. R., Keating, P., & Seidenberg, M. S. (2000). Language deficits in dyslexic children: Speech perception, phonology, and morphology. Journal of experimental child psychology, 77(1), 30-60.

Jorm, A. F. (1979). The cognitive and neurological basis of developmental dyslexia: A theoretical framework and review. Cognition, 7(1), 19-33.

Kaas, J. H., Hackett, T. A., & Tramo, M. J. (1999). Auditory processing in primate cerebral cortex. Current opinion in neurobiology, 9(2), 164-170.

Kanai, R., & Rees, G. (2011). The structural basis of inter-individual differences in human behaviour and cognition. Nature Reviews Neuroscience, 12(4), 231-242.

Klein, D., Zatorre, R. J., Milner, B., & Zhao, V. (2001). A cross-linguistic PET study of tone perception in Mandarin Chinese and English speakers. Neuroimage, 13(4), 646-653.

Klingberg, T., Hedehus, M., Temple, E., Salz, T., Gabrieli, J. D., Moseley, M. E., & Poldrack, R. A. (2000). Microstructure of temporo-parietal white matter as a basis for reading ability: evidence from diffusion tensor magnetic resonance imaging. Neuron, 25(2), 493-500.

Kopell, N., Ermentrout, G. B., Whittington, M. A., & Traub, R. D. (2000). Gamma rhythms and beta rhythms have different synchronization properties. Proceedings of the National Academy of Sciences, 97(4), 1867-1872.

Kovelman, I., Norton, E. S., Christodoulou, J. A., Gaab, N., Lieberman, D. A., Triantafyllou, C., ... & Gabrieli, J. D. (2012). Brain basis of phonological awareness for spoken language in children and its disruption in dyslexia. Cerebral Cortex, 22(4), 754-764.

Lakatos, P., Shah, A. S., Knuth, K. H., Ulbert, I., Karmos, G., & Schroeder, C. E. (2005). An oscillatory hierarchy controlling neuronal excitability and stimulus processing in the auditory cortex. Journal of neurophysiology, 94(3), 1904-1911.

Lakatos, P., Karmos, G., Mehta, A. D., Ulbert, I., & Schroeder, C. E. (2008). Entrainment of neuronal oscillations as a mechanism of attentional selection. science, 320(5872), 110-113.

Lallier, M., Thierry, G., Tainturier, M. J., Donnadieu, S., Peyrin, C., Billard, C., & Valdois, S. (2009). Auditory and visual stream segregation in children and adults: an assessment of the amodality assumption of the 'sluggish attentional shifting'theory of dyslexia. Brain research, 1302, 132-147.

Larsen, J. P., Høien, T., Lundberg, I., & Ødegaard, H. (1990). MRI evaluation of the size and symmetry of the planum temporale in adolescents with developmental dyslexia. Brain and language, 39(2), 289-301.

Lehongre, K., Ramus, F., Villiermet, N., Schwartz, D., & Giraud, A. L. (2011). Altered low-gamma sampling in auditory cortex accounts for the three main facets of dyslexia. Neuron, 72(6), 1080-1090.

Lehongre, K., Morillon, B., Giraud, A. L., & Ramus, F. (2013). Impaired auditory sampling in dyslexia: further evidence from combined fMRI and EEG.

Leonard, C. M., Eckert, M. A., Lombardino, L. J., Oakland, T., Kranzler, J., Mohr, C. M., ... & Freeman, A. (2001). Anatomical risk factors for phonological dyslexia. Cerebral Cortex, 11(2), 148-157.

Leong, V., & Goswami, U. (2014). Assessment of rhythmic entrainment at multiple timescales in dyslexia: evidence for disruption to syllable timing. Hearing research, 308, 141-161.

Liberman, I. Y., Shankweiler, D., Fischer, F. W., & Carter, B. (1974). Explicit syllable and phoneme segmentation in the young child. Journal of experimental child psychology, 18(2), 201-212.

Liégeois-Chauvel, C., Lorenzi, C., Trébuchon, A., Régis, J., & Chauvel, P. (2004). Temporal envelope processing in the human left and right auditory cortices. Cerebral Cortex, 14(7), 731-740.

Lizarazu, M., Lallier, M., Molinaro, N., Bourguignon, M., Paz-Alonso, P. M., Lerma-Usabiaga, G., & Carreiras, M. (2015). Developmental evaluation of atypical auditory sampling in dyslexia: Functional and structural evidence. Human brain mapping, 36(12), 4986-5002.

Lonigan, C. J., Burgess, S. R., & Anthony, J. L. (2000). Development of emergent literacy and early reading skills in preschool children: evidence from a latent-variable longitudinal study. Developmental psychology, 36(5), 596.

Lorenzi, C., Dumont, A., & Fullgrabe, C. (2000). Use of temporal envelope cues by children with developmental dyslexia. Journal of speech, language, and hearing research, 43(6), 1367-1379.

Luo, H., & Poeppel, D. (2007). Phase patterns of neuronal responses reliably discriminate speech in human auditory cortex. Neuron, 54(6), 1001-1010.

Luria, A. R. (1976). Basic problems of neurolinguistics (Vol. 73). Walter de Gruyter.

MacSweeney, M., Brammer, M. J., Waters, D., & Goswami, U. (2009). Enhanced activation of the left inferior frontal gyrus in deaf and dyslexic adults during rhyming. Brain, 132(7), 1928-1940.

Magnotta, V. A., Andreasen, N. C., Schultz, S. K., Harris, G., Cizadlo, T., Heckel, D., ... & Flaum, M. (1999). Quantitative in vivo measurement of gyrification in the human brain: changes associated with aging. Cerebral Cortex, 9(2), 151-160.

Magri, C., Whittingstall, K., Singh, V., Logothetis, N. K., & Panzeri, S. (2009). A toolbox for the fast information analysis of multiple-site LFP, EEG and spike train recordings. BMC neuroscience, 10(1), 1.

Majerus, S. (2013). Language repetition and short-term memory: an integrative framework.

Mattout, J., Phillips, C., Penny, W. D., Rugg, M. D., & Friston, K. J. (2006). MEG source localization under multiple constraints: an extended Bayesian framework. NeuroImage, 30(3), 753-767.

Menell, P., McAnally, K. I., & Stein, J. F. (1999). Psychophysical sensitivity and physiological response to amplitude modulation in adult dyslexic listeners. Journal of Speech, Language, and Hearing Research, 42(4), 797-803.

Merzenich, M. M., & Brugge, J. F. (1973). Representation of the cochlear partition on the superior temporal plane of the macaque monkey. Brain research, 50(2), 275-296.

Miceli, G., Caltagirone, C., Gainotti, G., & Payer-Rigo, P. (1978). Discrimination of voice versus place contrasts in aphasia. Brain and Language, 6(1), 47-51.

Middlebrooks, J. C. (2008). Auditory cortex phase locking to amplitude-modulated cochlear implant pulse trains. Journal of neurophysiology, 100(1), 76-91.

Miendlarzewska, E. A., & Trost, W. J. (2014). How musical training affects cognitive development: rhythm, reward and other modulating variables. Frontiers in neuroscience, 7, 279.

Miles, T. (2006). Fifty years in dyslexia research. John Wiley & Sons.

Minagawa-Kawai, Y., Van Der Lely, H., Ramus, F., Sato, Y., Mazuka, R., & Dupoux, E. (2010). Optical brain imaging reveals general auditory and language-specific processing in early infant development. Cerebral Cortex, bhq082.

Modersitzki, J. (2004). Numerical methods for image registration. Oxford University Press on Demand.

Molinaro, N., Lizarazu, M., Lallier, M., Bourguignon, M., & Carreiras, M. (2016). Out-of-synchrony speech entrainment in developmental dyslexia. Human brain mapping.

Molnar, M., Lallier, M., & Carreiras, M. (2014). The amount of language exposure determines nonlinguistic tone grouping biases in infants from a bilingual environment. Language Learning, 64(s2), 45-64.

Moncrieff, D. W., & Black, J. R. (2008). Dichotic listening deficits in children with dyslexia. Dyslexia, 14(1), 54-75.

Morais, J., Alegría, J., & Content, A. (1987). The relationships between segmental analysis and alphabetic literacy: An interactive view. Cahiers de psychologie cognitive, 7(5), 415-438.

Morel, A., & Kaas, J. H. (1992). Subdivisions and connections of auditory cortex in owl monkeys. Journal of Comparative Neurology, 318(1), 27-63.

Morest, D. K. (1965). The laminar structure of the medial geniculate body of the cat. Journal of anatomy, 99(Pt 1), 143.

Morillon, B., Liégeois-Chauvel, C., Arnal, L. H., Bénar, C. G., & Giraud, A. L. (2012). Asymmetric function of theta and gamma activity in syllable processing: an intra-cortical study. Frontiers in psychology, 3, 248.

Morosan, P., Rademacher, J., Schleicher, A., Amunts, K., Schormann, T., & Zilles, K. (2001). Human primary auditory cortex: cytoarchitectonic subdivisions and mapping into a spatial reference system. Neuroimage, 13(4), 684-701.

Munck, D. J., & Peters, M. J. (1993). A fast method to compute the potential in the multisphere model. IEEE transactions on biomedical engineering, 40(11), 1166-1174.

Nichols, T. E., & Holmes, A. P. (2002). Nonparametric permutation tests for functional neuroimaging: a primer with examples. Human brain mapping, 15(1), 1-25.

Niogi, S. N., & McCandliss, B. D. (2006). Left lateralized white matter microstructure accounts for individual differences in reading ability and disability. Neuropsychologia, 44(11), 2178-2188.

Okada, K., Rong, F., Venezia, J., Matchin, W., Hsieh, I. H., Saberi, K., ... & Hickok, G. (2010). Hierarchical organization of human auditory cortex: evidence from acoustic invariance in the response to intelligible speech. Cerebral Cortex, 20(10), 2486-2495.

Oostenveld, R., Fries, P., Maris, E., & Schoffelen, J. M. (2011). FieldTrip: open source software for advanced analysis of MEG, EEG, and invasive electrophysiological data. Computational intelligence and neuroscience, 2011.

Panzeri, S., Brunel, N., Logothetis, N. K., & Kayser, C. (2010). Sensory neural codes using multiplexed temporal scales. Trends in neurosciences, 33(3), 111-120.

Park, H., Ince, R. A., Schyns, P. G., Thut, G., & Gross, J. (2015). Frontal top-down signals increase coupling of auditory low-frequency oscillations to continuous speech in human listeners. Current Biology, 25(12), 1649-1653.

Paxinos, G., & Mai, J. K. (2004). *The human nervous system*. Academic Press.

Peelle, J. E., Johnsrude, I., & Davis, M. H. (2010). Hierarchical processing for speech in human auditory cortex and beyond. Frontiers in human neuroscience, 4, 51.

Penhune, V. B., Zatorre, R. J., MacDonald, J. D., & Evans, A. C. (1996). Interhemispheric anatomical differences in human primary auditory cortex: probabilistic mapping and volume measurement from magnetic resonance scans. Cerebral Cortex, 6(5), 661-672.

Pennington, B. F., Orden, G. C., Smith, S. D., Green, P. A., & Haith, M. M. (1990). Phonological processing skills and deficits in adult dyslexics. Child development, 61(6), 1753-1778.

Pennington, B. F., Filipek, P. A., Lefly, D., Churchwell, J., Kennedy, D. N., Simon, J. H., ... & DeFries, J. C. (1999). Brain morphometry in reading-disabled twins. Neurology, 53(4), 723-723.

Peretz, I. (2013). The biological foundations of music: insights from congenital amusia. The psychology of music, 3, 551-564.

Peretz, I., Vuvan, D., Lagrois, M. É., & Armony, J. L. (2015). Neural overlap in processing music and speech. Phil. Trans. R. Soc. B, 370(1664), 20140090.

Pernet, C. R., Wilcox, R. R., & Rousselet, G. A. (2013). Robust correlation analyses: false positive and power validation using a new open source Matlab toolbox. Frontiers in psychology, 3, 606.

Peyrin, C., Lallier, M., Demonet, J. F., Pernet, C., Baciu, M., Le Bas, J. F., & Valdois, S. (2012). Neural dissociation of phonological and visual attention span disorders in developmental dyslexia: FMRI evidence from two case reports. Brain and language, 120(3), 381-394.

Poelmans, H., Luts, H., Vandermosten, M., Boets, B., Ghesquière, P., & Wouters, J. (2012). Auditory steady state cortical responses indicate deviant phonemic-rate processing in adults with dyslexia. Ear and hearing, 33(1), 134-143.

Poeppel, D. (2003). The analysis of speech in different temporal integration windows: cerebral lateralization as 'asymmetric sampling in time'. Speech communication, 41(1), 245-255.

Poeppel, D., & Monahan, P. J. (2008). Speech perception: Cognitive foundations and cortical implementation. Current Directions in Psychological Science, 80-85.

Poeppel, D., Idsardi, W. J., & Van Wassenhove, V. (2008). Speech perception at the interface of neurobiology and linguistics. Philosophical Transactions of the Royal Society of London B: Biological Sciences, 363(1493), 1071-1086.

Power, A. J., Mead, N., Barnes, L., & Goswami, U. (2013). Neural entrainment to rhythmic speech in children with developmental dyslexia.

Rae, C., Harasty, J. A., Dzendrowskyj, T. E., Talcott, J. B., Simpson, J. M., Blamire, A. M., ... & Richardson, A. J. (2002). Cerebellar morphology in developmental dyslexia. Neuropsychologia, 40(8), 1285-1292.

Rademacher, J., Caviness, V. S., Steinmetz, H., & Galaburda, A. M. (1993). Topographical variation of the human primary cortices: implications for neuroimaging, brain mapping, and neurobiology. Cerebral Cortex, 3(4), 313-329.

Ramus, F. (2003). Developmental dyslexia: specific phonological deficit or general sensorimotor dysfunction?. Current opinion in neurobiology, 13(2), 212-218.

Ramus, F. (2014). Neuroimaging sheds new light on the phonological deficit in dyslexia. Trends in cognitive sciences, 18(6), 274-275.

Ramus, F., Nespor, M., & Mehler, J. (1999). Correlates of linguistic rhythm in the speech signal. Cognition, 73(3), 265-292.

Ramus, F., Rosen, S., Dakin, S. C., Day, B. L., Castellote, J. M., White, S., & Frith, U. (2003). Theories of developmental dyslexia: insights from a multiple case study of dyslexic adults. Brain, 126(4), 841-865.

Ramus, F., & Szenkovits, G. (2008). What phonological deficit?. The Quarterly Journal of Experimental Psychology, 61(1), 129-141.

Rauschecker, J. P., Tian, B., & Hauser, M. (1995). Processing of complex sounds in the macaque nonprimary auditory cortex. Science, 268(5207), 111.

Rauschecker, J. P., & Tian, B. (2004). Processing of band-passed noise in the lateral auditory belt cortex of the rhesus monkey. Journal of Neurophysiology, 91(6), 2578-2589.

Rauschecker, J. P., & Scott, S. K. (2009). Maps and streams in the auditory cortex: nonhuman primates illuminate human speech processing. Nature neuroscience, 12(6), 718-724.

Rey, V., De Martino, S., Espesser, R., & Habib, M. (2002). Temporal processing and phonological impairment in dyslexia: Effect of phoneme lengthening on order judgment of two consonants. Brain and language, 80(3), 576-591.

Robichon, F., Levrier, O., Farnarier, P., & Habib, M. (2000a). Developmental dyslexia: atypical cortical asymmetries and functional significance. European Journal of Neurology, 7(1), 35-46.

Robichon, F., Bouchard, P., Démonet, J. F., & Habib, M. (2000b). Developmental dyslexia: re-evaluation of the corpus callosum in male adults. European Neurology, 43(4), 233-237.

Rocheron, I., Lorenzi, C., Füllgrabe, C., & Dumont, A. (2002). Temporal envelope perception in dyslexic children. Neuroreport, 13(13), 1683-1687.

Rouiller, E. M., Rodrigues-Dagaeff, C., Simm, G., De Ribaupierre, Y., Villa, A., & De Ribaupierre, F. (1989). Functional organization of the medial division of the medial geniculate body of the cat: tonotopic organization, spatial distribution of response properties and cortical connections. Hearing research, 39(1), 127-142.

Saygin, Z. M., Norton, E. S., Osher, D. E., Beach, S. D., Cyr, A. B., Ozernov-Palchik, O., ... & Gabrieli, J. D. (2013). Tracking the roots of reading ability: white matter volume and integrity correlate with phonological awareness in prereading and early-reading kindergarten children. The journal of Neuroscience, 33(33), 13251-13258.

Schneider, T., & Neumaier, A. (2001). Algorithm 808: ARfit—A Matlab package for the estimation of parameters and eigenmodes of multivariate autoregressive models. ACM Transactions on Mathematical Software (TOMS), 27(1), 58-65.

Schroeder, C. E., & Lakatos, P. (2009). Low-frequency neuronal oscillations as instruments of sensory selection. Trends in neurosciences, 32(1), 9-18.

Schultz, R. T., Cho, N. K., Staib, L. H., Kier, L. E., Fletcher, J. M., Shaywitz, S. E., ... & Shaywitz, B. A. (1994). Brain morphology in normal and dyslexic children: The influence of sex and age. Annals of Neurology, 35(6), 732-742.

Scott, S. K., & Johnsrude, I. S. (2003). The neuroanatomical and functional organization of speech perception. Trends in neurosciences, 26(2), 100-107.

Scott, S. K., Rosen, S., Beaman, C. P., Davis, J. P., & Wise, R. J. (2009). The neural processing of masked speech: Evidence for different mechanisms in the left and right temporal lobes. The Journal of the Acoustical Society of America, 125(3), 1737-1743.

Ségonne, F., Dale, A. M., Busa, E., Glessner, M., Salat, D., Hahn, H. K., & Fischl, B. (2004). A hybrid approach to the skull stripping problem in MRI. Neuroimage, 22(3), 1060-1075.

Serniclaes, W., Sprenger-Charolles, L., Carré, R., & Demonet, J. F. (2001). Perceptual discrimination of speech sounds in developmental dyslexia. Journal of Speech, Language, and Hearing Research, 44(2), 384-399.

Serniclaes, W., Van Heghe, S., Mousty, P., Carré, R., & Sprenger-Charolles, L. (2004). Allophonic mode of speech perception in dyslexia. Journal of experimental child psychology, 87(4), 336-361.

Shapleske, J., Rossell, S. L., Woodruff, P. W. R., & David, A. S. (1999). The planum temporale: a systematic, quantitative review of its structural, functional and clinical significance. Brain Research Reviews, 29(1), 26-49.

Shaw, P., Kabani, N. J., Lerch, J. P., Eckstrand, K., Lenroot, R., Gogtay, N., ... & Giedd, J. N. (2008). Neurodevelopmental trajectories of the human cerebral cortex. The Journal of Neuroscience, 28(14), 3586-3594.

Snowling, M. J. (1981). Phonemic deficits in developmental dyslexia. Psychological research, 43(2), 219-234.

Snowling, M. J. (2008). Specific disorders and broader phenotypes: The case of dyslexia. The Quarterly Journal of Experimental Psychology, 61(1), 142-156.

Soroli, E., Szenkovits, G., & Ramus, F. (2010). Exploring dyslexics' phonological deficit III: foreign speech perception and production. Dyslexia, 16(4), 318-340.

Sowell, E. R., Peterson, B. S., Thompson, P. M., Welcome, S. E., Henkenius, A. L., & Toga, A. W. (2003). Mapping cortical change across the human life span. Nature neuroscience, 6(3), 309-315.

Sowell, E. R., Thompson, P. M., Leonard, C. M., Welcome, S. E., Kan, E., & Toga, A. W. (2004). Longitudinal mapping of cortical thickness and brain growth in normal children. *The Journal of neuroscience*, *24*(38), 8223-8231.

Stanovich, K. E. (2000). Progress in understanding reading: Scientific foundations and new frontiers. Guilford Press.

Stein, J.F. & Talcott, J.B. (1999). The magnocellular theory of dyslexia. Dyslexia: An International Journal of Research and Practice, 5(2), 59-78.

Stein, J. (2001). The magnocellular theory of developmental dyslexia. Dyslexia, 7(1), 12-36.

Stevens, K. N. (2002). Toward a model for lexical access based on acoustic landmarks and distinctive features. The Journal of the Acoustical Society of America, 111(4), 1872-1891.

Stoodley, C. J. (2015). The Role of the Cerebellum in Developmental Dyslexia. The Linguistic Cerebellum, 199.

Swan, D., & Goswami, U. (1997). Phonological awareness deficits in developmental dyslexia and the phonological representations hypothesis. Journal of experimental child psychology, 66(1), 18-41.

Tallal, P. (1980). Auditory temporal perception, phonics, and reading disabilities in children. Brain and language, 9(2), 182-198.

Tallal, P., & Gaab, N. (2006). Dynamic auditory processing, musical experience and language development. Trends in neurosciences, 29(7), 382-390.

Taulu, S., & Kajola, M. (2005). Presentation of electromagnetic multichannel data: the signal space separation method. Journal of Applied Physics, 97(12), 124905.

Temple, E., Deutsch, G. K., Poldrack, R. A., Miller, S. L., Tallal, P., Merzenich, M. M., & Gabrieli, J. D. (2003). Neural deficits in children with dyslexia ameliorated by behavioral remediation: evidence from functional MRI. Proceedings of the National Academy of Sciences, 100(5), 2860-2865.

Thevenet, M., Bertrand, O., Perrin, F., Dumont, T., & Pernier, J. (1991). The finite element method for a realistic head model of electrical brain activities: preliminary results. Clinical Physics and Physiological Measurement, 12(A), 89.

Thomson, J. M., Leong, V., & Goswami, U. (2013). Auditory processing interventions and developmental dyslexia: a comparison of phonemic and rhythmic approaches. Reading and Writing, 26(2), 139-161.

Tierney, A., Dick, F., Deutsch, D., & Sereno, M. (2013). Speech versus song: multiple pitch-sensitive areas revealed by a naturally occurring musical illusion. Cerebral Cortex, 23(2), 249-254.

Torgesen, J. K., Wagner, R. K., Rashotte, C. A., Rose, E., Lindamood, P., Conway, T., & Garvan, C. (1999). Preventing reading failure in young children with phonological processing disabilities: Group and individual responses to instruction. Journal of Educational Psychology, 91(4), 579.

Tort, A. B., Komorowski, R., Eichenbaum, H., & Kopell, N. (2010). Measuring phase-amplitude coupling between neuronal oscillations of different frequencies. Journal of neurophysiology, 104(2), 1195-1210.

Uhry, J. K. (2002). Kindergarten phonological awareness and rapid serial naming as predictors of Grade 2 reading and spelling. In Basic functions of language, reading and reading disability (pp. 299-313). Springer US.

Vandermosten, M., Boets, B., Wouters, J., & Ghesquière, P. (2012). A qualitative and quantitative review of diffusion tensor imaging studies in reading and dyslexia. Neuroscience & Biobehavioral Reviews, 36(6), 1532-1552.

Vandermosten, M., Poelmans, H., Sunaert, S., Ghesquière, P., & Wouters, J. (2013). White matter lateralization and interhemispheric coherence to auditory modulations in normal reading and dyslexic adults. Neuropsychologia, 51(11), 2087-2099.

Van Veen, B. D., Van Drongelen, W., Yuchtman, M., & Suzuki, A. (1997). Localization of brain electrical activity via linearly constrained minimum variance spatial filtering. IEEE Transactions on biomedical engineering, 44(9), 867-880.

Vanvooren, S., Poelmans, H., Hofmann, M., Ghesquière, P., & Wouters, J. (2014). Hemispheric asymmetry in auditory processing of speech envelope modulations in prereading children. The Journal of Neuroscience, 34(4), 1523-1529.

Vellutino, F. R. (1979). Dyslexia: Theory and research.

Vellutino, F. R., Fletcher, J. M., Snowling, M. J., & Scanlon, D. M. (2004). Specific reading disability (dyslexia): what have we learned in the past four decades?. Journal of child psychology and psychiatry, 45(1), 2-40.

Von Economo, C., & Horn, L. (1930). Über Windungsrelief, Maße und Rindenarchitektonik der Supratemporalfläche, ihre individuellen und ihre Seitenunterschiede. Zeitschrift für die gesamte Neurologie und Psychiatrie, 130(1), 678-757.

von Plessen, K., Lundervold, A., Duta, N., Heiervang, E., Klauschen, F., Smievoll, A. I., ... & Hugdahl, K. (2002). Less developed corpus callosum in dyslexic subjects—a structural MRI study. Neuropsychologia, 40(7), 1035-1044.

Wagner, R. K., & Torgesen, J. K. (1987). The nature of phonological processing and its causal role in the acquisition of reading skills. Psychological bulletin, 101(2), 192.

Wagner, R. K., Torgesen, J. K., & Rashotte, C. A. (1999). CTOPP: Comprehensive test of phonological processing. Pro-ed.

Wechsler, D. (1974). Wechsler intelligence scale for children-revised. Psychological Corporation.

Wechsler, D. (2008). Wechsler adult intelligence scale-fourth. San Antonio, TX: The Psychological Corporation Google Scholar.

Wenstrup, J. J. (1999). Frequency organization and responses to complex sounds in the medial geniculate body of the mustached bat. Journal of neurophysiology, 82(5), 2528-2544.

Wernicke, C. (1969). The symptom complex of aphasia. In Proceedings of the Boston Colloquium for the Philosophy of Science 1966/1968 (pp. 34-97). Springer Netherlands.

Wessinger, C. M., VanMeter, J., Tian, B., Van Lare, J., Pekar, J., & Rauschecker, J. P. (2001). Hierarchical organization of the human auditory cortex revealed by

functional magnetic resonance imaging. Journal of cognitive neuroscience, 13(1), 1-7.

Wheat, K. L., Cornelissen, P. L., Frost, S. J., & Hansen, P. C. (2010). During visual word recognition, phonology is accessed within 100 ms and may be mediated by a speech production code: evidence from magnetoencephalography. The Journal of Neuroscience, 30(15), 5229-5233.

Wild, C. J., Yusuf, A., Wilson, D. E., Peelle, J. E., Davis, M. H., & Johnsrude, I. S. (2012). Effortful listening: the processing of degraded speech depends critically on attention. The Journal of Neuroscience, 32(40), 14010-14021.

Winer, J. A., & Larue, D. T. (1987). Patterns of reciprocity in auditory thalamocortical and corticothalamic connections: study with horseradish peroxidase and autoradiographic methods in the rat medial geniculate body. Journal of Comparative Neurology, 257(2), 282-315.

Witelson, S. F., & Pallie, W. (1973). Left hemisphere specialization for language in the newborn. Brain, 96(3), 641-646.

Witton, C., Stein, J. F., Stoodley, C. J., Rosner, B. S., & Talcott, J. B. (2002). Separate influences of acoustic AM and FM sensitivity on the phonological decoding skills of impaired and normal readers. Journal of cognitive neuroscience, 14(6), 866-874.

Wolf, M., & Bowers, P. G. (1999). The double-deficit hypothesis for the developmental dyslexias. Journal of educational psychology, 91(3), 415.

Woods, D. L., Herron, T., Kang, X., Cate, A. D., & Yund, E. W. (2011). Phonological processing in human auditory cortical fields. Frontiers in human neuroscience, 5, 42.

Yildiz, I. B., von Kriegstein, K., & Kiebel, S. J. (2013). From birdsong to human speech recognition: Bayesian inference on a hierarchy of nonlinear dynamical systems. PLoS Comput Biol, 9(9), e1003219.

Zatorre, R. J., & Evans, A. C. (1992). Lateralization of phonetic and pitch discrimination in speech processing. Science, 256(5058), 846.

Ziegler, J. C., & Goswami, U. (2005). Reading acquisition, developmental dyslexia, and skilled reading across languages: a psycholinguistic grain size theory. Psychological bulletin, 131(1), 3.